CHESTER

Compressed Heat Energy Storage for Energy from Renewable sources

D4.5 Full scale CHEST system optimization and techno-economic assessment

PROJECT	**CHESTER**
PROJECT NO.	**764042**
DELIVERABLE NO.	**D4.5**
DOCUMENT VERSION	**V5.0/REV2.1**
DOCUMENT PREPARATION DATE	**23/09/2021**
RESPONSIBLE PARTNER	**USTUTT**
DISSEMINATION LEVEL	**Public**

Type of Deliverable		
R	Document, Report	**X**
DEM	Demonstrator, pilot, prototype	
DEC	Websites, patent fillings, videos, etc.	
OTHER		
ETHICS	Ethics requirements	
ORDP	Open Research Data Pilot	

This project has received funding from the European Union's Horizon 2020 research and innovation programme under grant agreement No. 764042.

EC Grant Agreement	No.764042
Project Acronym	CHESTER
Project Title	Compressed Heat Energy Storage for Energy from Renewable sources
Programme	HORIZON 2020
Start Date of Project	01-04-2018
Duration	48 Months

Financial/Administrative Coordinator	
Project Coordinator Organization Name	TECNALIA
Address	Parque Tecnológico de Bizkaia C/Geldo, Edificio 700 (Spain)
Phone Numbers	+34 946 430 850
E-mail Address	nora.fernandez@tecnalia.com
Project web-site	www.chester-project.eu

Version Management			
Filename	CHESTER D4.5: Full scale CHEST system optimization and techno-economic assessment		
Authors	Sven Stark, Dominik Bestenlehner (USTUTT)		
Reviewed by	Magdalena Komoszynska, Rasmus Lund (PlanEnergi)		
Approved by	Nora Fernandez Perez (Tecnalia)		
Revision No.	**Date**	**Author**	**Modification description**
V1.0	08/09/2020	S. Stark	First version
V2.0	06/10/2020	S. Stark	First complete version
V2.1	21/10/2020	M. Komoszynska	Review of the deliverable
V3.0	26/10/2020	S. Stark	Revised version of the deliverable
V3.1	28/10/2020	N. Fernandez	Review of the deliverable
V3.2	29/10/2020	D. Bestenlehner	Review of the deliverable
V4.0	30/10/2020	S. Stark	Revised version of the deliverable
V5.0	03/11/2020	S. Stark	Final corrections
REV1.0	07/09/2021	S. Stark	First revision after deliverable rejection
REV2.0	15/09/2021	D. Bestenlehner	Second revision after delv. rejection
REV2.1	23/09/2021	S. Stark	Minor changes after review

Contents

List of Figures

List of Tables

Glossary, Abbreviations and Acronyms

CAPEX	Capital expenditure
CHEST	Compressed Heat Energy Storage
COP	Coefficient of performance
CSP	Concentrated solar power
DH	District heating
DSO	Distribution system operator
EES	Electrical energy storage
FRR	Frequency restoration reserve
GWP	Global warming potential
HP	Heat pump
HT	High temperature
HTTES	High-temperature thermal energy storage
HTWT	High-temperature water tank
IRR	Internal rate of return
KPI	Key performance indicator
LCA	Life cycle analysis
LCOS	Levelized costs of storage
LCOE	Levelized costs of energy/electricity
LCOH	Levelized costs of heat
LHS	Latent heat storage (latent part of the HTTES)
LT	Low temperature
LTTES	Low-temperature thermal energy storage (seasonal thermal energy storage)
LTWT	Low-temperature water tank
NPV	Net present value
O&M	Operation and maintenance
OPEX	Operational expenditure
ORC	Organic Rankine Cycle
PCM	Phase change material
P2P	Power-to-power
PV	Photovoltaics
RES	Renewable energy source
ROI	Return on investment
SHS	Sensible heat storage (sensible part of the HTTES)
SoC	State of charge
TES	Thermal energy storage
TRNSYS	Transient System Simulation (software)
VAT	Value-added tax
WP	Work package

1. Introduction

1.1. Executive summary

This report deals with the techno-economic assessment of the CHEST system integrated into the energy system (electric and thermal grids, production and demand side, heat source and sink temperatures). For this purpose, the two selected case studies Aalborg (Denmark) and Ispaster (Spain) were considered, but also the characteristics of these case studies were modified to look for the optimum framework in which the CHEST system could fit better. For instance, the integration of CHEST into an island energy system in Ispaster was considered, which is a new potential hypothetical use case of CHEST. In order to carry out the techno-economic assessment, the first step was to define key performance indicators (KPIs) that describe and assess the performance of the CHEST system and its components from a technical, operational, energetic, environmental and economic point of view.

After this, the integration of the CHEST system into the energy system of the two case studies and new potential hypothetical case studies and also related to that, the respective business cases, were defined. The potential use cases, the related business models and other inputs for the models herein presented are based on the results of Task 6.2. Furthermore, they include the outcome of the parallel Task 4.4 regarding the optimization of the CHEST system by the selection of more suitable PCM and refrigerant combinations.

Dynamic simulations were then carried out for the respective case studies with the help of the TRNSYS model that was developed in Task 4.2 and that was adapted to the respective case study in this task. Finally, the KPIs defined at the beginning were applied to the simulation results for the techno-economic assessment of the CHEST system.

The main outcome of the techno-economic assessment for the Aalborg case study is that the electricity prices of the Danish spot and tertiary regulation market are very disadvantageous for the operation of the CHEST system. On the one hand, there are only a few hours with very low and very high electricity prices and on the other hand, also the fluctuation of the electricity prices is quite low. Together with the currently existing tax scheme for the purchase and sale of electricity and the considerable operation and maintenance (O&M) costs of the CHEST system, the hours of operation of the heat pump (HP) and the Organic Rankine Cycle (ORC) are too limited to achieve a profitable business case in the Danish electricity market. The limitation of the hours of operation also leads to very low annual primary energy savings and annual savings of CO_2 emissions.

For the Ispaster case study, the economic assessment is much more advantageous, at least in comparison to the battery storage. Indeed, from the economic point of view, it is the best option to install no electrical energy storage at all, but if electrical energy storage is used, CHEST is the favorable option. This is especially true for larger storage capacities like required for an island energy system since the CHEST system becomes more and more advantageous concerning investment costs compared to a conventional battery storage, the higher the storage capacity is. Due to a heat generation that is already completely based on renewables (solar thermal + biomass), there are only small differences in the annual primary energy savings and annual savings of CO_2 emissions between CHEST and the battery storage.

A general finding for both case studies is that the CHEST system is a net heat consumer, i.e. the operation of the CHEST system leads to additional heat demand. If the heat source is not truly excess heat, which would not be usable otherwise, this leads to increased annual costs, but it also leads to a decrease of the annual primary energy savings and the annual savings of CO_2 emissions. As the production of the CHEST system according to current knowledge is connected to a quite high energy demand and to quite high CO_2 emissions due to the PCM, there is a relatively long energetic as well as CO_2 payback time for the CHEST system. However, the primary energy and CO_2 emission values for the PCM production are only preliminary numbers here. Certainly, the work in Task 4.6 about life cycle analysis (LCA) of the CHEST system will bring more light into this.

1.2. Purpose and Scope

This deliverable presents the outcome of the work carried out in Task 4.3. This task mainly deals with the following subtasks:

- defining key performance indicators (KPIs), which describe and assess the performance of the CHEST system itself and in comparison to a reference energy system as regards to for instance energetic, environmental and economic benefit,
- based on the previous work in the project, defining the integration and business case of the CHEST system to be analyzed in T4.3 for the two case studies considered in WP4: Aalborg and Ispaster,
- carrying out simulations with the dynamic TRNSYS simulation model developed in T4.2 for the two case studies Aalborg and Ispaster,
- through these simulations, analyzing and optimizing the dimensions and operation (parameter settings, control strategy) of the CHEST system for the respective case study and given boundary conditions,
- based on the simulation results and the KPIs defined, evaluating the performance of the CHEST system itself and in comparison to the reference energy system.

Task 4.3 started with the definition of several KPIs that were grouped into five categories. The first and second group of KPIs comprise parameters that evaluate the performance of the CHEST system itself or its main components, respectively. In contrast to that, the KPIs of the other three groups are performance parameters that are defined in relation to a reference energy system. This reference energy system can be given by the currently existing situation of the respective case study without CHEST system or can be an alternative storage solution, i.e. a competitor energy system.

As the second step of Task 4.3, the integration of the CHEST system into the energy system of the two case studies Aalborg and Ispaster, the respective business cases and the intended extent of simulations to be carried out in T4.3 were defined. The definition of the CHEST integration was built upon the work of previous tasks of the project, for more details see Chapter 1.4.

After the definition of the CHEST integration, simulations for the two case studies Aalborg and Ispaster were carried out. In order to do this, some adaptions of the TRNSYS model that was developed in T4.2 had to be undertaken, especially for the case study of Ispaster. The simulations that were carried out in Task 4.3 were done with the “optimized” combination of refrigerant and PCM, which was an outcome of Task 4.4.

The simulation results were then used to calculate the KPIs defined at the beginning of the task in order to evaluate the performance of the CHEST system itself and in comparison to the reference energy system.

1.3. Structure of the document

Following the several subtasks mentioned above, the document is composed of five main parts.

In the first part (Chapter 2), a range of key performance indicators (KPIs) that describe and assess the CHEST system from a technical, operational, energetic, environmental and economic point of view are defined.

Chapter 3 then deals with the description of the CHEST integration into the energy system of the two case studies Aalborg and Ispaster. This means that the basic role that the CHEST system plays in the case studies and which was analyzed by simulations in Task 4.3 is explained in this part of the document.

In Chapter 4, some adaptions of the WP4 TRNSYS model that were undertaken in order to properly simulate the CHEST system in the respective case study are described.

Chapter 5 shows selected results of the simulation studies with a focus on finding a suitable sizing of the CHEST system for the respective case study and given boundary conditions. In this chapter, KPIs of the first two groups (technical and operational KPIs) are already shown as they are inherent to the CHEST system.

In the last part of this document (Chapter 6), a detailed techno-economic assessment of the CHEST systems in the two case studies with the help of the KPIs evaluating the energetic, environmental and economic performance of the CHEST system is presented.

Finally, Chapter 7 concludes the results of the CHEST simulations and techno-economic assessment that were presented in this document.

1.4. Relations with other tasks and deliverables

This deliverable D4.5 and the associated Task 4.3 have multiple relations to other tasks and deliverables, which are explained in the following.

First of all, there are several relations given for the subtask of the integration of the CHEST system into the energy system of the two case studies Aalborg and Ispaster. In earlier tasks of the CHESTER project, there have already been analyses of the CHEST integration into the energy system of the respective case study. Namely, this was done in Task 2.1 (description of the case studies including CHEST potential), Task 2.2 and 2.3 (CHEST performance evaluation through simulations with the first TRNSYS model), Task 4.2 (analysis of CHEST integration into the several electricity markets) and Task 6.2 (definition and assessment of several business cases).

Second, there is a relation between the Tasks 4.3 and 4.4 concerning the simulations for Aalborg and Ispaster. It was decided to carry out the T4.3 simulations with an optimized combination of refrigerant and PCM in order to get results with increased CHEST performance. Therefore, the workflow here was the following:

- at first, the TRNSYS simulation model was adapted to the respective case study in the course of T4.3,
- then, simulations for the analysis of the best combination of refrigerant and PCM were done with this model in T4.4 with the refrigerants and PCMs, which had been identified through a literature research,
- the best combination found for each case study was then taken for the simulations in T4.3,
- whereupon, some modifications in the TRNSYS model were done in T4.3, for instance, the T4.4 simulations were carried out with large enough SHS, that means, without the recharge mechanism described in Chapter 4.2, this was later added only for T4.3 in order to further improve the results on the thermal side.

A further relation to be mentioned here is the use of data from D4.3, but also from WP2 for the work in T4.3. For Aalborg case study, most of the profiles were already given in WP2. In Ispaster case study, there is a continuous development concerning heat generation (new boilers) and heat demand (further buildings connected to the DH network), but also concerning the connection of further buildings to the electric micro-grid. As regards to the annual heat and electricity demand of Ispaster, it was decided to stick to the annual values that were presented in D4.3. So, the profiles of heat and electricity demand were changed compared to T2.3, with for instance new information from another project in the Basque country incorporated for the electric profile. Compared to WP2, DH temperatures were changed for Ispaster from 75/55 °C to 60/40 °C, which is the lowest temperature level possible for Ispaster according to the currently available information on this case study.

Concerning the environmental assessment of the CHEST system, this Task 4.3 will only supply selected preliminary and approximate results, respectively, as this will be analyzed more in detail in the upcoming Task 4.6. There are also only two environmental KPIs defined in this deliverable, the savings of CO_2 emissions and the CO_2 payback time (see Chapter 2.5) being considered as the most significant ones. In a complete environmental impact analysis, there are a lot more parameters to consider, for instance, the total use of resources, particulate matter, acidification of soil and water, land use, contribution to ozone layer depletion, etc.

Beside CO_2 payback time, the same applies to the energetic payback time defined in Chapter 2.4.4. At the current status of the project, there is simply no sound information about how much primary energy is needed for the production, installation and removal of a CHEST system and so, how much CO_2 emission this results in. These questions will be answered in Task 4.6, which deals with an environmental assessment from a life cycle perspective.

A further relation is given to Task 6.2, which already presented economic results for the two case studies Aalborg and Ispaster. To make clear the distinction of this Task 4.3 and the previous work, especially in comparison to T6.2, the main differences are explained in the following:

<u>**General differences**</u>

- **Detailed TRNSYS model**: In T4.3, the detailed TRNSYS model developed in T4.2 is used, whereas, in WP6, the energyPro software simulating a simplified CHEST system was used. For some T6.2 calculations of Ispaster case study, also TRNSYS results were used, but they were obtained with the less detailed model of WP2. The advanced TRNSYS model has been developed allowing for a more detailed simulation of the CHEST components and their interaction between each other and the environment, including for instance, the calculation of refrigerant states at the different points of the thermodynamic cycle and the incorporation of heat transfer limitations in the latent heat storage. The energyPro software does not simulate the CHEST system in such a detailed level.
- **Availability of heat**: In T6.2, the available thermal power of the heat source is infinite, i.e. there is no constraint of the CHEST operation by this. In contrast to this, the WP4 TRNSYS model takes the limited availability of the heat sources (excess heat in Aalborg case study, biomass boiler and/or solar thermal heat in Ispaster case study) into account. This means that times can occur when the heat pump of the CHEST system cannot work because of a lack of available heat.
- **Scope of evaluation**: T6.2 was nearly solely dedicated to the economic assessment of the CHEST system running in different business case scenarios. In contrast to this, T4.3 considers not only the economic side but also a detailed techno-economic assessment. So, a lot of further key performance indicators (KPIs) like for instance the savings of primary energy and the savings of CO_2 emissions have been defined and are presented as an outcome of the simulations in T4.3. On the other hand, in terms of the economic assessment, T6.2 does not only focus on pure KPIs, but includes several further calculations and considerations.
- **General scope of the two tasks 4.3 and 6.2 in the context of WP4 and WP6**: The WP4 TRNSYS model was developed to describe the operation of the CHEST system in its technical details including temperatures, state of working fluid, heat transfer etc. This was done in order to optimize the performance not only in terms of the economic

profitability but also from the technical and energetic side. So, the basic scope of WP4 is to describe the CHEST operation and its link to the electric and thermal grid as precisely as possible and then to optimize it, e.g. concerning working fluids, PCM and operation strategy (→T4.4). In comparison to that, the WP6 analyses are carried out on a superordinate level of CHEST operation description, focusing on the identification and evaluation of potential business cases.

Specific differences for the Aalborg case study

- **P2P ratio**: In T6.2, the P2P ratio used for the economic calculations accounted for about 59 %. In contrast to that, the P2P ratio in T4.3 is significantly higher, about 115 - 135 %, which is much more advantageous for a business case that considers the participation in the national electricity markets. This significantly higher P2P ratio is a result of the optimized refrigerant/PCM selection together with the adaption of the HP evaporation and ORC condensation temperature level.
- **Thermal power of heat source and heat sink**: In T6.2, the thermal power made available by the heat source and the thermal power, which can be discharged to the heat sink are assumed to be infinite, i.e. there is no constraint of the CHEST operation by this. In contrast to this, the available excess heat is limited in T4.3 (given by the hourly excess heat profile). In case it is lower than the heat required by the HP evaporator, an additional gas-fired backup heater must be used. Concerning the heat sink (i.e. the DH network), the ORC of the CHEST system can only transfer as much heat to the DH network as is given by the current DH heat demand. If at a certain point of time, the DH heat demand is lower than the available ORC condensation heat, a part of this condensation heat gets lost to the environment. As will be shown with the results (see Chapter 5.1), there is anyway no transfer of ORC condensation heat to the DH network at all, because the ORC condensation temperature level is too low for this.
- **No LTTES**: In T4.3, there is no low-temperature thermal energy storage (LTTES), i.e. no seasonal thermal energy storage, considered for the Aalborg case study. Compared to the previous simulation results of WP2, this gives the possibility to decouple the HP evaporation and ORC condensation temperatures from each other. When both the HP and the ORC are connected to a LTTES, a high temperature level in the LTTES is advantageous for the COP of the HP, but at the same time, this high temperature level in the LTTES is disadvantageous for the ORC efficiency. Without the LTTES, the HP and ORC are directly connected to the heat source (= excess heat) and heat sink (= DH network). A further main reason for not considering an LTTES in Aalborg is the high HP evaporation temperature of 100 °C (see Chapter 4.3), which does not allow for a non-pressurized LTTES. This high HP evaporation temperature was an outcome of T4.4 considering a maximum temperature lift in the HP of 60 K and the PCM to be used here having a melting temperature of 160 °C, cf. Deliverable 4.4.

Specific differences for the Ispaster case study

- **P2P ratio**: In T6.2, the P2P ratio accounted for about 46 - 53 %. Due to the optimized refrigerant/PCM selection and the adaption of the HP evaporation and ORC condensation temperature level, the P2P ratio was higher in T4.3: about 65 - 69 % for Ispaster 2.0 case and 95 - 101 % for Ispaster Island case.
- **Thermal power of heat source and heat sink**: In T6.2, the thermal power made available by the heat source and the thermal power, which can be discharged to the heat sink are assumed to be infinite, i.e. there is no constraint of the CHEST operation by this. In contrast to this, the available heat at the HP evaporator is limited in T4.3. Depending on the exact settings in the thermal circuit (e.g. set point temperature of the boiler, settings of the controllers for the solar collectors and the boiler), there might be hours when the HP cannot operate due to the unavailability of heat. Concerning the heat sink (i.e. the DH network), the ORC of the CHEST system can only transfer as much heat to the DH network as is given by the current DH heat demand. If at a certain point of time, the DH heat demand is lower than the available ORC condensation heat, a part of this condensation heat gets lost to the environment.
- **Thermal storage (no LTTES in the original sense of the CHESTER concept)**: In T2.3, a thermal storage, i.e. a LTTES in the original sense of the CHESTER concept as described in Chapter 2.1.4. served as heat source for the HP and as heat sink for the ORC. In contrast to this, in T4.3, the thermal storage (which is fed by heat from the solar thermal collectors and the biomass boiler) only serves as heat source for the HP. The ORC is directly coupled to the DH network allowing for lower ORC condensation temperatures and thus higher ORC efficiencies. However, this measure has the following drawback: In times where the DH heat demand is lower than the available ORC condensation heat, a part of the ORC condensation heat gets lost, because it cannot be transfered to the DH network (and its temperature level is also too low to transfer it to the thermal storage, if the ORC would have been connected to it). Therefore, this thermal storage in T4.3 is not an LTTES in the original sense of the CHESTER concept being coupled to both HP and ORC. Furthermore, the thermal storage in the Ispaster case study allows for storage temperatures of > 95 °C and thus, it is considered to be a pressurized storage, in contrast to a typical LTTES (see Chapter 2.1.4). The reason for this higher storage temperature level is due to the relatively high HP evaporation temperature of 82 °C (see Chapter 4.4). Taking into account the required temperature difference of 5 K at the HP evaporator, this gives a minimum useful temperature in the thermal storage (at least for the HP operation, not for the DH network) of 87 °C. Allowing a maximum storage temperature of only 95 °C would mean a relatively small useful temperature difference, which limits the storage capacity.
- **DH temperatures**: As already said above, the DH temperatures used in T4.3 accounted for 60/40 °C forward and return temperature of the DH network, respectively, in contrast to 75/55 °C in all previous calculations (T2.3/T6.2). This leads to higher ORC efficiencies for cases when there is heat transferred to the DH network.
- **Change of energy profiles**: In T6.2, the electricity and heat production and demand profiles from T2.3 were taken. Here in T4.3, the demand profiles were changed to follow

the annual numbers presented in D4.3. The energy production was in both cases modelled in TRNSYS with the same TRNSYS types and basic settings used for PV and solar thermal collectors. However, changes arise especially for the thermal side due to changes in the thermal circuit including boiler and the thermal storage (which is not considered an "LTTES", see above). Furthermore, some detail settings like for instance the boiler set point temperature had to be changed due to the different HP evaporation temperature level, which is a consequence of the different PCM/refrigerant combination used in T4.3.

- **Changes in the economic boundary conditions**: One change compared to the calculations of T6.2 is the consideration of an investment cost reduction for HP and ORC under the assumption that both will form one single component in the future. Another change is the use of a fixed electricity price (as part of a bilateral contract with the DSO) instead of fluctuating prices dependent on the Spanish spot electricity market.
- **Ispaster Island case**: So far, no scenario was considered where PV + the electrical energy storage (i.e. either the CHEST system or the lead-acid batteries) provide electrical self-sufficiency for Ispaster, which means complete independence from the DSO. Compared to the previous work, the integration of CHEST into an island energy system is a new promising potential use case, because an island energy system based on PV as the only electricity generator necessarily requires a form of electrical energy storage.
- **Solar thermal collector area**: Compared to the previous studies, the solar thermal collector area was doubled due to the findings of WP2 to meet the large heat requirements of the CHEST system.
- **Installed PV peak power**: In contrast to the previous work, the installed PV peak power was varied in T4.3 (both for Ispaster 2.0 and Ispaster Island case). For Ispaster 2.0 case, an increase of the installed PV power has only smaller impact because of the limited size of the electrical energy storage system. But for achieving electrical self-sufficiency in Ispaster Island case, an increase of the installed PV peak power leads to considerable reductions of the storage sizes as is shown in Chapter 5.2.3 of this deliverable.

Concerning the simulative and economic analysis of CHEST, it can be added that in WP6, there is ongoing work on identifying the technological and economic potential of CHEST using EnergyPLAN software. However, in contrast to the consideration of specific case studies, this analysis is done on a national level.

A further relation is given between T4.3 and T6.5 dealing with the development of the CHEST public tool. This is an online tool that provides the user with information on the feasibility and impact of the implementation of a CHEST system into an energy system according to the user´s specifications. The most important KPIs that were defined in T4.3 are calculated in the online tool and made available to the user in a short report.

2. Definition of key performance indicators

2.1. General definitions

Chapter 2 deals with the definition of key performance indicators (KPIs) that describe and assess the performance of the CHEST system and its components from a technical, operational, energetic, environmental and economic point of view. The KPIs are used in Chapter 5 and 6 of this deliverable to give a techno-economic assessment of the CHEST system in the different case studies considered in T4.3. Furthermore, the KPIs will be used for the CHEST public tool that will be developed in T6.5. Based on the inputs of the user, the CHEST public tool will calculate the KPIs and provide them to the user showing the feasibility and the performance of the CHEST system that can be expected when implementing a CHEST system into the user-specified energy system.

Before the KPIs of the different groups are defined in Chapters 2.2 to 2.6, this section 2.1 provides explanations and clarifications concerning some essential parameters of the CHEST system so that their meaning and their dimensions (units) are clear for the reader of this document.

2.1.1. Nominal electric HP power [MW_{el}]

This is the maximum electric power in MW that the heat pump can take up when operating under nominal conditions, i.e. in permanent operation. In partial load operation, the electric power taken up by the heat pump is less than the nominal power.

2.1.2. Nominal electric ORC power [MW_{el}]

This is the maximum electric power in MW that the ORC can generate when operating under nominal conditions, i.e. in permanent operation. In partial load operation, the electric power generated by the ORC is less than the nominal power.

2.1.3. Capacity of latent heat storage [MWh_{th}]

The capacity of the latent heat storage is given by the mass of PCM [kg] in the storage, multiplied by the specific heat of fusion [kJ/kg] of the PCM. The latent heat storage is completely discharged (SoC = 0 %) when the whole PCM is in a solid state. The latent heat storage is completely charged (SoC = 100 %) when the whole PCM is in a liquid state.

2.1.4. Capacity of sensible heat storages (SHS/LTTES) [MWh_{th}]

The capacity of sensible heat storage is given by the mass of the fluid (water) in the storage, multiplied by the specific heat capacity of the fluid and the temperature difference of its operation.

For the sensible heat storage (SHS) as part of the HTTES, formed by the two water tanks HTWT and LTWT, the definition of the storage capacity and the state of charge (SoC) via the upper and lower temperature limit does not directly apply here, because their tank temperature is always kept constant. Instead, fluid is sent from one of the tanks to the other, while either taking up heat from the heat pump circuit or delivering heat to the ORC circuit. That is why in this case, the state of charge is defined by the fluid level in the respective tank. When the complete amount of water is located in the LTWT and none of the fluid is located in the HTWT, then the sensible part of the HTTES is completely discharged (SoC = 0 %). Vice versa, when the complete amount of water is located in the HTWT and none of the fluid is located in the LTWT, then the sensible part of the HTTES is completely charged (SoC = 100 %). The capacity of the sensible part of the HTTES is defined by the mass of water in the two tanks, the specific heat capacity of water and the temperature levels of the two tanks HTWT and LTWT. These temperature levels are different for the two case studies, because they are dependent on the refrigerant and PCM.

For the LTTES as a non-pressurized (seasonal) thermal energy storage, a typical upper temperature limit of operation is 95 °C. This means that when the whole water in the storage has a temperature of 95 °C, then the LTTES is completely charged (SoC = 100 %). The lower temperature for the definition of a completely discharged storage (SoC = 0 %) actually depends on the specific boundary conditions of the case study, because it is a question of which temperature level is still useful. For the analyses carried out in T4.3, no LTTES was considered for the Aalborg case study and at least no LTTES in its original sense (as a non-pressurized thermal storage and coupled with both HP and ORC) was considered for the Ispaster case study (see explanations in Chapter 1.4). Thus, the LTTES storage capacity is not relevant for the results presented here, but in principle, it must be considered if a LTTES is used.

2.1.5. Clean-up thermal energy [MWh_{th}]

An even state of charge in the latent and sensible part of the HTTES is desired for optimum use of the HTTES. Because otherwise, one of the storage parts can block the operation of the heat pump or the ORC, as this storage part is completely charged or discharged while the other storage part is not.

To ensure an even state of charge of the two parts of the HTTES, heat can be removed from the latent or sensible part of the HTTES. When excessive latent heat is present (i.e. the SoC of the latent part of the HTTES is higher than SoC of the sensible part), this excessive heat will be removed from the latent part of the HTTES. On the contrary, when excessive sensible heat is present (i.e. the SoC of the sensible part of the HTTES is higher than SoC of the latent part), then, this excessive heat will be removed from the sensible part of the HTTES.

This removed excessive heat is called “clean-up thermal energy”. The removed heat does not get lost, but can, for instance, be fed into the LTTES. Details about the clean-up mechanisms can be found in Deliverable 2.2 and Deliverable 2.3.

In the WP4 TRNSYS model, no such clean-up mechanism was implemented due to the different nature of the model compared to WP2. Therefore, the clean-up thermal energy is not relevant for the results presented in T4.3, but in principle, it must be considered if such a mechanism is used. Instead of a clean-up mechanism for the HTTES, a recharge for its sensible part (SHS) was implemented in the WP4 model, see paragraph 2.1.6.

2.1.6. Recharge thermal energy [MWh_{th}]

The WP4 model is different from the WP2 model concerning the modelling of the HTTES. First of all, the HTTES is modelled much more in detail in the WP4 model, e.g. through the consideration of the heat transfer between refrigerant and PCM in the LHS and through the two tank model of the SHS. Furthermore, the general approach for the HTTES sizing and control of its energy input and output is focused on the fact that the energy input into the PCM storage has to be the same as its energy output on the yearly basis, cf. Deliverable 4.4.

As a consequence of this and since the CHEST system is a net heat consumer, the SoC of the SHS becomes smaller and smaller over the year. Depending on the choice of refrigerant and PCM, the HP evaporation temperature level and the ORC condensation temperature level, as well as the HP and ORC operating hours, this negative heat balance of the SHS can be more or less pronounced. The eventual problem for the simulation work in WP4 is that, once the SHS becomes completely discharged, the SHS limits the ORC operation for the rest of the year. To prevent this, the SHS could be dimensioned big enough, but this is not realistic as regards to investment costs and space demand. Therefore, the SHS must be recharged from time to time, i.e. heat is added to the SHS, which increases its SoC again.

Like in a normal charging operation of the HTTES, water is pumped from the LTWT to the HTWT and the temperature of this water is increased from LTWT temperature level to HTWT temperature level in a heat exchanger. However, the heat that is required for this does not come from the HP circuit (via the subcooler) now, but needs to be taken from an external heat source. In the Aalborg case study, this is preferably excess heat. If there is not enough excess heat available, the required recharge thermal energy is provided by gas boilers. In the Ispaster case study, the required recharge thermal energy is exclusively provided by the biomass boiler.

2.2. Performance of the CHEST system and of its main components

2.2.1. COP of the heat pump $\boldsymbol{COP_{HP}}$ [-]

The COP of the heat pump is the sum of the thermal energy delivered during the simulation period (one year) to the latent + sensible part of the HTTES by the heat pump, divided by the electricity required by the heat pump. Furthermore, the effort for e.g. pumps and for the control of the HP operation has to be included. In the WP4 TRNSYS model, this miscellaneous electricity required for the heat pump operation is given by the electricity demand of the water pump, which pumps water from the LTWT to the HTWT during HP operation. The COP is calculated by:

$$COP_{HP} = \frac{Q_{HTTES,in}}{W_{el,HP,tot}} = \frac{Q_{HTTES,LHS,in} + Q_{HTTES,SHS,in}}{W_{el,HP,comp} + W_{el,HP,misc}}$$

With:

- Thermal energy delivered to the latent + sensible part of the HTTES by the heat pump $Q_{HTTES,in}$ [MWh]
- Total electricity required for the heat pump operation $W_{el,HP,tot}$ [MWh]
- Thermal energy delivered to the latent part of the HTTES by the heat pump $Q_{HTTES,LHS,in}$ [MWh]
- Thermal energy delivered to the sensible part of the HTTES by the heat pump $Q_{HTTES,SHS,in}$ [MWh]
- Electricity required for the compressor of the heat pump $W_{el,HP,comp}$ [MWh]
- Miscellaneous electricity required for heat pump operation $W_{el,HP,misc}$ [MWh]

2.2.2. ORC efficiency $\boldsymbol{\eta_{ORC}}$ [%]

The ORC efficiency is the electricity generated by the ORC, divided by the thermal energy taken from the latent + sensible part of the HTTES by the ORC. Furthermore, the effort for e.g. pumps and control of the ORC operation has to be included. In the WP4 TRNSYS model, this miscellaneous electricity required for the ORC operation is composed of two parts: (1) the electricity demand of the water pump, which pumps water from the HTWT to the LTWT during ORC operation and (2) the electricity demand of the condensate pump in the ORC circuit.

$$\eta_{ORC} = \frac{W_{el,ORC,net}}{Q_{HTTES,out}} = \frac{W_{el,ORC,exp} - W_{el,ORC,misc}}{Q_{HTTES,LHS,out} + Q_{HTTES,SHS,out}}$$

With:

- Net electricity generated by the ORC $W_{el,ORC,net}$ [MWh]
- Thermal energy taken from the latent + sensible part of the HTTES by the ORC $Q_{HTTES,out}$ [MWh]
- Electricity generated by the expander of the ORC $W_{el,ORC,exp}$ [MWh]
- Miscellaneous electricity required for ORC operation $W_{el,ORC,misc}$ [MWh]
- Thermal energy taken from the latent part of the HTTES by the ORC $Q_{HTTES,LHS,out}$ [MWh]
- Thermal energy taken from the sensible part of the HTTES by the ORC $Q_{HTTES,SHS,out}$ [MWh]

2.2.3. Efficiency of the HTTES η_{HTTES} [%]

The efficiency of the HTTES is the ratio of the thermal energy taken from the HTTES by the ORC and the thermal energy delivered to the HTTES by the HP. As the state of charge (SoC) of the HTTES can vary between the beginning and the end of the simulation/evaluation period (one year), the change of energy content of the HTTES ΔQ_{HTTES} has to be considered in this definition as well. For all T4.3 simulations, the SoC of the HTTES was 50 % at the beginning of the simulation period. In case that the SoC is > 50 % at the end of the simulation period, the change of energy content is positive while it is negative in case that the SoC is < 50 % at the end of the simulation period. As regards to the definition of the SoC of the latent and sensible part of the HTTES, please refer to Chapters 2.1.3 and 2.1.4 of this document.

The efficiency of the HTTES can also be calculated by subtracting the heat losses of the HTTES from the thermal energy delivered to the HTTES by the HP and dividing this by this thermal energy delivered to the HTTES by the HP. The HTTES efficiencies can also be calculated separately for each of the two storage parts.

If there is a removal of clean-up thermal energy from the latent or sensible part of the HTTES (cf. Chapter 2.1.5) or if a recharge mechanism is applied (cf. Chapter 2.1.6), this heat should be included in the calculation of the efficiency of the HTTES or its part, respectively. For this Task 4.3, there is no clean-up strategy for the HTTES applied, but a recharge mechanism for the SHS. In this case, the heat into the SHS consists of two parts: the thermal energy delivered to the SHS by the heat pump and the thermal energy delivered to the SHS during recharge by external heat.

$$\eta_{HTTES} = \frac{Q_{HTTES,out} + \Delta Q_{HTTES}}{Q_{HTTES,in}} = 1 - \frac{Q_{HTTES,loss}}{Q_{HTTES,in}}$$

$$\eta_{HTTES,LHS} = \frac{Q_{HTTES,LHS,out} + \Delta Q_{HTTES,LHS}}{Q_{HTTES,LHS,in}} = 1 - \frac{Q_{HTTES,LHS,loss}}{Q_{HTTES,LHS,in}}$$

$$\eta_{HTTES,SHS} = \frac{Q_{HTTES,SHS,out} + \Delta Q_{HTTES,SHS}}{Q_{HTTES,SHS,in,HP} + Q_{HTTES,SHS,in,Rch}} = 1 - \frac{Q_{HTTES,SHS,loss}}{Q_{HTTES,SHS,in,HP} + Q_{HTTES,SHS,in,Rch}}$$

With:

- Thermal energy delivered to the latent part of the HTTES by the HP $Q_{HTTES,LHS,in}$ [MWh]
- Thermal energy delivered to the sensible part of the HTTES by the HP $Q_{HTTES,SHS,in,HP}$ [MWh]
- Thermal energy delivered to the sensible part of the HTTES by the recharge mechanism $Q_{HTTES,SHS,in,Rch}$ [MWh]
- Total thermal energy delivered to the latent + sensible part of the HTTES by the HP + recharge mechanism $Q_{HTTES,in}$ [MWh]
- Thermal energy taken from the latent part of the HTTES by the ORC $Q_{HTTES,LHS,out}$ [MWh]
- Thermal energy taken from the sensible part of the HTTES by the ORC $Q_{HTTES,SHS,out}$ [MWh]
- Thermal energy taken from the latent + sensible part of the HTTES by the ORC $Q_{HTTES,out}$ [MWh]
- Thermal losses of the latent part of the HTTES $Q_{HTTES,LHS,loss}$ [MWh]
- Thermal losses of the sensible part of the HTTES $Q_{HTTES,SHS,loss}$ [MWh], this is the sum of the thermal losses of the HTWT and the LTWT
- Thermal losses of the latent + sensible part of the HTTES $Q_{HTTES,loss}$ [MWh]
- Difference of the energy content of the latent part of the HTTES between beginning and end of the evaluation period $\Delta Q_{HTTES,LHS}$ [MWh]
- Difference of the energy content of the sensible part of the HTTES between beginning and end of the evaluation period $\Delta Q_{HTTES,SHS}$ [MWh]
- Difference of the energy content of the latent + sensible part of the HTTES between beginning and end of the evaluation period ΔQ_{HTTES} [MWh]

2.2.4. Efficiency of the LTTES η_{LTTES} [%]

Similar to the efficiency of the HTTES, the efficiency of the LTTES describes the ratio of the thermal energy taken from the LTTES and the thermal energy delivered to the LTTES, with possible changes in the energy content of the storage ΔQ_{LTTES} considered.

Also here, the efficiency of the LTTES can be calculated via the thermal losses of the storage.

$$\eta_{LTTES} = \frac{Q_{LTTES,out} + \Delta Q_{LTTES}}{Q_{LTTES,in}} = 1 - \frac{Q_{LTTES,loss}}{Q_{LTTES,in}}$$

With:

- Thermal energy delivered to the LTTES $Q_{LTTES,in}$ [MWh]
- Thermal energy taken from the LTTES $Q_{LTTES,out}$ [MWh]

- Difference of the energy content of the LTTES between beginning and end of the evaluation period ΔQ_{LTTES} [MWh]
- Thermal losses of the LTTES $Q_{LTTES,loss}$ [MWh]

Again, the difference of the energy content of the LTTES can be positive or negative, depending on whether the energy content has increased or decreased when comparing the end and the beginning of the evaluation period (one year). If heat is supplied to the LTTES by clean-up thermal energy coming from the HTTES, this must be included in the term $Q_{LTTES,in}$.

Here in Task 4.3, this KPI Efficiency of the LTTES is not relevant, because there was no LTTES present in both case studies analyzed (see explanations in Chapter 1.4).

2.2.5. P2P ratio of the CHEST system $\boldsymbol{P2P}$ [%]

The P2P ratio is defined as the ratio of the net electricity generated by the ORC and the total electricity consumed by the HP operation. As described more in detail in Chapters 2.2.1 and 2.2.2, the miscellaneous electricity required for HP and ORC operation have to be considered in this calculation.

$$P2P\ ratio = \frac{W_{el,ORC,net}}{W_{el,HP,tot}} = \frac{W_{el,ORC,exp} - W_{el,ORC,misc}}{W_{el,HP,comp} + W_{el,HP,misc}}$$

With:

- Net electricity generated by the ORC $W_{el,ORC,net}$ [MWh]
- Total electricity required for the heat pump operation $W_{el,HP,tot}$ [MWh]
- Electricity generated by the expander of the ORC $W_{el,ORC,exp}$ [MWh]
- Electricity required for the compressor of the heat pump $W_{el,HP,comp}$ [MWh]
- Miscellaneous electricity required for ORC operation $W_{el,ORC,misc}$ [MWh]
- Miscellaneous electricity required for heat pump operation $W_{el,HP,misc}$ [MWh]

2.2.6. Electrical efficiency of the CHEST system $\boldsymbol{\eta_{CHEST,el}}$ [%]

The electrical efficiency of the CHEST system is defined by the ratio of the useful electrical energy delivered by the CHEST system and the total energy input (electrical + thermal) into the CHEST system. The change of energy content of the HTTES has to be considered as well.

$$\eta_{CHEST,el} = \frac{W_{el,ORC,exp} - W_{el,ORC,misc}}{\left(W_{el,HP,comp} + W_{el,HP,misc}\right) + \Delta Q_{HTTES} + Q_{heatsource}}$$

The term $Q_{heatsource}$ is the thermal energy input into the CHEST system and it comprises three parts: (1) the thermal energy that is needed at the HP evaporator, (2) the recharge thermal energy that is delivered to the SHS by an external heat source, and (3) the thermal energy that is required for the compensation of the thermal losses of the HTTES (which in its turn is composed of the thermal losses of the LHS and the SHS).

$$Q_{heatsource} = Q_{HP,evap} + Q_{SHS,rech} + Q_{HTTES,loss}$$

Note: in the WP4 TRNSYS model, only the thermal losses of the SHS are compensated by an external heat source (excess heat, gas or biomass boiler). The thermal losses of the LHS are not compensated; heat is supplied to the LHS only through the HP operation. Therefore, here in T4.3, the term $Q_{HTTES,loss}$ only comprises the thermal losses of the SHS. But indirectly, these thermal losses of the LHS do play a role for the electrical efficiency, because they affect the energy content of the LHS and thus of the whole HTTES.

With:

- Electricity generated by the expander of the ORC $W_{el,ORC,exp}$ [MWh]
- Miscellaneous electricity required for ORC operation $W_{el,ORC,misc}$ [MWh]
- Electricity required for the compressor of the heat pump $W_{el,HP,comp}$ [MWh]
- Miscellaneous electricity required for heat pump operation $W_{el,HP,misc}$ [MWh]
- Difference of the energy content of the latent + sensible part of the HTTES between beginning and end of the evaluation period ΔQ_{HTTES} [MWh]
- Thermal energy delivered to the CHEST system by RES + conventional heat sources $Q_{heatsource}$ [MWh]
- Thermal energy that is supplied to the evaporator of the HP in order to operate the HP of the CHEST system $Q_{HP,evap}$
- Thermal energy that is supplied to the SHS from an external source (i.e. not via the HP operation) in order to increase the SoC of the SHS $Q_{SHS,rech}$
- Thermal losses of the latent + sensible part of the HTTES $Q_{HTTES,loss}$ [MWh]

2.2.7. Thermal efficiency of the CHEST system $\eta_{CHEST,th}$ [%]

The thermal efficiency of the CHEST system is defined by the ratio of the useful thermal energy delivered by the CHEST system and the total energy input (electrical + thermal) into the CHEST system. The change of energy content of the HTTES has to be considered as well. In principle, this change of energy content of the HTTES could also be seen as a benefit of useful thermal energy (if it is positive) or a reduction of useful thermal energy (if it is negative) and therefore be written above the fraction line here. However, this amount of heat will not directly come out of the CHEST system, but will be used to generate electricity and heat (at variable portions, dependent on the ORC conditions) during the operation of the ORC at a later point of time. Therefore, and following the definition in Chapter 2.2.6, it was decided to write this term below the fraction line, where there are anyway electrical and thermal energy summed up to form the total energy input into the CHEST system.

$$\eta_{CHEST,th} = \frac{Q_{ORC,DH}}{(W_{el,HP,comp} + W_{el,HP,misc}) + \Delta Q_{HTTES} + Q_{heatsource}}$$

With:

- Thermal energy supplied from the CHEST system to the DH network at the ORC condenser $Q_{ORC,DH}$ [MWh]
- Electricity required for the compressor of the heat pump $W_{el,HP,comp}$ [MWh]
- Miscellaneous electricity required for heat pump operation $W_{el,HP,misc}$ [MWh]
- Difference of the energy content of the latent + sensible part of the HTTES between beginning and end of the evaluation period ΔQ_{HTTES} [MWh]
- Thermal energy delivered to the CHEST system by RES + conventional heat sources $Q_{heatsource}$ [MWh]

For the calculation of the term $Q_{heatsource}$ see above Chapter 2.2.6.

2.2.8. Overall energy efficiency of the CHEST system $\eta_{CHEST,el+th}$ [%]

The overall energy efficiency of the CHEST system is defined by the ratio of the useful energy (electrical + thermal) delivered by the CHEST system and the total energy input (electrical + thermal) into the CHEST system. This overall energy efficiency is the sum of the electrical and thermal efficiency.

$$\eta_{CHEST,el+th} = \frac{(W_{el,ORC,exp} - W_{el,ORC,misc}) + Q_{ORC,DH}}{(W_{el,HP,comp} + W_{el,HP,misc}) + \Delta Q_{HTTES} + Q_{heatsource}} = \eta_{CHEST,el} + \eta_{CHEST,th}$$

With:

- Electricity generated by the expander of the ORC $W_{el,ORC,exp}$ [MWh]
- Electricity required for the compressor of the heat pump $W_{el,HP,comp}$ [MWh]
- Miscellaneous electricity required for heat pump operation $W_{el,HP,misc}$ [MWh]
- Miscellaneous electricity required for ORC operation $W_{el,ORC,misc}$ [MWh]
- Thermal energy supplied from the CHEST system to the DH network at the ORC condenser $Q_{ORC,DH}$ [MWh]
- Difference of the energy content of the latent + sensible part of the HTTES between beginning and end of the evaluation period ΔQ_{HTTES} [MWh]

- Thermal energy delivered to the CHEST system by RES + conventional heat sources $Q_{heatsource}$ [MWh]

For the calculation of the term $Q_{heatsource}$ see above Chapter 2.2.6.

2.3. Operational performance indicators

2.3.1. Full-load hours of HP and ORC $\boldsymbol{\tau_{fullload,HP/ORC}}$ [h]

The full-load hours of the HP are defined by the ratio of the electricity consumed by the compressor of the heat pump and the nominal electric power of the heat pump. For the ORC, the full-load hours are defined by the ratio of the electricity generated by the expander of the ORC and the nominal electric power of the ORC.

$$\tau_{fullload,HP} = \frac{W_{el,HP,comp}}{W_{el,HP,nom}}$$

$$\tau_{fullload,ORC} = \frac{W_{el,ORC,exp}}{W_{el,ORC,nom}}$$

With:

- Electricity required for the compressor of the heat pump $W_{el,HP,comp}$ [MWh]
- Electricity generated by the expander of the ORC $W_{el,ORC,exp}$ [MWh]
- Nominal electric power of the heat pump $P_{el,HP,nom}$ [MW]
- Nominal electric power of the ORC $P_{el,ORC,nom}$ [MW]

2.3.2. Time in each operation mode [h]

It can be interesting to know how many hours per year the CHEST system is in each of the operation modes "Charging", "Discharging" and "Idleness" as well as how many hours per year a recharge of the SHS needs to be done. The time in charging and discharging mode can also be compared to the time in which there is a charging or discharging demand. A charging or discharging demand for the CHEST system is either given by the availability of acceptable electricity prices in the electricity grid (Aalborg case study) or by the availability of electricity surplus or deficit (Ispaster case study). If there is a point of time with charging or discharging demand, but without HP/ORC operation, it is interesting to know, what was the limiting factor for this. The HP operation can be limited by a completely charged LHS or SHS or by the non-availability of heat at the HP evaporator. As was explained in Chapter 1.4, a limitation of the HP operation by a non-availability of heat only occurs in Ispaster case study. In Aalborg case study, if there is not enough excess heat available, the HP heat demand is covered by gas-fired backup heating. The ORC operation can be limited by a completely discharged LHS or SHS. The following scheme gives a better comprehension of the aforementioned times of interest:

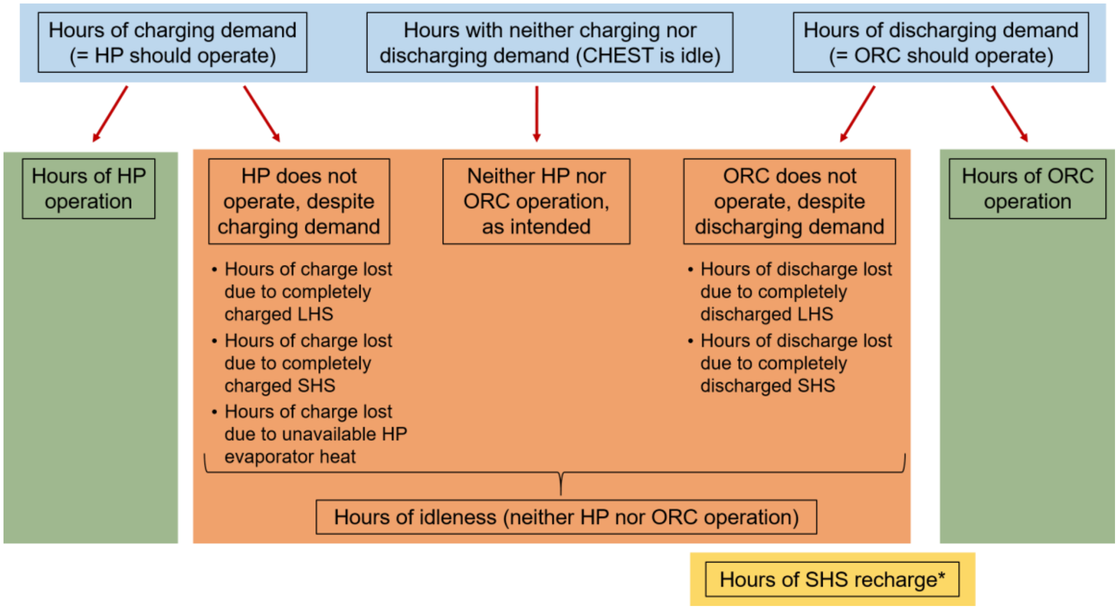

Figure 1: Overview of demand and operating times of the CHEST system.

*Normally, the SHS recharge is supposed to happen during CHEST idle times. However, this might be not sufficient, because there are too few idle times or they do not match with the demand times for SHS recharge. In this case, SHS recharge could also be done during ORC operation times. Details to the SHS recharge as it was implemented in the WP4 TRNSYS model can be found in Chapter 4.2.

All these parameters shown above in Figure 1 are a direct output of the WP4 TRNSYS model.

2.3.3. Response time τ_{resp} [min]

The response time of discharge is the period of time between the moment in which the discharge request is issued and the moment the system reaches the requested power, i.e. the ORC can deliver this power. Accordingly, the response time of charge is the interval of time between the moment in which the charge request is issued and the moment the heat pump can consume the requested power.

This is not a direct output of the TRNSYS model nor can it be calculated by other outputs of the model, because up to now, there is not sufficient information on this. However, this KPI is presented here, because it is an important operational performance indicator for the ability of the CHEST system to participate in the different electricity markets. When the first-of-its-kind prototype of the CHEST system is built-up and tested in the laboratory (WP5), more information can be given on the response time of the CHEST system.

2.4. Energetic assessment of the CHEST system

2.4.1. Savings of electricity $S_{el,fin}$ [MWh$_{el}$]

Compared to a situation without CHEST system or compared to another reference energy system, respectively, there is a saving of electricity (on a final energy basis). This saving originates from the reduction of the electricity deficit (of the district or the national electricity grid considered).

In Ispaster case study, for instance, the CHEST system takes up excess PV electricity and generates electricity in times of electricity deficit, which leads to a reduction of electricity that needs to be purchased from the DSO. So, the saving of electricity here is given by this reduction of electricity import. It is equal to the net electricity generation of the CHEST system, i.e. of the ORC. The savings of electricity can also be calculated in comparison to the reference energy system with battery storage here.

For the Aalborg case study, the saving of electricity of the CHEST system compared to the situation without CHEST system is in principle also given by the net electricity generation of the CHEST system. However, as there is no **hourly** information about the electricity grid, i.e. as regards to electricity production by the different conventional and renewable energy sources over time, it can actually not be said, if the electricity consumed by CHEST was excess (renewable) electricity or conventionally generated electricity. In Aalborg, the interaction between CHEST and the electricity grid is solely based on electricity prices, i.e. for the CHEST system, the source of generation of the consumed electricity is not of interest.

For the calculations in this Task 4.3, it is assumed that all the electricity taken up by the CHEST system was excess electricity from renewable sources. With this assumption, the saving of electricity in Aalborg case study is also equal to the net electricity generation of the ORC like in the Ispaster case study (see above). This assumption is quite justified given (1) the high share of renewables in the Danish electricity grid of 71 % (**on an annual basis**), cf. Chapter 6.1.1, and (2) the fact that low electricity prices are actually a result of an excess of electricity in the grid, and this excess of electricity is normally due to the high electricity production from wind and/or PV.

$$S_{el,fin} = W_{el,deficit,NoCHEST} - W_{el,deficit,CHEST} = W_{el,ORC,net}$$

With:

- Electricity deficit, which has to be covered by the grid in the case without $W_{el,deficit,NoCHEST}$ and with CHEST system $W_{el,deficit,CHEST}$ [MWh]
- Net electricity generated by the ORC $W_{el,ORC,net}$ [MWh]

2.4.2. Savings of thermal energy $S_{th,fin}$ [MWh$_{th}$]

Compared to a situation without CHEST system, there might be a saving of thermal energy (on a final energy basis), particularly, in CHEST systems with low P2P ratio, low thermal losses of the HTTES and a high share of the ORC condensation heat transferred to the DH network. However, there might also be an increase of the total heat demand by the CHEST system, as it needs heat for its operation and might only partly deliver heat back into a DH system. Whether the CHEST system increases or decreases the heat demand, depends on several parameters, e.g. on the size of the CHEST system, on the ORC condensation temperature and the heat sink temperature, on the selected refrigerant/PCM combination, on the thermal losses of the HTTES.

As can be seen in the results section later, the CHEST system is in most cases a net heat consumer, i.e. it increases the total heat demand and thus, there is a negative “saving” of thermal energy.

$$S_{th,fin} = Q_{Heatdemand,NoCHEST} - Q_{Heatdemand,CHEST}$$

With:

- Heat demand in the case without $Q_{Heatdemand,NoCHEST}$ and with CHEST system $Q_{Heatdemand,CHEST}$ [MWh]

2.4.3. Savings of primary energy $S_{el+th,prim}$ [MWh]

These are the savings of energy based on primary energy, i.e. the savings of final energy have to be multiplied by the primary energy factors of the respective energy source.

For the electrical side, the primary energy factor for the electrical grid $PEF_{el,grid}$ is calculated according to the known mix of electric sources in the grid.

For the thermal side, the resulting primary energy factor $PEF_{th,tot}$ is calculated according to the known mix of heat sources used for the heat generation.

In Ispaster case study, as can be seen from the results later, the CHEST system on the one hand reduces the electricity that needs to be purchased from the grid and on the other hand increases the biomass demand. In this case, the savings of the grid electricity have to be multiplied by a primary energy factor which is representative for the Spanish electricity grid or the Basque region. On the thermal side, the increased biomass demand has to be multiplied by the primary energy factor for biomass (wood chips). The resulting sum of primary energy consumption can be a saving, i.e. the primary energy consumption is less for the CHEST system compared to the situation without CHEST system, or vice versa, can be negative, i.e. the CHEST system is disadvantageous as regards to primary energy consumption compared to the situation without CHEST system.

In the Aalborg case study, the ORC net electricity generation has to be multiplied by a primary energy factor which is representative for the Danish electricity grid or the Aalborg region. On the thermal side, the CHEST system causes an additional demand of excess heat and, dependent on the CHEST size, also a demand of heat from gas boilers. If we assume the excess heat not to be usable in case of no CHEST system, only the gas demand has to be multiplied by the primary energy factor for natural gas.

A detailed information of the primary energy factors used in T4.3 is given in Chapter 6.1.1.

$$S_{el,prim} = (W_{el,deficit,NoCHEST} - W_{el,deficit,CHEST}) * PEF_{el,grid}$$

$$S_{th,prim} = [Q_{fueldemand,NoCHEST} - Q_{fueldemand,CHEST}] * PEF_{th,tot}$$

$$S_{el+th,prim} = (W_{el,deficit,NoCHEST} - W_{el,deficit,CHEST}) * PEF_{el} + (Q_{fueldemand,NoCHEST} - Q_{fueldemand,CHEST}) * PEF_{th,tot}$$

$$PEF_{el,grid} = \sum_{i}^{m} PEF_{el,source,i} * \psi_{el,source,i}$$

$$PEF_{th,tot} = \sum_{i}^{n} PEF_{th,source,i} * \psi_{th,source,i}$$

With:

- Electricity deficit, which has to be covered by the grid in the case without $W_{el,deficit,NoCHEST}$ and with CHEST system $W_{el,deficit,CHEST}$ [MWh]
- Fuel demand (natural gas, biomass) in the case without $Q_{fueldemand,NoCHEST}$ and with CHEST system $Q_{fueldemand,CHEST}$ [MWh]
- Resulting primary energy factor for electricity in the grid $PEF_{el,grid}$ [-]
- Primary energy factor for the respective electric source i in the grid $PEF_{el,source,i}$ [-]
- Share of the electric source i in the grid $\psi_{el,source,i}$ [-]
- Number of electric sources in the grid m [-]
- Resulting primary energy factor for the (conventional) backup heating $PEF_{th,tot}$ [-]
- Primary energy factor for the respective heat source i $PEF_{th,source,i}$ [-]
- Share of the heat source i in the (conventional) backup heat $\psi_{th,source,i}$ [-]
- Number of heat sources in the (conventional) backup heat n [-]

Note: The primary energy factors PEF used here consider only the **non-renewable share** of primary energy.

2.4.4. Energetic payback time $\tau_{payback,en}$ [a]

The operation of the CHEST system should result in primary energy savings compared to a scenario without CHEST system (see above). On the other hand, primary energy is required for the production and installation of the CHEST system. The energetic payback time is defined as the time until the primary energy savings of the CHEST system have become equal to the primary energy which was required to produce and install the CHEST system.

In a broader sense, also the removal phase of the CHEST system has to be considered.

$$\tau_{payback,en,P} = \frac{CED_P}{S_{el+th,prim}}$$

$$\tau_{payback,en,P+R} = \frac{CED_P + CED_R}{S_{el+th,prim}}$$

With:

- Primary energy savings of the CHEST system compared to the situation without CHEST system or compared to another reference energy system $S_{el+th,prim}$ [MWh/a]
- Cumulative energy demand for the production and installation CED_P and for the removal of the CHEST system CED_R [MWh]

Note: As was stated in Chapter 1.4, only preliminary and approximate CED values could be used in T4.3 (and they also only apply to the production phase of the CHEST system´s components), because this will be analyzed more in detail in T4.6.

2.4.5. Reduction of peak deficit power $\boldsymbol{RedP_{el,peak}}$ [MWel]

A CHEST system reduces the electricity deficit not only with regards to energy but also with regards to power. This can result in an ease of the electricity grid and in a reduction of the provision of conventional power. The reduction of peak power is calculated by the difference of the maximum electricity deficit power between the case with and without CHEST system.

Furthermore, the reduction of peak deficit power could be part of the business model, because the fixed costs for the connection to the electricity grid depend on the maximum available power. In Task 4.3, this KPI is only relevant for Ispaster, but no economic benefit was assumed for this (due to lacking information about the contract with the DSO and as it is thought to be a negligible benefit here). For Aalborg, it is in principle also a relevant KPI, because the CHEST system contributes to the ease of the national electricity grid. However, no electricity supply and demand profiles are considered in Aalborg case study, so there is no further information about the grid here to calculate this KPI for Aalborg case study.

$$RedP_{el,peak} = P_{el,deficit,max,NoCHEST} - P_{el,deficit,max,CHEST}$$

With:

- Maximum electricity deficit power, which has to be covered by the grid in the case without $P_{el,deficit,max,NoCHEST}$ and with CHEST system $P_{el,deficit,max,CHEST}$ [MW]

2.4.6. Curtailment reduction $\boldsymbol{RedW_{surplus}}$ [MWh$_{el}$]

The reduction of the curtailment of the renewable power source is calculated by the difference of the electricity surplus in the cases with and without CHEST system.

In Ispaster case study, the CHEST system leads to a curtailment reduction of excess PV electricity. For Aalborg case study, given the abovementioned assumption that all the electricity taken up by the CHEST system is excess renewable electricity, the CHEST system leads to a curtailment reduction of the renewables in general.

$$RedW_{surplus} = W_{el,surplus,NoCHEST} - W_{el,surplus,CHEST}$$

With:

- Electricity surplus in the case without $W_{el,surplus,NoCHEST}$ and with CHEST system $W_{el,surplus,CHEST}$ [MWh]

2.5. Environmental assessment of the CHEST system

2.5.1. Savings of CO_2 emissions E_{CO2} [t]

The savings of CO_2 emissions can be calculated by multiplying the savings of final energy (see Chapters 2.4.1 and 2.4.2) with the relevant CO_2 emission factors, dependent on the energy source. These CO_2 emission factors consider the global warming potential over a certain time (in this case, 100 years, i.e. GWP_{100}) and they are expressed in t of CO_2 equivalent per MWh of final energy. A detailed information of the CO_2 emission factors used in T4.3 is given in Chapter 6.1.1.

$$E_{CO2} = \left(W_{el,deficit,NoCHEST} - W_{el,deficit,CHEST}\right) * CEF_{el,grid} + \left(Q_{Heatdemand,NoCHEST} - Q_{Heatdemand,CHEST}\right) * CEF_{th,tot}$$

$$CEF_{el,grid} = \sum_{i}^{m} CEF_{el,source,i} * \psi_{el,source,i}$$

$$CEF_{th,tot} = \sum_{i}^{n} CEF_{th,source,i} * \psi_{th,source,i}$$

With:

- Electricity deficit, which has to be covered by the grid in the case without $W_{el,deficit,NoCHEST}$ and with CHEST system $W_{el,deficit,CHEST}$ [MWh]
- Fuel demand (natural gas, biomass) in the case without $Q_{fueldemand,NoCHEST}$ and with CHEST system $Q_{fueldemand,CHEST}$ [MWh]
- Resulting CO_2 emission factor for electricity in the grid $CEF_{el,grid}$ [t/MWh]
- CO_2 emission factor for the respective electric source i $CEF_{el,source,i}$ [t/MWh]
- Share of the electric source i in the grid $\psi_{el,source,i}$ [-]
- Number of electric sources in the grid m [-]
- Resulting CO_2 emission factor for the (conventional) backup heating $CEF_{th,tot}$ [t/MWh]
- CO_2 emission factor for the respective thermal source i $CEF_{th,source,i}$ [t/MWh]
- Share of the thermal source i in the (conventional) backup heat $\psi_{th,source,i}$ [-]
- Number of thermal sources in the (conventional) backup heat n [-]

2.5.2. CO_2 payback time $\tau_{payback,CO2}$ [a]

The operation of the CHEST system can result in CO_2 savings compared to the reference scenario without CHEST system (see above). On the other hand, CO_2 is emitted during the production and installation of the CHEST system. The CO_2 payback time is defined as the time until the CO_2 savings of the CHEST system have become equal to the CO_2 emitted during the production and installation of the CHEST system. As mentioned in Chapter 2.5.1 for the CEF values, also the GWF values consider a period of 100 years for the global warming potential (GWP_{100}) that arises from the production and installation of the CHEST system.

In a broader sense, also the removal phase of the CHEST system has to be considered.

$$\tau_{payback,CO2,P} = \frac{GWF_P}{E_{CO2}}$$

$$\tau_{payback,CO2,P+R} = \frac{GWF_P + GWF_R}{E_{CO2}}$$

With:

- Savings of CO_2 emissions E_{CO2} [t/a]
- Global warming factor (equivalent CO_2 emissions) of the production and installation GWF_P and of the removal of the CHEST system GWF_R [t]

Note: As was stated in Chapter 1.4, only preliminary and approximate GWF values could be used in T4.3 (and they also only apply to the production phase of the CHEST system´s components), because this will be analyzed more in detail in T4.6.

2.6. Economic assessment of the CHEST system

2.6.1. Investment costs (CAPEX) [€]

The investment costs of the CHEST system comprise the costs for the production of its components and the costs for the installation of the CHEST system, which include, for instance, construction measures, hydraulics, measuring and control devices, etc. In this Task 4.3, the investment costs of the CHEST system were calculated according to the component costs given in Deliverable 6.2. For some scenarios, an investment cost reduction for HP and ORC under the assumption that both will form one single component in the future was assumed, see Chapter 6.1.2 for more details.

2.6.2. Operational costs (OPEX) [€/a]

The operational costs encompass energy costs (electricity that still has to be bought from the grid, backup boiler heating), costs for the CHEST system operation (O&M costs given by, for instance, personnel costs and maintenance costs) and financial costs (depreciation, interests). The calculation of the O&M costs of the CHEST system and the assumptions and boundary conditions for the calculation of the financial costs are detailed in Chapter 6.1.2. The energy costs for the respective source of energy are given in Chapter 3.1.3 for Aalborg case study and in Chapter 3.2.3 for Ispaster case study, respectively.

2.6.3. Turnover [€/a]

The CHEST system operator can earn money with the sale of electricity, heat and/or making available positive/negative electrical power. Depending on the use case, the CHEST system can also be used for the reduction of costs, for instance, through savings of electricity and heat or through savings of CO_2 payments.

Depending on the country and the concrete business model, turnover is reduced by different taxes and fees.

2.6.4. Profit/loss [€/a]

The difference between turnover and operational costs results in the annual profit or loss of the CHEST system operation:

$$Profit/loss = Turnover - OPEX$$

2.6.5. Return on Investment (ROI) [-]

This KPI is a result of a dynamic economic calculation. Generally, this KPI is given by:

$$ROI = \frac{Profit}{Invested\ capital}$$

2.6.6. Net present value (NPV) [€]

This KPI is a result of a dynamic economic calculation. Generally, this KPI is given by:

$$NPV = \sum_{t=1}^{n} \frac{Profit_t}{(1+j)^t}$$

With:

- Current year of calculation t [-]
- Calculated profit in the current year $Profit_t$ [€/a]
- Total number of years that form the calculation period (= lifetime of the CHEST system) n [-]
- Assumed interest rate j [%]

Note: The profit of the first year includes the investment costs here. And if there are further investment costs within the calculation period (as for the battery storage due its shorter lifetime compared to the CHEST system), the NPV also includes these further investment costs at the point of time when they arise.

2.6.7. Internal rate of return (IRR) [%]

This KPI is a result of a dynamic economic calculation. In principle, this KPI is calculated with the same formula as for the NPV, but here, the interest rate is searched for the case that the NPV becomes 0:

$$0 = NPV = \sum_{t=1}^{n} \frac{Profit_t}{(1+IRR)^t}$$

Note: As said above for the NPV, this formula also includes the initial and all further investment costs at the point of time when they arise.

2.6.8. Economic payback time [a]

This KPI is a result of a dynamic economic calculation. Generally, this KPI is given by:

$$\tau_{payback,econ} = \frac{CAPEX}{Profit}$$

The detailed assumptions for the dynamic economic calculation (expected lifetimes, assumed inflation and increase of energy prices, etc.) are given in Chapter 6.1.2.

2.6.9. Levelized costs of energy (LCOE) [€/MWh]

The levelized costs of energy are expressed by the total capital expenditure of a generation plant or an energy system over its whole lifetime (or a certain calculation period) divided by the amount of energy the plant or system generated over this lifetime. The numerator considers all relevant discounted costs such as investment, operation and maintenance costs as well as fuel costs. Furthermore, possible end-of-life costs and residual values are taken into account. The denominator contains the discounted sum of the amount of energy delivered:

$$LCOE = \frac{I_0 + \sum_{t=1}^{n}\left[\frac{O\&M_t + F_t}{(1+j)^t}\right] + \frac{EOL - RV}{(1+j)^n}}{\sum_{t=1}^{n}\frac{E_t}{(1+j)^t}}$$

With:

- Current year of calculation t [-]
- Investment costs at the beginning of the lifetime I_0 [€]
- Investment costs in the current year I_t [€]
- Operation and maintenance costs in the current year $O\&M_t$ [€/a]
- Fuel costs in the current year F_t [€/a]
- End-of-life costs at the end of the lifetime EOL [€]
- Residual value at the end of the lifetime RV [€]
- Energy delivered in the current year E_t [€/a]
- Total number of years that form the calculation period (= lifetime of the CHEST system) n [-]
- Assumed interest rate j [%]

LCOE expresses the average revenues (net present value) per unit of energy generated in order to cover all costs. Due to this, LCOE presents the minimum price at which energy must be sold for a plant or system to reach break-even point.

If no end-of-life costs and residual costs are taken into account and if investment costs arise several times during the calculation period (e.g. for an energy system with batteries, since electrical energy storage devices only have a relatively short lifetime of 10 or 15 years, see Chapter 6), above equation can be written the following way:

$$LCOE = \frac{\sum_{t=1}^{n} \frac{I_t + O\&M_t + F_t}{(1+j)^t}}{\sum_{t=1}^{n} \frac{E_t}{(1+j)^t}}$$

Usually, electricity is the energy form of interest. Thus, LCOE can also be termed as levelized costs of electricity. However, also the calculation of *levelized costs of heat (LCOH)*, is possible in the same manner. CHEST systems deliver both heat and electricity; so, actually both could be taken into account. However, it depends on the type of application and related business model, which is the energy form to consider. When, for instance, CHEST participates in electricity markets to offer grid services, electrical energy storage (EES) is the main purpose and heat will rather be an additional cost factor that needs to be considered instead of a true output, since in such a case, the CHEST system very likely consumes more heat than it generates.

When it comes to energy storage technologies, such as CHEST or batteries, a similar KPI termed *levelized costs of storage (LCOS)* can be defined. Following the approach of Schmidt et al. [Schm 2019] and neglecting end-of-life costs and residual values, LCOS can be calculated by the following equation:

$$LCOS = \frac{\sum_{t=1}^{n} \frac{I_t + O\&M_t + C_{Charge,t}}{(1+j)^t}}{\sum_{t=1}^{n} \frac{E_{Discharge,t}}{(1+j)^t}}$$

With:

- Investment costs in the current year I_t [€]
- Operation and maintenance costs in the current year $O\&M_t$ [€/a]
- Costs for storage charging in the current year $C_{Charge,t}$ [€/a]
- Discharged energy in the current year by the $E_{Discharge,t}$ [MWh]

In case of CHEST, the costs for charging can comprise fuel costs required for the net heat demand of the CHEST system. On the other hand, when EES technology like CHEST or a battery participates in electricity markets, charging can also generate revenues, e.g. through payments in the regulation market or in case of negative prices in the spot market.

We should note that there exist several similar definitions for LCOE and LCOS including or excluding parameters like replacement, disposal, capacity degradation, taxes, inflation, etc. For storage applications that focus on providing power instead of energy, the above equations can also be written in terms of power to calculate the lifetime cost per unit of power.

Furthermore, it should be noted that a comparison of LCOS for different storage technologies should only be done on an application-specific basis. In principle, LCOS for storage technologies and LCOE for generation technologies can also be compared with each other. However, due to the different concepts of energy provision (electricity, heat, electrical power) and the resulting different cost calculation methods, this should be done with caution [Schm 2019]. Further details on the calculation of the LCOE in the analyses that are the subject of this report are given separately for the two case studies in the techno-economic assessment in chapter 6.

2.7. KPI importance and targets

In the following, a brief overview is given on the target values for the several KPIs presented above – where applicable and reasonable at the current point of time – in order to better assess later whether the KPI values derived from the simulation results are promising or not. As for some of the KPIs it is quite difficult to define targets at the moment, only indicative values are given.

Table 1: Overview of the KPIs and their target values.

Key performance indicator (KPI)	Target value
Performance of the CHEST system and of its main components	
COP of heat pump	3.0 for 50 °C heat source and > 130 °C heat sink temperature 6.8 for 100 °C heat source and > 130 °C heat sink temperature
ORC efficiency	12 % for > 150 °C heat source and 40 °C heat sink temperature 15.5 % for > 150 °C heat source and 15 °C heat sink temperature
Efficiency of HTTES	> 90 %, i.e. less than 10 % heat losses
Efficiency of LTTES	> 90 %, i.e. less than 10 % heat losses
P2P ratio	depends on rather electrical or thermal focus, but should be > 70 % to compete with other electrical energy storage solutions
CHEST electrical efficiency	depends on rather electrical or thermal focus, but should be > 10 % to have significant electricity output
CHEST thermal efficiency	depends on rather electrical or thermal focus, but should be > 75 % to cause as little as possible additional heat demand
CHEST overall energy efficiency	> 85 %, i.e. less than 15 % overall losses
Operational performance indicators	
Full-load hours of HP and ORC	> 1,500 h for HP and ORC each
Time in each operation option	no specific target, but hours of operation limitation of the HP and ORC by a completely charged or discharged LHS/SHS or by unavailable heat at the HP evaporator should be in the order of magnitude of some hundreds at most, not of several thousands
Response time	< 15 min for FRR participation
Energetic benefit of the CHEST system	
Savings of electricity	according to abovementioned targeted ORC full-load hours: > 1,500 MWh per MW_{el} of ORC

Savings of thermal energy	> 0, i.e. causing no additional heat demand
Savings of primary energy	depends on electricity and fuel mix of the reference energy system
Energetic payback time	< 5 a
Reduction of peak deficit power	no specific target for grid-connected systems, 100 % for island energy systems
Curtailment reduction	according to abovementioned targeted HP full-load hours: > 1,500 MWh per MW_{el} of HP
Environmental benefit of the CHEST system	
Savings of CO_2 emissions	depends on electricity and fuel mix of the reference energy system
CO_2 payback time	< 5 a
Economic assessment of the CHEST system	
Investment costs	depends on system size
Operational costs	depends on system size
Turnover	depends on system size
Profit	depends on system size
Return on investment	no specific target at the moment
Net present value	depends on system size
Internal rate of return	no specific target at the moment
Economic payback time	< 3 a

The importance of each KPI can vary from case to case or some of the KPIs might not be relevant for a specific case, respectively.

For instance, the efficiency of the LTTES does not need to be considered for both Aalborg and Ispaster case, because there is no LTTES considered. Another example are the two economic parameters return on investment (ROI) and internal rate of return (IRR): a calculation of these only makes sense if there is a payback of the investment within the lifetime of the CHEST system.

So, not all of the KPIs can and will be presented in detail in the results sections Chapter 5 and 6, but these sections will concentrate on the most important ones for the respective case study.

3. CHEST integration into the energy system

3.1. Aalborg case study

3.1.1. General information of the case study

In the Aalborg case study, the city of Aalborg in the Northern part of Jutland Peninsula in Denmark with a population of about 115,000 people is considered. The entire Aalborg Municipality has 215,000 citizens of whom nearly 75 % is currently connected to a DH network. In the reference energy system, i.e. without a CHEST system, there is a certain heat demand, which is covered by several waste and excess heat sources. This excess heat mostly comes from coal-fired power plants and industrial plants, see Chapter 6.1.1. In times where this available excess heat is lower than the heat demand of the DH network, the remaining heat comes from conventional backup heating, which is considered to be natural gas fired here. An LTTES is not taken into account here, because it has not been installed, yet, and it would also not fit regarding the HP evaporation temperature level of the CHEST system, see explanation in Chapter 1.4.

On the electricity side, there is a certain electricity demand for this part of the city connected to the DH network, and this electricity is taken from the national electricity grid. This grid electricity is partly generated by renewables, i.e. onshore and offshore wind farms and PV systems, and partly, it is generated by conventional sources (according to the current Danish electricity generators on national level). For more details, refer to Chapter 6.1.1 of this deliverable.

There are two separate companies for the heat and electricity supply side, Netselskabet N1 acting as a DSO and Aalborg Forsyning acting as the operator of the DH network. Figure 2 illustrates this in a simple form showing the role of the DSO and the role of the operator of the DH network with their purchase and sale of energy.

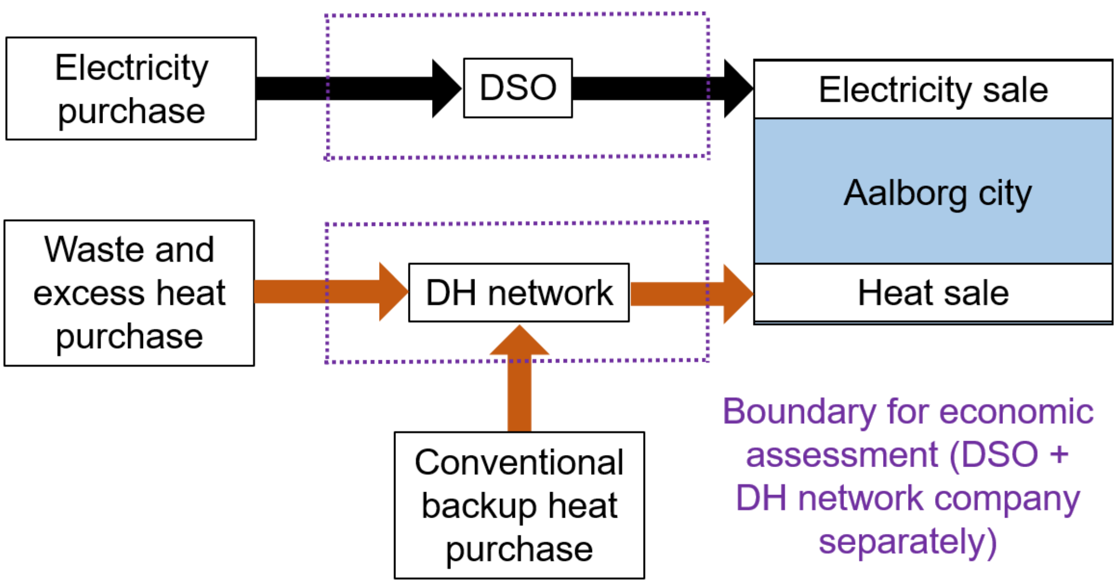

Figure 2: Purchase and sale of energy by two separate companies in the reference energy system in Aalborg case study.

Further general information about the case study of Aalborg can be found in the Deliverables 2.1, 2.2 and 4.3.

3.1.2. Role of CHEST in the Aalborg case study

Figure 3 illustrates the basic role the CHEST system plays in the Aalborg case study.

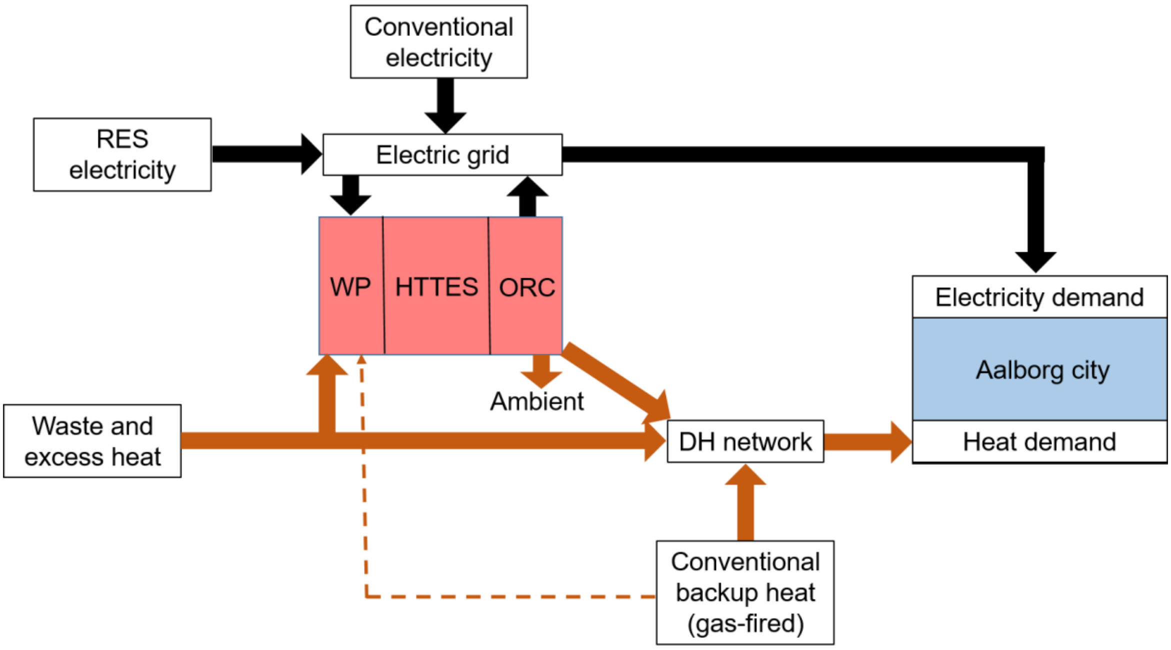

Figure 3: Schematic drawing of the role of the CHEST system integrated into the energy system in Aalborg case study.

The main objective of the CHEST system from an economic point of view will be to take up electricity from the grid at low price and give back electricity to the grid at high price. This general intention is similar to the business case defined in Deliverable 6.2. However, the decisive difference here is, that concerning the heat side, the availability of the excess heat has to be taken into account. That means that the operation of the heat pump can be limited, in terms of operation time or power, if there is not enough waste heat available to cover the DH demand and the demand of the heat pump of the CHEST system. If such a limitation is present, conventional backup heat from a gas-fired heater is used for the operation of the heat pump.

Similar to T6.2, the electrical power taken up by the CHEST system from the grid and the electrical power delivered by the CHEST system to the grid are only limited by the CHEST size, i.e. by the nominal powers of HP and ORC and the current state of charge of the HTTES. In this case, it is not interesting for the charging of the CHEST system whether there is much renewable electricity available and it is not interesting for the discharging of the CHEST system what is the actual electricity demand of the Aalborg city. The operation of the CHEST system is purely driven by the electricity price. In order to get substantial profit on the electricity side, the CHEST system participates in both the tertiary regulation market and the spot electricity market. This is done with a similar control strategy as indicated in T6.2., i.e. the decision for the operation of the HP and the ORC includes the given taxes and fees and the O&M costs of the CHEST system.

For the economic assessment of the CHEST system, the boundary line is drawn around the CHEST system as shown in Figure 4. It indicates that beside the DSO and the operator of the DH network, there is a third party that only operates the CHEST system. For energetic and environmental assessment, as stated in Chapter 2.4.1, it is assumed that all the electricity taken up by the HP of the CHEST system is excess RES electricity in the grid.

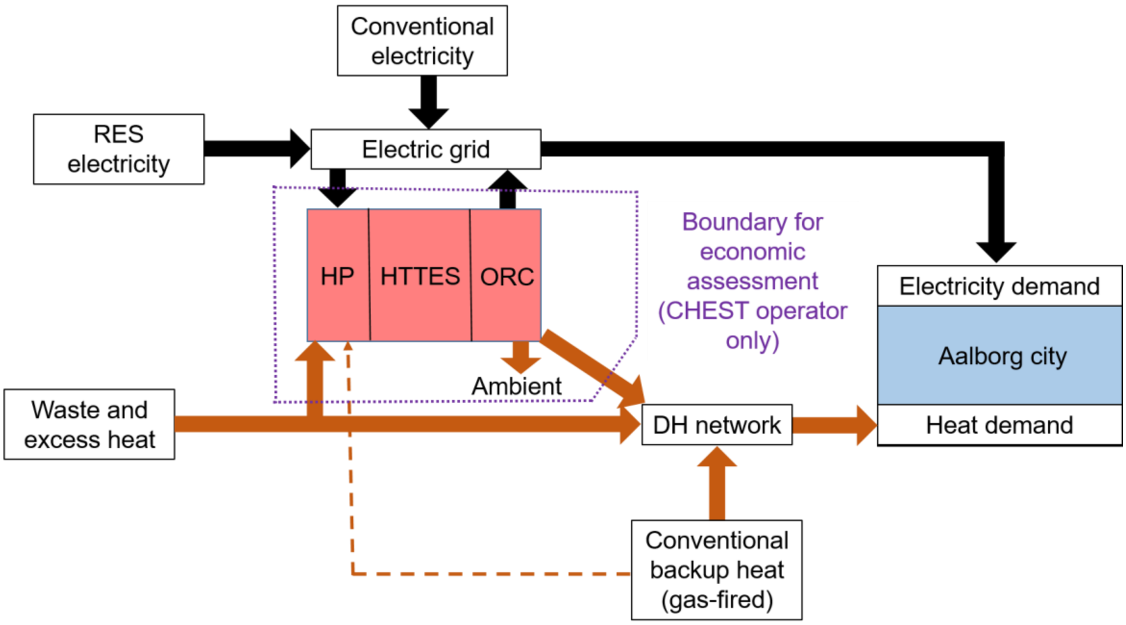

Figure 4: Schematic drawing of the role of the CHEST system in the business model for a CHEST only operator in Aalborg case study.

The heat of the ORC condenser can be supplied either to the ambient or to the DH network. This depends on the availability of enough excess heat and the temperature level of the DH network at this point of time. For the PCM/refrigerant combination chosen here (see Chapter 4.3), the ORC condensation temperature level is too low to use this heat for the DH network. Therefore, all the heat from the ORC condenser is transferred to the ambient.

3.1.3. Profiles and boundary conditions

The profiles for the heat demand of the DH system and the available waste and excess heat used in this task were the same as have been presented in Deliverable 2.2. The annual heat demand of the DH system accounts for about 1,930 GWh and the available waste and excess heat accounts for about 1,000 GWh. The forward and return temperatures of the DH system have a constant value of 90 and 45 °C throughout the year, respectively. Figure 5 shows the profiles of DH heat demand and excess heat generation together with the forward and return temperatures of the DH network.

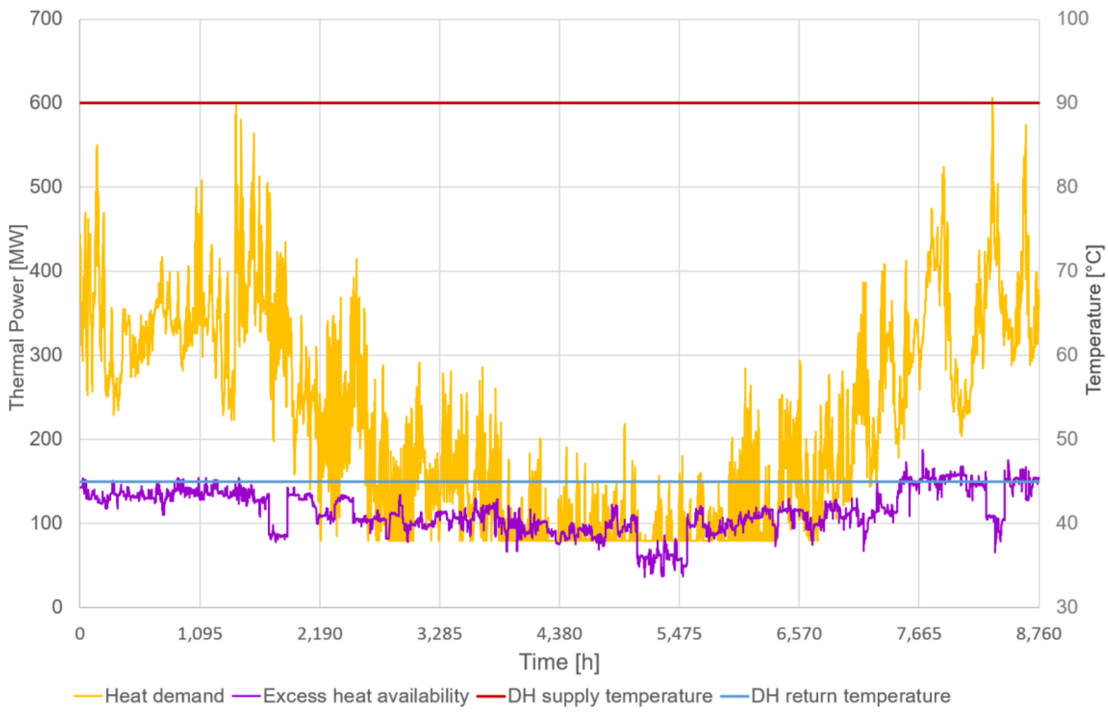

Figure 5: Profiles of DH heat demand, excess heat generation and DH temperatures used for the simulations of the Aalborg case study.

As was said above, the operation of the CHEST system is purely driven by the current electricity prices and does not depend on the actual renewable electricity generation and the electricity demand of Aalborg city. So, for the simulations carried out for this case study in T4.3, no electricity demand and production profiles are considered for the operation of the CHEST system. The exchange of electricity between the CHEST system and the electricity grid is not limited by the availability of a surplus or a deficit of electricity but is only limited by the size of the HP and ORC as well as the state of charge of the HTTES, respectively.

The electricity price profiles of the Danish tertiary regulation market and of the Danish spot market used in this task are shown in Figure 6 and Figure 7, respectively. For the up regulation, the minimum and maximum electricity prices account for -29.6 €/MWh and +335.0 €/MWh, while for the down regulation, these numbers are -40.3 €/MWh and +80.0 €/MWh. The average spot market electricity price accounts for 26.7 €/MWh, with minimum and maximum prices of -53.6 €/MWh and +105.0 €/MWh, respectively.

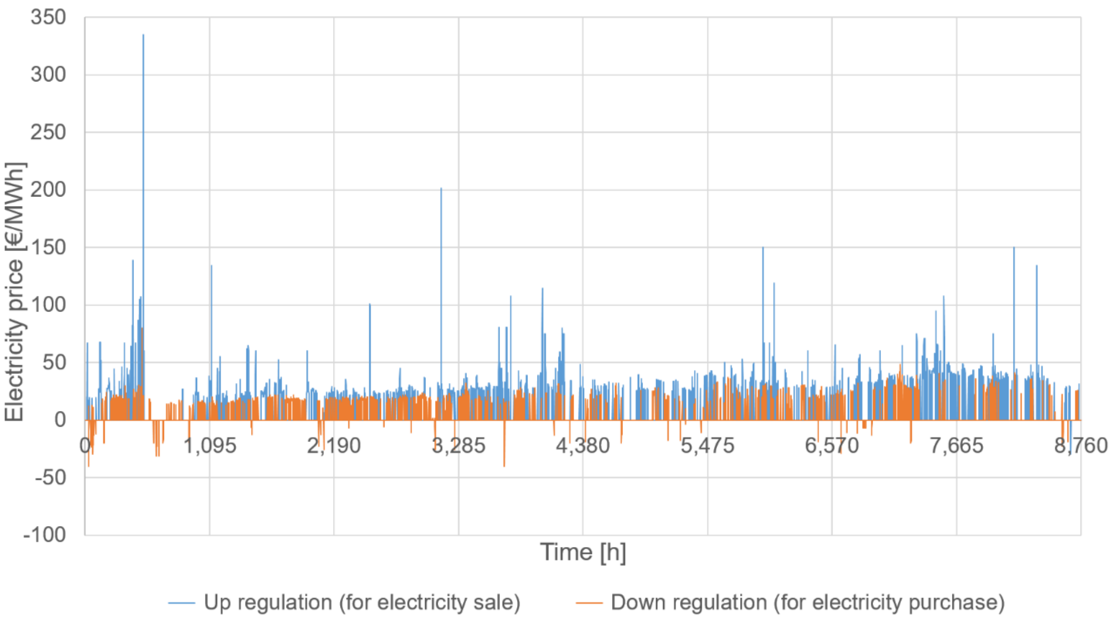

Figure 6: Electricity price profiles of the Danish tertiary regulation market (2016); Up regulation: delivery of electricity into the grid; Down regulation: taking up electricity from the grid.

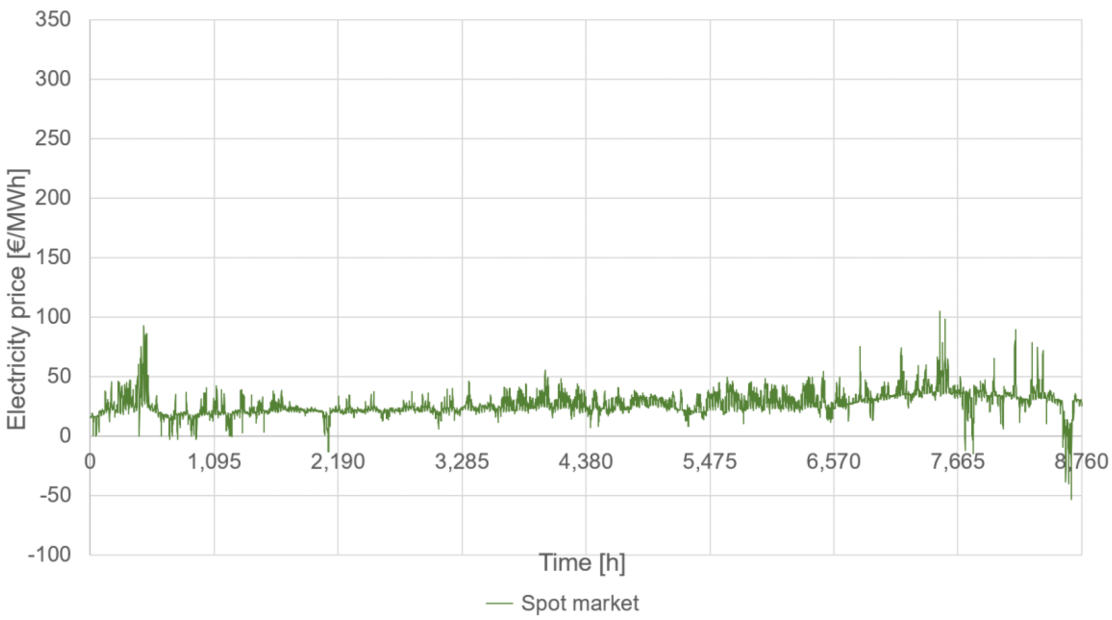

Figure 7: Electricity price profile of the Danish spot market (2016).

Figure 8 shows the sorted annual curves for the electricity prices of the Danish tertiary regulation market and the Danish spot market. First of all, it can be seen that negative prices are available just for some hours per year in each of the markets. Furthermore, there are also just a few hours per year with really high prices. In the regulation market, the electricity price is 0 €/MWh at most time of the year, i.e. there is no regulation volume, which limits the potential of the CHEST participation in this electricity market. Up regulation electricity prices are > 0 €/MWh at only about 1,740 hours per year, while it is 1,370 hours for a down regulation electricity price of > 0 €/MWh.

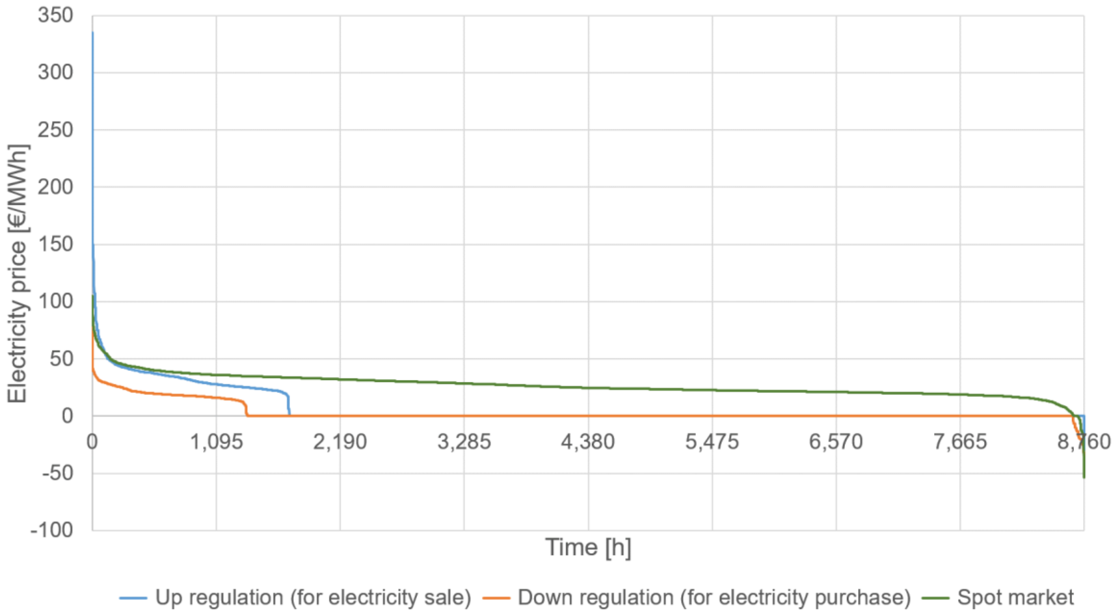

Figure 8: Sorted annual electricity price curves of the Danish tertiary regulation and spot market (2016).

Beside the price that the CHEST system needs to pay or gets rewarded for the exchange of electricity with the grid in the regulation market, there is also an availability payment considered for each hour the CHEST makes available a certain electrical power to the grid. However, this availability payment is only granted for the ORC electricity generation. Furthermore, as was shown more in detail in Deliverable 6.2, the availability payment is quite low, in most cases < 1 € per MW_{el} and hour of availability.

It is assumed that all prices are not affected by the operation of the CHEST system, because its size is small compared to the rest of the market.

3.2. Ispaster case study

3.2.1. General information of the case study

In the small town of Ispaster (about 700 inhabitants), which is located in the Basque country about 50 km northeast of Bilbao, Spain, several (public) buildings are connected to a DH network and an electrical micro-grid. This part of the town, with an annual gross heat demand of about 108.4 MWh and an annual electricity demand of about 23.5 MWh, is considered in the Ispaster case study. The maximum electricity load of the buildings in the electric micro-grid accounts for about 5.5 kW, while the maximum thermal load of the DH network is about 24.2 kW, see Chapter 3.2.3.

Renewable electricity is locally generated by 100 PV panels with a total peak power of 25 kW_p. In case the PV electricity generation is higher than the current electricity demand of the buildings in the electrical micro-grid, this surplus of PV electricity is stored in lead-acid batteries with a total gross capacity of 197 kWh. The storage efficiency of the batteries accounts for 70 %. When the batteries are completely charged, the PV electricity generation is normally curtailed, because this excess PV electricity cannot be sold to the DSO for legislative reasons.

The heat demand of the DH network is covered on the one hand by solar thermal collectors with thermal power of about 41.5 kW and on the other hand by a wood chips boiler with thermal power of about 90 kW. This means that all the heat is already generated by renewables. Furthermore, there are three storage tanks installed: one store of 2,000 l for the solar collectors, one store of 5,000 l for the biomass boiler and one store of 2,000 l in one of the buildings. The DH network itself has a volume of another about 1,000 l. Figure 9 shows a schematic drawing of the reference energy system for Ispaster case study.

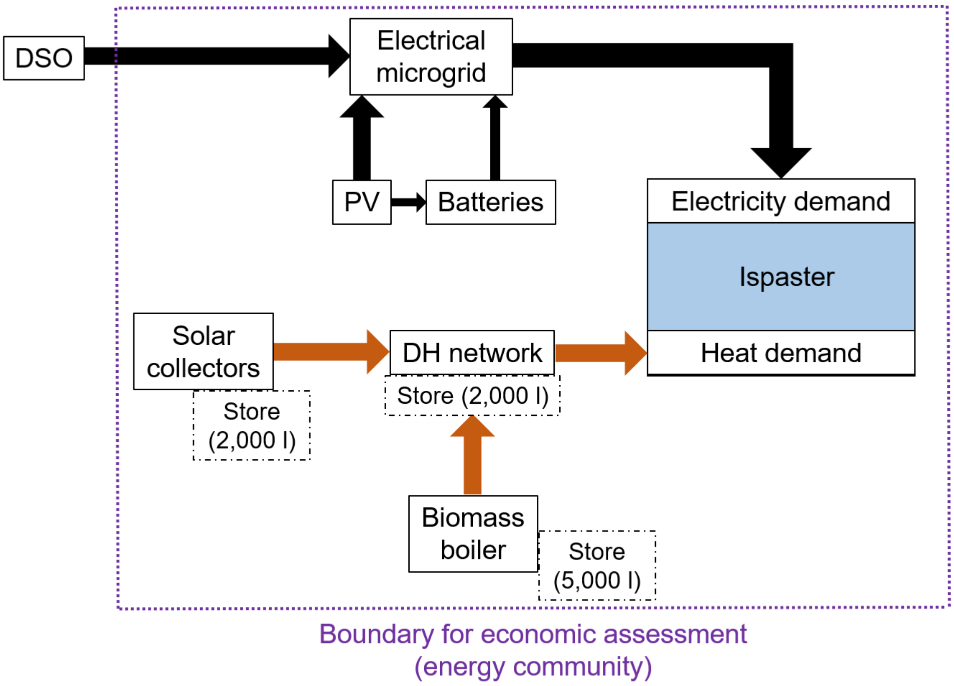

Figure 9: Schematic drawing of the reference energy system and its boundary for the economic assessment in Ispaster case study.

In Ispaster case study, energy supply is not managed by a profit-orientated public utility company, but by a public-private collaboration. Therefore, the business case considered here for the reference energy system is not to make a profit with the production/purchase and sale of heat and electricity but to minimize the costs of energy supply for this energy community. Another intention of the public-private company with the micro-grid is to increase the reliability of the electricity supply, because there have been problems with this for the electricity supplied by the DSO.

The costs of energy supply comprise the investment and operational costs of the energy generators installed + the energy purchased from outside. As can be seen from Figure 9, no heat needs to be purchased from outside, as it is completely generated by the energy community itself. Also, there is a considerable part of the electricity generated by the energy community itself, through the PV + battery system. So, there is only some electricity, which has to be purchased from the DSO.

Further general information about the case study of Ispaster can be found in the Deliverables 2.1, 2.3 and 4.3.

3.2.2. Role of CHEST in the Ispaster case study

Basically, the role of the CHEST system in Ispaster case study is to replace the lead-acid batteries to provide a more efficient and perhaps also cheaper solution compared to the current way of electricity storage. In addition to that, the intention is to further reduce the purchase of electricity from the DSO, which can be achieved by an increase of the installed PV panels and a respective dimensioning of the electricity storage system, in this case, the CHEST system.

On the heat side, the solar thermal collectors and the biomass boiler act as a heat source for the CHEST system while the DH network is the heat sink for the CHEST system. As is explained more in detail in Chapter 4.4, one collective thermal storage was considered in the WP4 TRNSYS model of Ispaster, which is fed by heat from both the solar thermal collectors and the biomass boiler. Concerning the control of these two heat sources, there is a prioritization for the solar thermal collectors. If the available heat at the ORC condenser is higher than the current heat demand of the DH system, the remaining available ORC heat is transferred to the ambient.

For the Ispaster case study, two different scenarios are considered. The first one is called “Ispaster 2.0” and is schematically shown in Figure 10. In this scenario, there is still a connection to the DSO, i.e. only part of Ispaster´s electricity demand is covered by the PV + CHEST system. The reference energy system with the battery is the one shown in Figure 9.

In times where PV electricity generation is higher than the electricity demand and can also not been taken up by the CHEST system (or battery system), this PV electricity is curtailed. As was said above, a sale of excess PV electricity is currently not possible due to legislative reasons but could be possible in the future. In T4.3, no sale of excess PV electricity was considered since it worsens the economic assessment of both the CHEST system and the battery storage in comparison to the situation without any electrical storage (as the available excess PV in such a situation is higher and so would be the revenues for the electricity export).

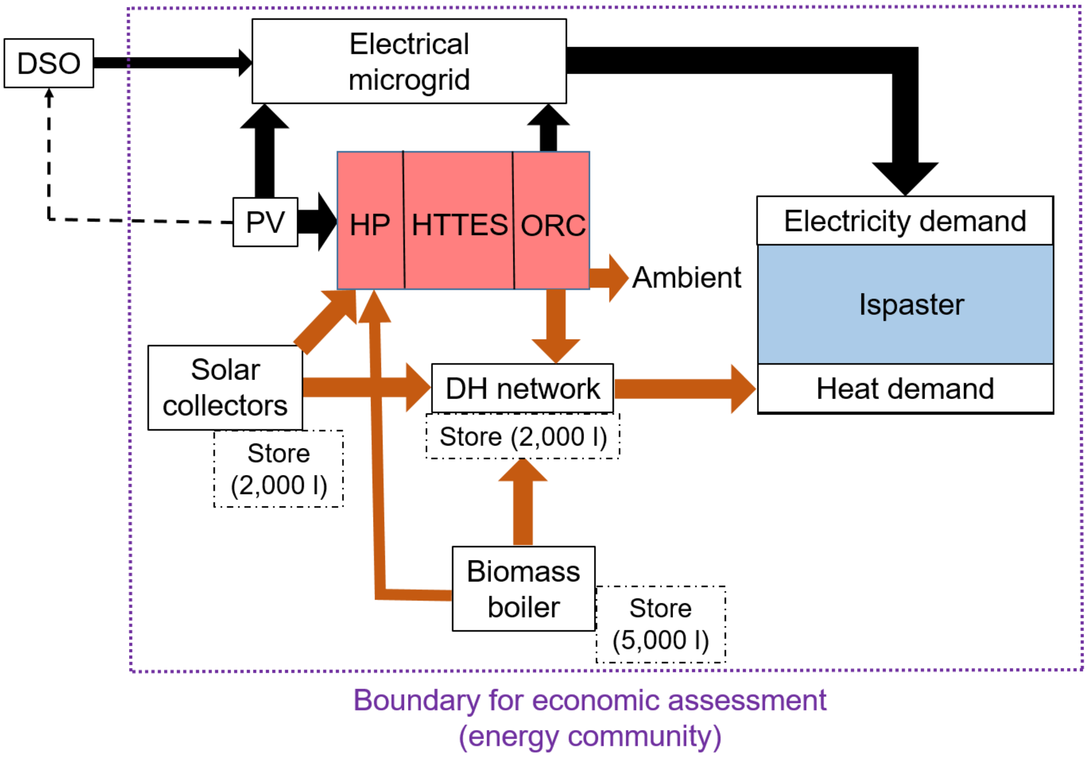

Figure 10: Schematic drawing of the role of the CHEST system integrated into the energy system in Ispaster case study ("Ispaster 2.0").

In contrast to the scenario explained above, the second scenario called "Ispaster Island" considers an island energy system, which means that all contracts with the DSO can be cancelled. The PV system and the CHEST system (and in the reference case the battery system) must be dimensioned in such a way that the electricity demand of Ispaster is completely covered at any time. For the CHEST system, this scenario is illustrated in Figure 11.

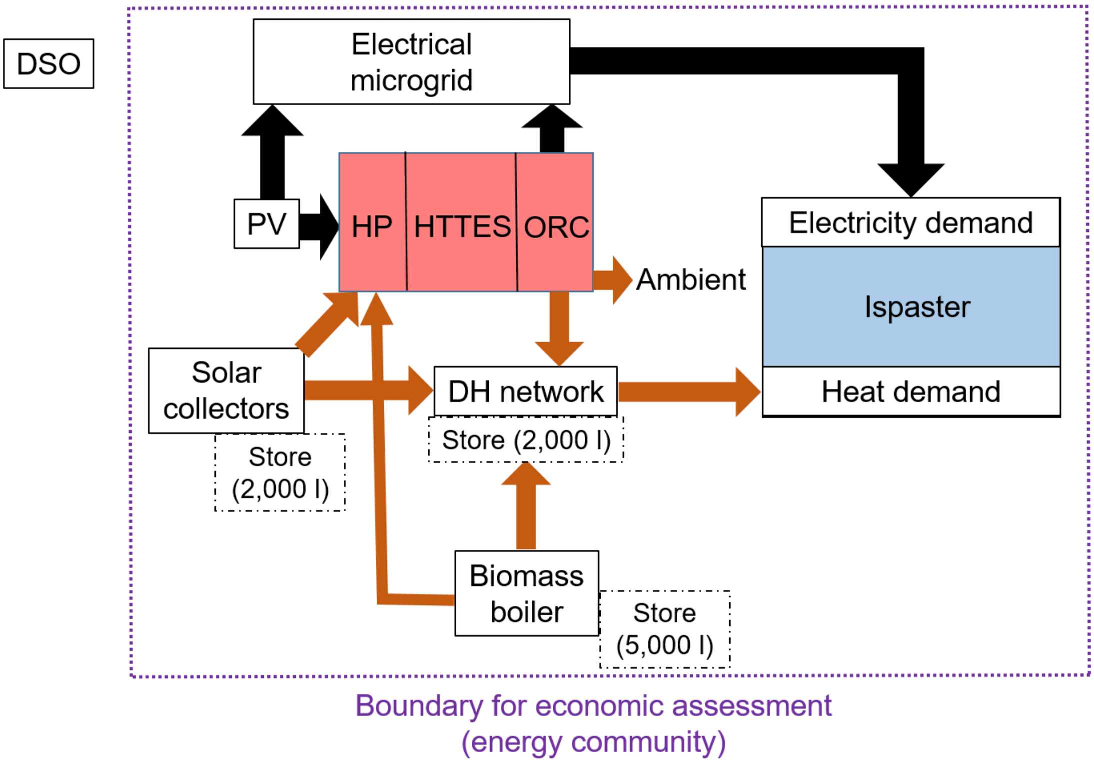

Figure 11: Schematic drawing of the role of the CHEST system integrated into the energy system in Ispaster case study ("Ispaster Island").

3.2.3. Profiles and boundary conditions

As was pointed out in Deliverable 4.3, the Ispaster pilot case could be monitored only partly. So, the gaps of the times series were filled with generated data (refer to Deliverable 4.3 for more detailed information). Furthermore, the situation in Ispaster is permanently changing, for instance as regards to further buildings that are connected to the DH network or as regards to a second wood chips boiler that was installed recently.

For the calculations carried out in Task 4.3, the annual heat and electricity demands presented in D4.3 were taken as the boundary condition, but new hourly profiles were created. As was shown in D4.3, the annual heat demand of Ispaster (gross demand including thermal losses of DH network) accounts for 108.4 MWh, while the annual electricity demand amounts to 23.5 MWh. For the electricity demand profile, data of the daily distribution of the electricity demand from another town in the Basque country were taken in order to generate a more realistic profile. For the heat demand profile, a TRNSYS simulation was used to generate a realistic profile.

Figure 12 shows the profile of DH heat demand together with the forward and return temperatures of the DH network. Compared to the simulations in WP2, lower DH temperatures of 60 and 40 °C, respectively, were assumed here to allow for more efficient integration of the CHEST system. Lower DH temperatures than this cannot be realized in Ispaster.

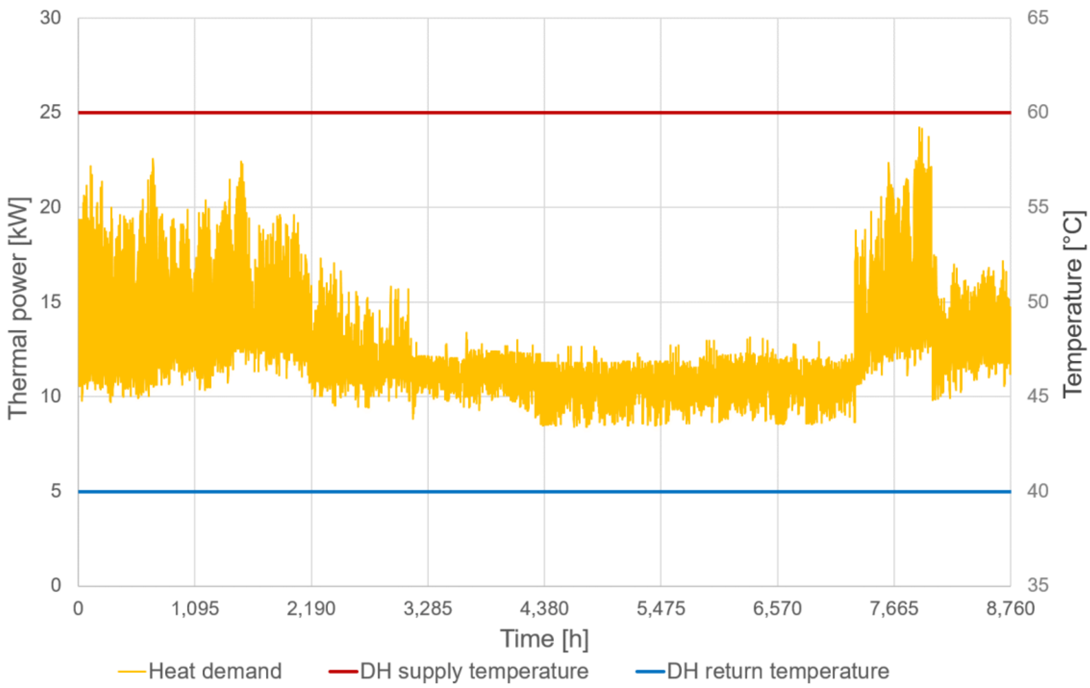

Figure 12: Profiles of the DH heat demand and the DH temperatures used for the simulations of the Ispaster case study.

As was said above, data for the daily electricity demand distribution from another town in the Basque country were used. This distribution was then applied to the known monthly and annual electricity demand values of Ispaster (i.e. it was scaled to fit the monthly and annual electricity demand), which finally gives the electricity demand profile for Ispaster.

Figure 13 shows the resulting daily and Figure 14 shows the resulting yearly electricity demand profile for Ispaster. As you can see from the two figures, the maximum electric power demand accounts for about 5.5 kW in winter while it is around 4.5 kW in summer.

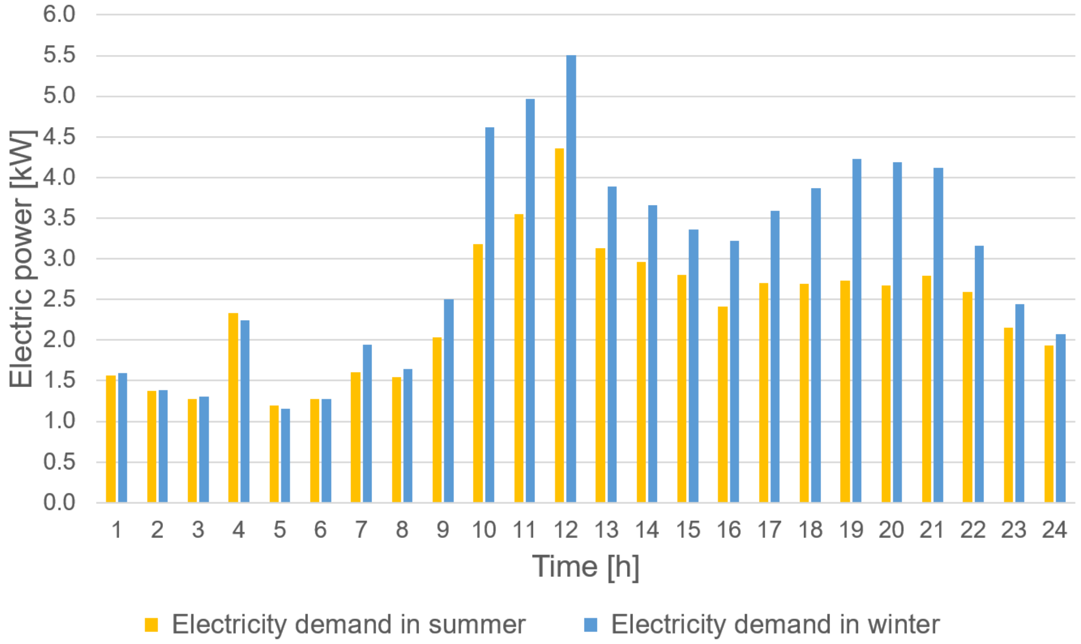

Figure 13: Profiles of the daily distribution of the electricity demand in summer and winter used for the simulations of the Ispaster case study.

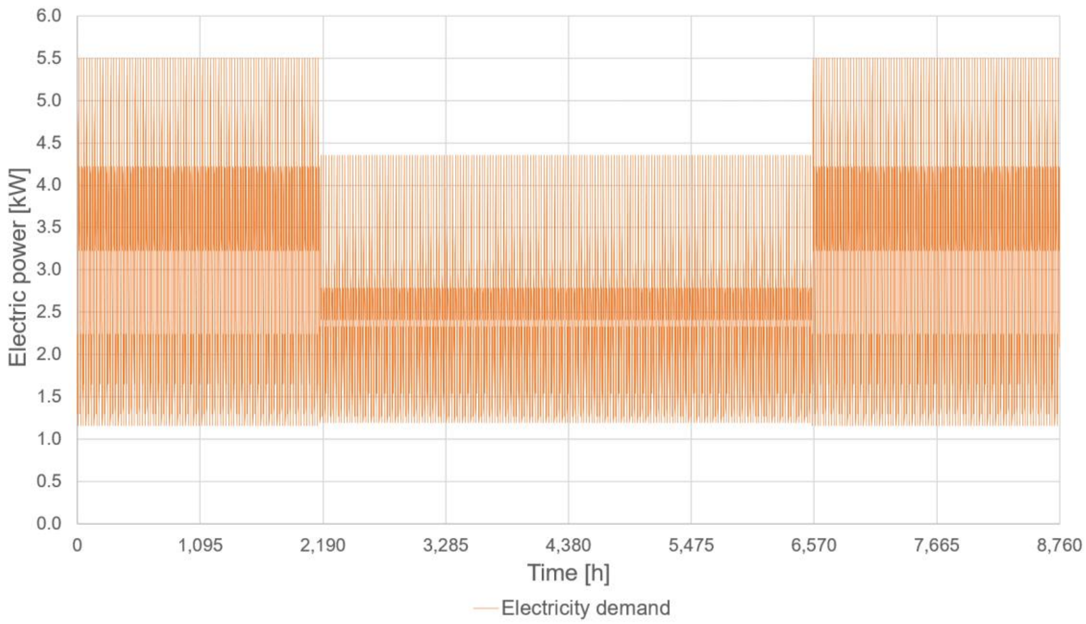

Figure 14: Profile of the electricity demand used for the simulations of the Ispaster case study.

The electricity price that has to be paid to the DSO for electricity purchase was assumed to be constant here (as part of a bilateral contract) at a level of 123.4 €/MWh, which is the average electricity price including taxes and fees for Ispaster, see Deliverable 6.2.

The price for the purchase of the wood chips was also assumed to be constant. It accounts for 25.6 €/MWh (including VAT and transport).

4. Adaptions of the simulation model

4.1. Basic model

The TRNSYS model that was developed in Task 4.2 and described in Deliverable 4.2 was the basic simulation model that was used for the simulations in Task 4.3.

Beside some specific changes for the respective case study, there were some general adaptions of the model implemented after the first simulations had been carried out in the Tasks 4.3 and 4.4. Such adaptions for example comprised additional output variables, minor bug fixing and the implementation of a recharge mechanism for the SHS storage, which is described paragraph 4.2.

4.2. Recharge mechanism for the SHS storage

Due to the different ratios of latent to sensible heat transferred from the HP to the HTTES during a charging cycle and transferred from the HTTES to the ORC during a discharging cycle, the states of charge (SoC) of the LHS and the SHS do not match each other if no other measures are taken. This is disadvantageous because one of the two storage parts might limit the operation of the CHEST system although the other part would allow for the operation. In the WP2 model, this mismatch between the two states of charges was solved by a so-called “clean-up strategy”, which removed excessive either latent or sensible heat in such a way that the two parts of the HTTES were charged and discharged uniformly, cf. Deliverables 2.2 and 2.3.

For the T4.3 simulations, a different approach was followed due to the following reason:

In the WP4 TRNSYS model, the general approach of the system sizing (and control) is that the energy input into the PCM storage has to be the same as its energy output on the yearly basis, cf. Deliverable 4.4. Depending on the ratios of latent to sensible heat for charging and discharging for the respective working fluid and depending on the HP and ORC operation hours, this leads to a more or less negative SHS heat balance as the results of Task 4.4 have shown. Consequently, the SHS limits the ORC operation once it is completely discharged unless the SHS is dimensioned big enough so that this does not happen. However, this is not realistic as regards to investment costs and space demand. Therefore, in order to keep the SHS sizes small and to allow for ORC operation with SHS heat, there must be recharging of the SHS from time to time, i.e. heat is added to the SHS, which increases its state of charge again.

When such a recharge happens, water is pumped from the LTWT to the HTWT like in the HP operation. However, this time, the water does not get heat via the subcooler, but via an additional heat exchanger. In the Aalborg case study, preferably, excess heat is taken for the recharge and if there is not enough excess heat available, additional gas firing is necessary. In Ispaster case study, the recharge heat is exclusively supplied by the biomass boiler due to the required temperature level of the HTWT.

Theoretically, to avoid this additional heat exchanger, an alternative solution is that cold water is pumped from the LTWT to the HTWT. The resulting temperature decrease in the HTWT would then be compensated in the same way the thermal losses of the HTWT are compensated, i.e. by an external heat source directly delivering heat to the HTWT. From an energetic point of view, this gives the same result as the procedure described above.

In the Aalborg case study, a recharge operation is normally carried out, if there is neither HP nor ORC operation at this time and if the state of charge of the SHS is below a certain threshold. For Ispaster 2.0, this operation logic was similar, but for Ispaster Island, it was necessary to allow recharge operation also in parallel to ORC operation. The reason for this is that for Ispaster Island case, there are nearly no times with neither HP nor ORC operation, because there is always a surplus or deficit of electricity that the CHEST system has to react to (and so, recharge would only happen if the PCM storage is completely charged or discharged, which is rarely the case). Further information about the implementation of the recharge mechanism is given below for the respective case study.

As will be shown with the results, the recharge heat increases the P2P ratio since this heat into the SHS is used at a later point of time to generate electricity with the ORC. So, the recharge heat increases the electricity output, but this is achieved at the expense of additional heat demand for this SHS recharge.

4.3. Model adaptions for the Aalborg case study

Beside the implementation of the recharge mechanism, only minor adaptions of the basic simulation model were done for the Aalborg case study. The main adaption concerns the control of the HP and ORC operation in the boundary conditions of the Danish electricity markets.

The basic idea is that the price difference between the purchase of electricity for the HP and the sale of electricity with the ORC must at least compensate the O&M costs and the Buy- and Sell-addons through taxes and fees. As was presented in Deliverable 6.2, the O&M costs account for 10 €/MWh_{el} for the HP and 15 €/MWh_{el} for the ORC, respectively. Furthermore, there is a Buy-Addon for purchased electricity of 21.53 €/MWh_{el} and a Sell-Addon for sold electricity of 0.52 €/MWh_{el}. Summing up these four parts results in a minimum required price difference between purchase and sale of electricity of 47.05 €/MWh_{el}.

However, this required price difference can actually be reduced, if the P2P ratio of the CHEST system is > 100 %. Because then, the amount of sold electricity is higher than the amount of purchased electricity. Such a P2P ratio of > 100 % can be achieved, when the HP evaporation temperature level is higher than the ORC condensation temperature level, assuming an ideal HP and ORC cycle and no thermal losses during energy storage. In a real system, the HP evaporation temperature level must be considerably higher than the ORC condensation temperature level, but this is given for the Aalborg case study, see below.

Basically, as will be shown later with the simulation results, the required price difference for the CHEST system control can be reduced compared to the abovementioned total addon sum of 47.05 €/MWh_{el} by a reduction factor F_R, which is equal to about the expected P2P ratio.

So, the control for the CHEST system was based on mainly two parameters: a buy-price limit, below which electricity is purchased, and the reduction factor F_R, which determines the price difference between purchase and sale of electricity and thus sets the control for the ORC operation.

As a result of Task 4.4, all Task 4.3 simulations were carried out with Cyclopentane as HP and ORC refrigerant and with $LiNO_3$-$NaNO_3$-KCl as the PCM having a melting temperature of 160 °C. The temperature levels for the HP evaporator and the ORC condenser (refrigerant-side) were 100 °C and 45 °C, respectively. The simulations were carried out for a complete year with a time step of 1.0 h.

4.4. Model adaptions for the Ispaster case study

As the basic WP4 simulation model was mainly developed for a CHEST system connected to the electricity grid and driven by the time-dependent electricity prices in both the spot and the regulation electricity market, the following main model modifications had to be done for the Ispaster case study:

- removal of electricity price signals
- implementation of the PV panels and the electricity demand profile for the calculation of electricity surplus and deficit
- change of CHEST system control from control based on electricity prices to control based on electricity surplus and deficit
- incorporation of a thermal circuit including solar thermal collector field, biomass boiler, water storage tank, hydraulics and the connection to both DH network and CHEST system (heat for HP evaporator, compensation of SHS thermal losses and SHS recharge)
- adaption of output variables and plots for the Ispaster case

As a result of Task 4.4, the simulations for Ispaster 2.0 were carried out with R1233zd(E) as HP and ORC refrigerant and with KNO_3-$NaNO_3$-$NaNO_2$ as the PCM having a melting temperature of 142 °C. The temperature levels for the HP evaporator and the ORC condenser (refrigerant-side) were 82 °C and 70 °C, respectively.

For Ispaster Island simulations, the refrigerant used was R601 due to its higher P2P ratio compared to R1233zd(E) in order to get to lower system sizes, especially for the PCM storage. The PCM used was the same as for Ispaster 2.0, i.e. KNO_3-$NaNO_3$-$NaNO_2$ with a melting temperature of 142 °C. The temperature levels for the HP evaporator and the ORC condenser (refrigerant-side) were 82 °C and 46 °C, respectively.

Based on the PV electricity generation and the electricity demand profile, the electricity surplus (excess PV power) and electricity deficit is calculated for the current time step, respectively. An electricity surplus means demand for HP operation for the CHEST system, while an electricity deficit means demand for the ORC operation. If there is no limitation given by a completely charged LHS or SHS and if there is no limitation by the available heat at the HP evaporator (see below), the HP runs with the maximum power possible. This maximum power is either determined by the nominal power of the HP or by the available electricity surplus – whatever is the smaller amount. Accordingly, if there is no limitation given by a completely discharged LHS or SHS, the ORC runs with the maximum power possible. This maximum power is either determined by the nominal power of the ORC or by the electricity deficit – whatever is the smaller amount.

The thermal circuit was built up of the solar thermal vacuum tube collectors, the biomass boiler and a collective water storage tank. A simplified scheme of the thermal circuit is shown below in Figure 15 for the battery model. The storage tank had a volume of 10 m³, which is equal to the total volume of the three single water storages installed in Ispaster (cf. Figure 9) + the water volume of the DH network itself.

Both the solar thermal collectors and the biomass boiler supply heat to the storage based on temperature control (with hysteresis). Basically, the solar thermal collectors feed the storage, whenever the collector outlet temperature is at a certain level above the storage temperature. The biomass boiler operates based on certain set point temperature for the storage temperature, which is chosen depending on the required temperature levels for the two heat consumers: the DH network and the HP evaporator. In this case, the required temperature at the HP evaporator (82 °C on refrigerant-side, + 5 K temperature difference for heat transfer at the HP evaporator, equals 87 °C required on water-side) is higher than for the DH network (60 °C) and so, this is the decisive temperature.

Both the DH network and the HP evaporator are connected to the water storage tank. Whenever the storage temperature is high enough for the respective application, heat is transferred from the water storage to the DH network and/or the HP evaporator. This means, a non-availability of heat at the HP evaporator is given in case of too low temperatures in the water storage tank. Depending on the settings for the set point temperature of the boiler and the settings for the hysteresis temperature differences, it is easy to avoid such a non-availability of heat at the HP evaporator. However, this results in higher temperatures in the water storage tank, which is disadvantageous for the solar thermal yield. This is why the settings were done in such a way that some hours of non-availability of heat at the evaporator are allowed for.

As was already mentioned, the ORC condenser is directly connected to the DH network but not to the water storage tank, because the ORC condensing temperature level is too low to transfer heat to the water storage tank. The DH heat demand is first of all covered by the ORC condensation heat. If there is not enough ORC condensation heat available, the remaining DH heat demand is covered by heat from the water storage, as was described above.

The heat for the compensation of the thermal losses of the SHS and the heat for the recharge of the SHS is always supplied by the biomass boiler due to the high temperature level of the HTWT (142 °C).

Beside the CHEST simulation model, also a simulation model for the reference energy system with battery storage was built up in TRNSYS. Figure 15 shows a screenshot of this model along with the labels of the most important components.

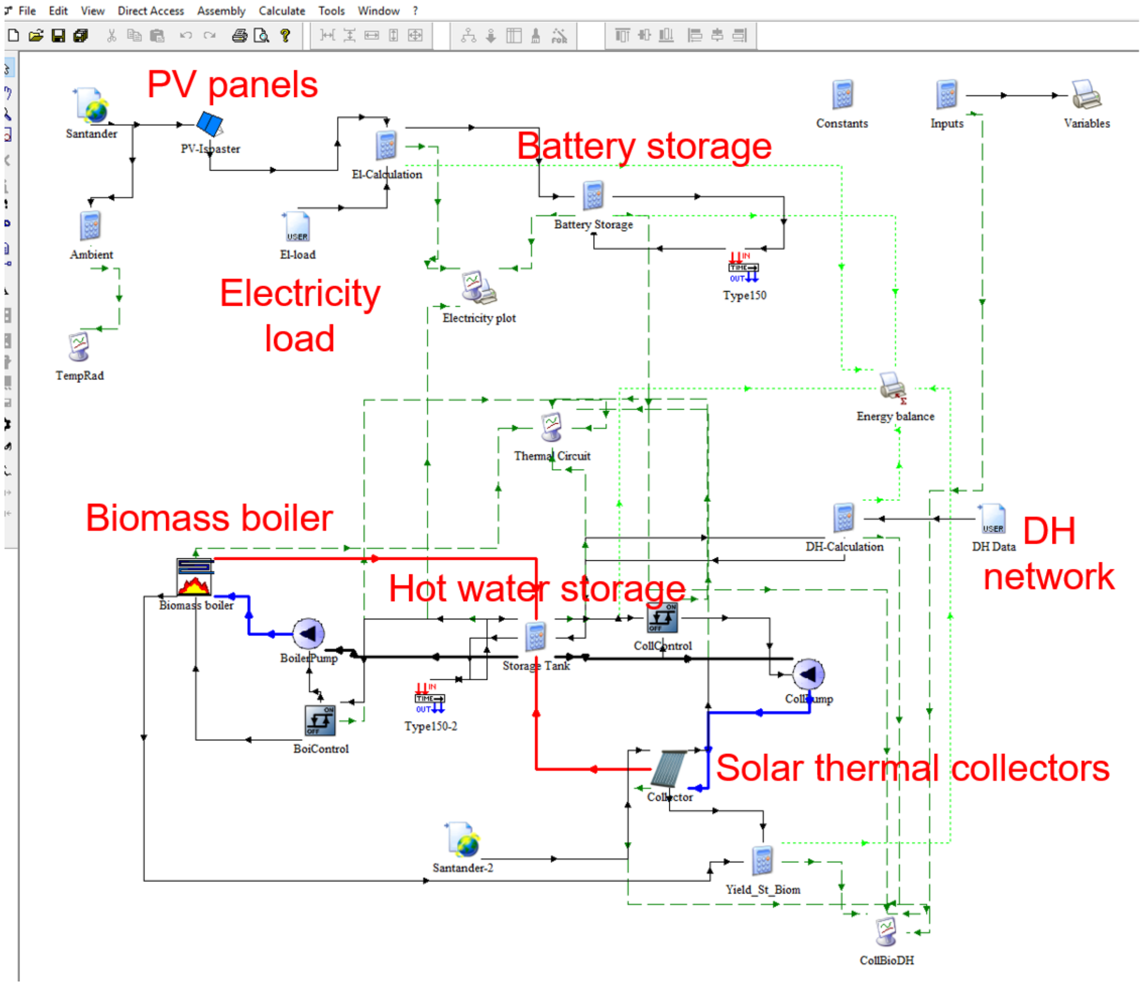

Figure 15: Screenshot of the TRNSYS simulation model for the reference energy system of Ispaster with the battery storage.

The battery storage is modelled via an equation block, which contains all necessary equations for the simulation of the battery storage. The characteristics of the battery storage are the same as given in Deliverable 2.3, i.e.:

- charging efficiency: 100 %
- discharging efficiency: 70 %
- depth of discharge (battery utilization factor): 60 %
- maximum charging power: 20 kW
- maximum discharging power: 20 kW

At the beginning of each simulation, the state of charge of the battery storage was set to 50 %, which is equal to the settings for the LHS and the SHS in the CHEST system.

The other main components shown above in Figure 15 are also part of the TRNSYS model, for explanation see above. In the reference energy system with the battery storage, the electric and the thermal side are completely decoupled from each other. This means that changes made in the thermal circuit like for instance a variation of the solar thermal collector area or adaptions of the biomass boiler control, do not influence the results of the electric side like the amount of purchased grid electricity. Similarly, changes made at the electric side, e.g. variations of the number of PV panels or the gross capacity of the battery storage, do not influence the thermal outputs like the solar thermal collector yield.

All simulations for the Ispaster Island case were done for a two-year period, because the initial state of charge of the battery storage / HTTES influences the output variables in the first year at the high storage capacities required for an island energy system. The results of the second year were taken for further analysis. For Ispaster 2.0, only one complete year was simulated, because the storage capacities are much smaller here and so, the initial state of charge has only negligible influence on the outcome of a simulation. As for the Aalborg simulations, the time step chosen was 1.0 h.

5. Simulation results

5.1. Simulation results for Aalborg case study

The basic objective of the simulations for the Aalborg case study is to find a CHEST system, which in terms of size and settings (control) results in a profitable business case. This means that a CHEST system, which utilizes the price differences in the spot and the tertiary regulation electricity market generates sufficient annual profit to provide an acceptable payback on the initial investment.

As regards to the size of the CHEST system, this concerns the following parameters:

- HP nominal electric power
- ORC nominal electric power
- LHS thermal storage capacity
- SHS thermal storage capacity (given by the HTWT and LTWT tank volumes)

As regards to the settings, this concerns the following parameters:

- buy-limit for the purchase of electricity, i.e. a defined price threshold below which electricity is purchased
- the required price difference between purchase and sale of electricity in the CHEST system control, determined by the reduction factor F_R

For clarification, these two setting parameters are briefly explained again in the following. As was mentioned in Chapter 4.3, the sum of Buy-Addon, Sell-Addon and O&M costs accounts for 47.05 €/MWh$_{el}$, i.e. the required price difference between purchase and sale of electricity has to be at least that high in order to make profit by the purchase and sale of electricity. However, due to a P2P ratio of > 100 % in the Aalborg case study (see results below), more electricity can be sold than electricity is purchased, which gives the possibility of reducing this required price difference. This is expressed by the reduction factor F_R according to the following formula:

$$Reduced\ price\ difference\ = \frac{Original\ price\ difference\ (47.05\ €/MWh_{el})}{F_R}$$

As an example, this gives for the reduced price difference:

- F_R=1.0 → Reduced price difference = 47.05 €/MWh$_{el}$ / 1.0 = 47.05 €/MWh$_{el}$
- F_R=1.2 → Reduced price difference = 47.05 €/MWh$_{el}$ / 1.2 = 39.21 €/MWh$_{el}$
- F_R=1.4 → Reduced price difference = 47.05 €/MWh$_{el}$ / 1.4 = 33.61 €/MWh$_{el}$

Together with the buy-limit indicating the threshold below which electricity is to be purchased, this sets the limits for the purchase and sale of electricity. For example, if the buy-limit is 10 €/MWh$_{el}$ and F_R is 1.2, then, electricity is purchased at either the spot or the tertiary regulation electricity market if the price in one of the two markets is below 10 €/MWh_{el}. And electricity is sold to one of the two markets if the electricity price is above 10 €/MWh_{el} + 39.21 €/MWh_{el} = 49.21 €/MWh_{el}. And the market to purchase electricity from or sell electricity to is chosen depending on which one has the more beneficial price at a certain point of time, i.e. the lower price in case of electricity purchase and the higher price in case of electricity sale.

Other setting parameters such as the temperature levels of the HP evaporator and ORC condenser or the HTWT state of charge limit to initiate SHS recharge are fixed in this analysis, as they were optimized beforehand, cf. for instance T4.4.

In the first run of simulations, the required HP and ORC nominal electric powers were analyzed. The minimum nominal electric power has to be 5 MW because otherwise, the CHEST system would not be allowed to participate in the Danish tertiary regulation electricity market, cf. Deliverable 6.2. Concerning the maximum power, the basic consideration was that for higher CHEST system sizes, the heat demand for the HP evaporator increases, and at a certain HP size, there won´t be enough excess and waste heat available anymore. If so, the HP operation would either be limited or the remaining heat demand would have to come from gas-fired auxiliary heating. Here in T4.3, the latter option is carried out in such a case.

However, auxiliary gas-fired heating should be avoided because this causes further costs. As will be shown later, it is already very difficult to generate economic profit in the two electricity markets considered here. So, on the heat side, basically no costs should arise. It is assumed that the excess heat needed for HP operation is received for free, which is already an optimistic assumption. However, for additional gas-fired auxiliary heating, this would clearly not be the case.

Figure 16 shows the dependence of the required gas-fired auxiliary heat demand on the HP nominal electric power for three different relative HP/ORC sizes. The figure shows that gas-fired auxiliary heating starts at HP nominal electric powers of about 10 MW and then increases more and more. The auxiliary heat demand is higher for lower HP/ORC relative sizes, because the higher ORC size causes the HP to run more hours to charge the HTTES again.

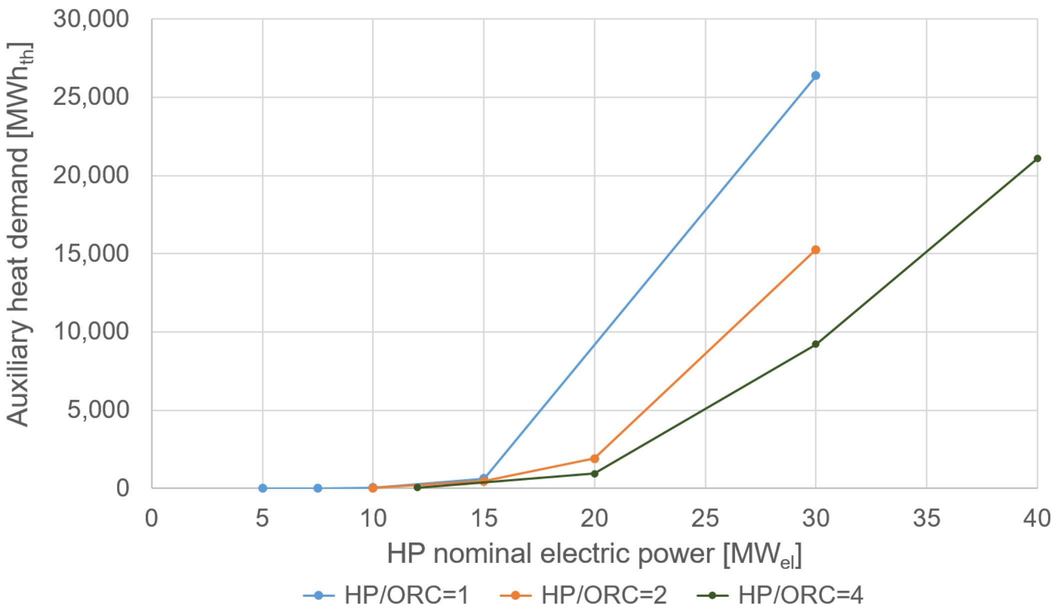

Figure 16: Dependence of the required additional gas-fired auxiliary heat demand on the HP size and the relative HP/ORC size.

Figure 17 shows a detail view of the figure above. It shows how auxiliary heat demand starts at HP nominal electric powers of about 10 MW. At a HP nominal electric power of 15 MW, the auxiliary heat demand accounts for about 466 MWh/a for a HP/ORC relative size of 2.0 while it accounts for 632 MWh/a for a HP/ORC relative size of 1.0. Assuming a gas-boiler efficiency of 0.95 and a gas price of 25 €/MWh, this would result in additional costs of > 10,000 €/a, which means significant costs compared to the low profit on the electric side (see Chapter 6.2.3). For HP/ORC relative sizes of 4.0, the minimum possible HP size is 20 MW (considering the minimum ORC size of 5 MW, see above). As can be seen in Figure 17, the auxiliary heat demand, in this case, accounts for about 953 MWh/a.

As a consequence of this analysis on the auxiliary heat demand shown here, it was decided to carry out the following simulations with HP and ORC nominal electric powers in the range of 5…10 MW and with a relative HP/ORC size of 1…2.

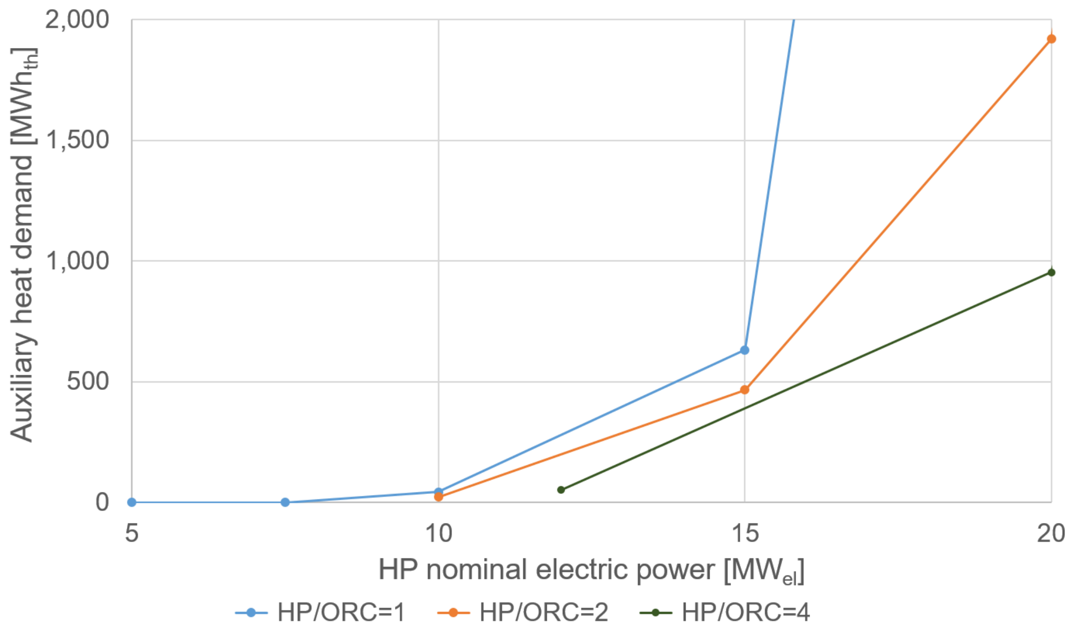

Figure 17: Dependence of the required additional gas-fired auxiliary heat demand on the HP size and the relative HP/ORC size (detail view).

The second run of simulation studies was the analysis of the demand times for HP and ORC, which is determined by the electricity price profiles and the abovementioned two setting parameters for the CHEST system control, the buy-limit and the reduction factor F_R. The basic question is, how many hours there is a demand for the purchase of electricity (and thus for the HP to operate) and for the sale of electricity (and thus for the ORC to operate). This demand does not mean that the HP and the ORC will really operate these hours, because of the limitation by the state of charge (SoC) of the LHS and SHS. Nevertheless, this will show the potential (= maximum possible) operating hours, i.e. the operating hours in case of an "unlimited" size of the HTTES.

Figure 18 shows the hours of demand for HP and ORC operation dependent on the two setting parameters. As was shown above, a reduction factor F_R = 1.0 means a price difference between purchase and sale of electricity of 47.05 €/MWh$_{el}$. A reduction factor of 1.2 reduces this price difference to 39.21 €/MWh$_{el}$ and a reduction factor of 1.4 means a price difference of 33.61 €/MWh$_{el}$. In the simulations of T4.3, mostly, a reduction factor of about 1.2 - 1.3 was applied, because the P2P ratio for most of the simulations is in the range of 120 - 130 %.

Figure 18 shows that an increase of the buy-limit increases the demand hours for the HP operation, which is due to the fact that more often, there are electricity prices below the buy-limit and so, electricity is to be purchased. For the same reduction factor F_R (and thus for the same required price difference between purchase and sale of electricity), the ORC demand decreases with increasing buy-limit.

Furthermore, the decrease of the required price difference between purchase and sale of electricity (i.e. an increase of the reduction factor F_R) leads to an increase of the total demand hours (HP + ORC) as is shown more clearly in Figure 19.

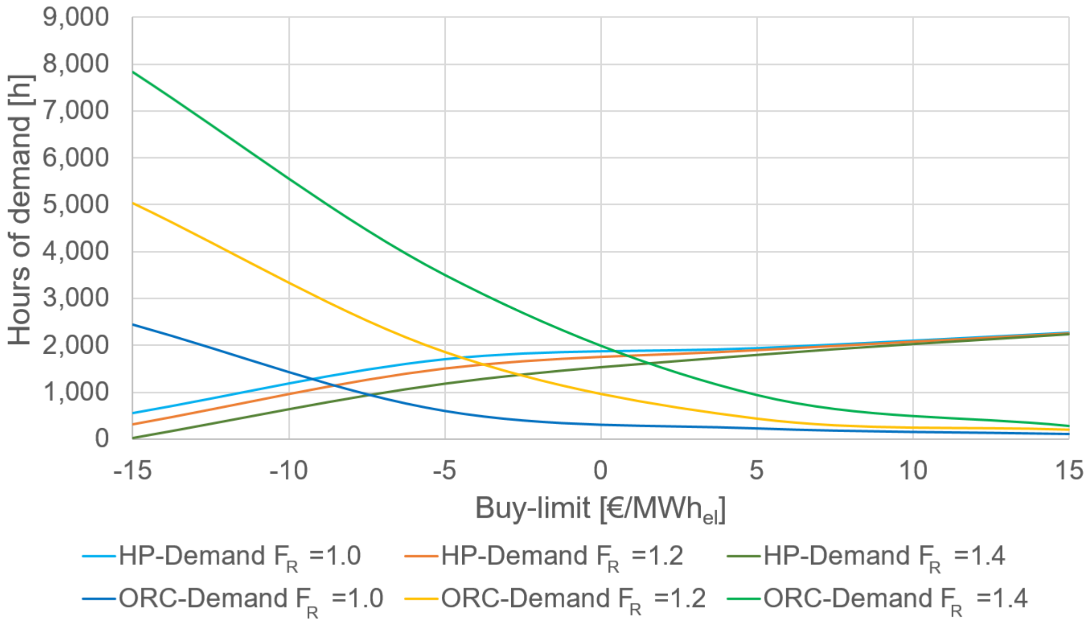

Figure 18: Hours of demand for HP and ORC operation dependent on the two setting parameters of the CHEST system control, the buy-limit (price threshold below which electricity is purchased) and the reduction factor F_R (reducing the gap between purchase and sale price of electricity), for the electricity profiles of the Danish spot and tertiary regulation market (2016).

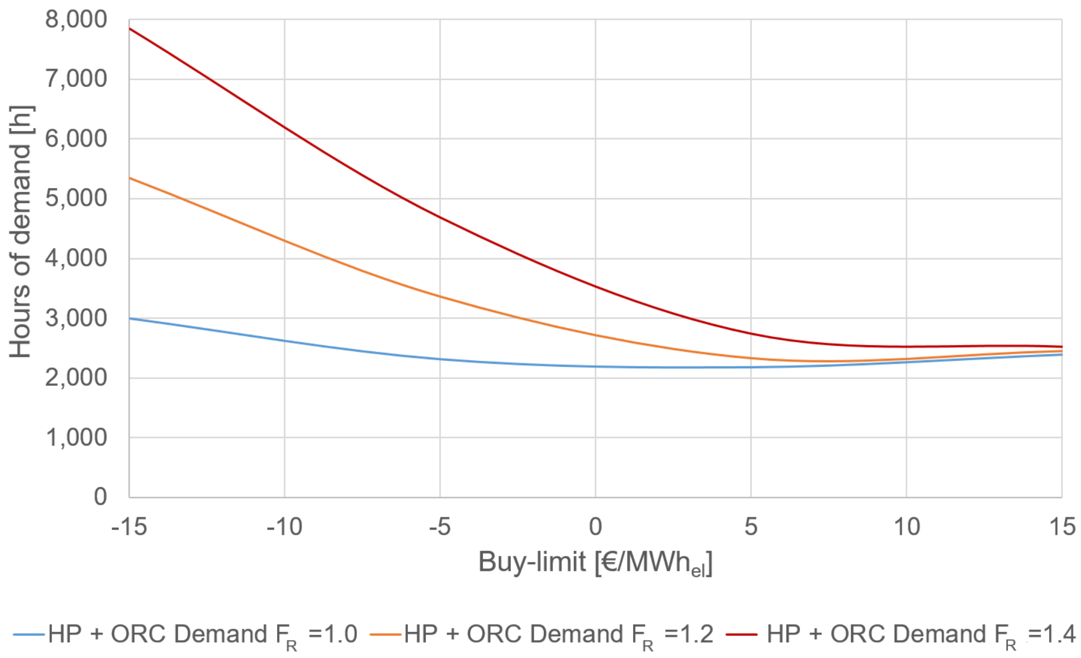

Figure 19: Total hours of demand for both HP and ORC operation dependent on the two setting parameters of the CHEST system control, the buy-limit (price threshold below which electricity is purchased) and the reduction factor F_R (reducing the gap between purchase and sale price of electricity), for the electricity profiles of the Danish spot and tertiary regulation market (2016).

The analysis of the demand hours for HP and ORC illustrated above shows how the required price difference between purchase and sale of electricity considerably reduces the potential operating hours of HP and ORC. A price difference between purchase and sale of electricity of 47.05 €/MWh$_{el}$, i.e. a reduction factor F_R = 1.0, means total (HP + ORC) operating demand of just about 3,000 hours per year. And as was already mentioned, the real operation hours are even lower due to the limitations of the HTTES.

The reason for the low operation demand of HP and ORC must be seen in the price profiles of the Danish electricity markets that were shown in Figure 8 in Chapter 3.1.3. As can be seen in that figure, there are only few hours with high and low prices for both the regulation and the spot electricity market. In most time of the year, the electricity price has a similar value, but this time cannot be used by the CHEST system, because it needs price differences that are high enough to compensate at least for the O&M costs and the fees and taxes that are subject to the electricity purchase and sale.

As will be shown more in detail in Chapter 6.2.3, it is not possible under such market conditions to generate sufficient economic profit in relation to the investment costs. Therefore, it was not reasonable to carry out detailed "optimization" concerning the sizing and setting parameters mentioned at the beginning of this chapter. Regardless of the selected values for the sizing and setting parameters, the business case is highly negative. As a consequence, the technical and operational KPIs are presented just for a selected example in the following.

The only optimization that was applied here was the implementation of flexible values for the buy-limit. This means, that not a fixed value was set for the buy-limit but different values during the year. This flexible setting was applied because a similar approach showed improved HP and ORC operation hours in the framework of T4.4, see Deliverable 4.4. However, here in T4.3, it was not possible to use the "optimizer" described in Deliverable 4.4, because this was a result at the end of the parallel Task 4.4 and it would have required major changes of the whole TRNSYS model. So, the flexible buy-limit approach followed here in T4.3 was much simpler and consisted of two main ideas:

- **Dependence of the buy-limit on the SoC of the LHS**: The higher the current SoC of the LHS, the lower the value for the buy-limit. As was shown in Figure 18, a decrease of the buy-limit (for a fixed reduction factor F_R) reduces the HP demand hours and increases the ORC demand hours. So, in times of a high SoC of the LHS, the demand hours are shifted towards more ORC demand and less HP demand in order to discharge the LHS and not get blocked by a completely charged LHS.
- **Monthly adaption of the buy-limit**: The abovementioned flexible setting of the buy-limit dependent on the SoC of the LHS already improves the operating hours of HP and ORC, but there are still longer periods with either predominantly HP or ORC demand, which leads to a blocking of CHEST operation by either completely charged or discharged LHS. Therefore, a monthly adaption of the buy-limit was added, which means that in months with predominantly HP demand, the buy-limit was lowered a bit and in months with predominantly ORC demand, the buy-limit was increased a bit.

Table 2 shows the sizing and setting parameters for an exemplary CHEST system in the Aalborg case study along with the simulation results for a fixed and for a flexible setting of the buy-limit, respectively. The reduction factor F_R was changed slightly for the flexible setting since this improved the economic balance a bit.

Table 2: Simulation results for an exemplary CHEST system.

Sizing parameter	Fixed buy-limit	Flexible buy-limit
HP nominal electric power [MW_{el}]	5.0	5.0
ORC nominal electric power [MW_{el}]	5.0	5.0
→ HP/ORC relative size	1.0	1.0
LHS capacity [MWh_{th}]	817.2	544.8
SHS capacity [MWh_{th}]	653.7	653.7
HTTES capacity [MWh_{th}]	1,470.9	1,198.5
Setting parameter	**Value**	**Comment**
Buy-limit [€/MWh_{el}]	0.0	flexible
Reduction factor F_R [-]	1.30	1.25
→ Required price difference between electricity purchase and electricity sale	36.19 €/MWh_{el}	37.64 €/MWh_{el}
Technical KPI	**Value**	**Comment**
COP [-]	6.54	6.26
ORC efficiency [%]	17.44	17.44
Efficiency of the LHS [%]	99.7	99.9
P2P ratio [%]	122.8	135.2
Electrical efficiency [%]	16.9	16.8
Thermal efficiency [%]	0.0	0.0
Overall energy efficiency [%]	16.9	16.8
Operational KPI	**Value**	**Comment**
HP demand time [h]	1,638	1,130
HP operation time [h]	606	855
→ Operation limitation by a completely charged LHS [h]	943	275
→ Operation limitation by a completely charged SHS [h]	89	0
ORC demand time [h]	1,359	1,395
ORC operating time [h]	764	1,186
→ Operation limitation by a completely discharged LHS [h]	595	207
→ Operation limitation by a completely discharged SHS [h]	0	2
Time in neither charging (HP) nor discharging (ORC) operation [h]	7,390	6,719
SHS recharging time [h]	199	693

The CHEST system considered here consists of a HP and an ORC with both a nominal electric power of 5 MW, which means a relative size of these two components of 1.0. The storage capacity of the HTTES in case of the **fixed buy-limit** is quite high and would theoretically allow for a full-load HP operation of about 45 h and a full-load ORC operation of about 51 h, respectively. However, as can be seen from the operational KPIs, there are still considerable times of HP and ORC operation limitation, especially by the LHS.

With the Buy-limit of 0 €/MWh$_{el}$ and the reduction factor F_R of 1.3 (which means a required price difference between electricity purchase and sale of 36.19 €/MWh$_{el}$) chosen, this results in a total HP + ORC demand time of about 3,000 hours, with a relatively equal distribution between HP and ORC. A closer look at the demand times shows that for the HP, there are only 64 hours of demand for electricity purchase from the spot market and 1,574 hours of demand for electricity purchase from the regulation market. For the ORC, this is 890 hours of demand for the sale of electricity at the spot market and 469 hours of demand for the sale of electricity at the regulation market.

Actually, as was said above, the HTTES storage is dimensioned quite large, which should result in lower limitation of the HP and the ORC operation. A closer look at the operation of the CHEST system shows that the actual reason for limitation of the HP and ORC operation by the state of charge of the HTTES does not lie in its size. Rather, it is the low fluctuation of the electricity prices that leads to the fact that the HP and ORC operation times are reduced considerably compared to the HP and ORC demand times.

For instance, there is a period of about 450 hours from late March until mid of April, where the LHS stays completely charged due to a lack of acceptable prices at both the spot and the regulation market that would cause a demand for the ORC to operate. However, there is a demand for HP operation of about 180 hours in the same period. This HP demand cannot be used due to the completely charged LHS. If there was a higher fluctuation of the electricity prices in that time causing a frequent change of HP and ORC demand times, the operation times for the HP and ORC would be higher for one and the same HTTES storage capacity. So, the reason for the eventually low HP and ORC operation times does not only lie in the low demand times as such, but also in the low fluctuation between HP and ORC demand.

As can be seen in Table 2, the **flexible setting of the buy-limit** changes the operation time of HP and ORC significantly, despite similar (ORC) or even lower (HP) demand times. The reason for this lies in the approach described above to couple the buy-limit to the SoC of the LHS (and furthermore, to adapt it monthly). This leads to a considerable decrease of the operation limitation by either a completely charged or a completely discharged LHS.

As a result, the optimization through the flexible buy-limit, compared to the fixed buy-limit, on the one hand leads to an increase of the total operation time of CHEST from 1,370 hours to 2,041, and on the other hand, also the LHS size could be reduced by about 30 %. From economic point of view, this means an increase of the annual profit from about 65,000 € to about 83,000 €, while simultaneously, the investment costs are reduced by about 25 % from about 102 million € to about 77 million € (for details refer to Chapter 6.2.3).

However, these numbers show that even with this optimized setting, the annual profits are much too low compared to the investment costs. The disadvantageous electricity price levels and profiles of the Danish electricity markets together with the given tax schemes and the relatively high O&M costs of the CHEST system do not allow for a profitable business case.

At least the key technical performance parameters are quite satisfying. The P2P ratio is very high, more than 120 % here. The main reason for this can be seen in the high COP of > 6 (which is mainly due to the high HP evaporation temperature of 100 °C) as well as the high ORC efficiency of 17.44 % (which is mainly due to the low ORC condensation temperature of 45 °C). A further effect on the P2P ratio is given by the recharge heat. As can be seen from the figures in Table 2, the P2P ratio is higher than the product of COP * ORC-efficiency. Actually, it should be vice versa considering the fact that there are thermal losses of the HTTES. However, the recharge heat that directly goes to the SHS is used at a later point of time (together with heat from the LHS) to drive the ORC and generate electricity. Thus, this recharge heat increases the electricity output and therefore the P2P ratio, but this is achieved at the expense of additional heat demand for this SHS recharge.

Due to the low ORC condensation temperature of only 45 °C, no heat from the ORC condenser is transferred to the DH network. Therefore, there is no heat output of the CHEST system and thus, its thermal efficiency is 0. Due to the required heat input (only excess heat here, no gas-fired auxiliary heat), which is considerably higher than the exchanged amounts of electricity, the electrical efficiency and the overall energy efficiency of the CHEST system are quite low, around 17 %. However, this is acceptable for such a case where we assume free excess heat and the only interest lies in the profit to be made from the exchange of electricity with the grid. At the cost of heat, the CHEST system is designed for maximum performance on the electricity side.

5.2. Simulation results for Ispaster case study

5.2.1. Results for the reference energy system (Battery storage)

The following paragraph briefly presents the most important results on the electric and thermal side for the reference energy system with the lead-acid batteries for Ispaster. Further results will later be shown in comparison to the CHEST system in Chapter 5.2.2 and 5.2.3 as well as in the techno-economic assessment in Chapter 6.

Figure 20 shows, which share of the annual electricity demand (23.5 MWh) is covered by the PV + Battery system dependent on the PV peak power and the gross capacity of the battery storage. With no battery installed, this share accounts for about 50 - 55 % dependent on the PV peak power. For the currently installed system in Ispaster, i.e. for a PV peak power of 25 kW_p (=100 PV panels) and a gross capacity of the battery storage of 197 kWh_{el}, the share of the annual electricity demand covered by this system is already quite high, ca. 83.5 %. A further increase of the battery capacity leads to an only minor increase of this share, i.e. the electricity that has to be purchased from the DSO is reduced only slightly.

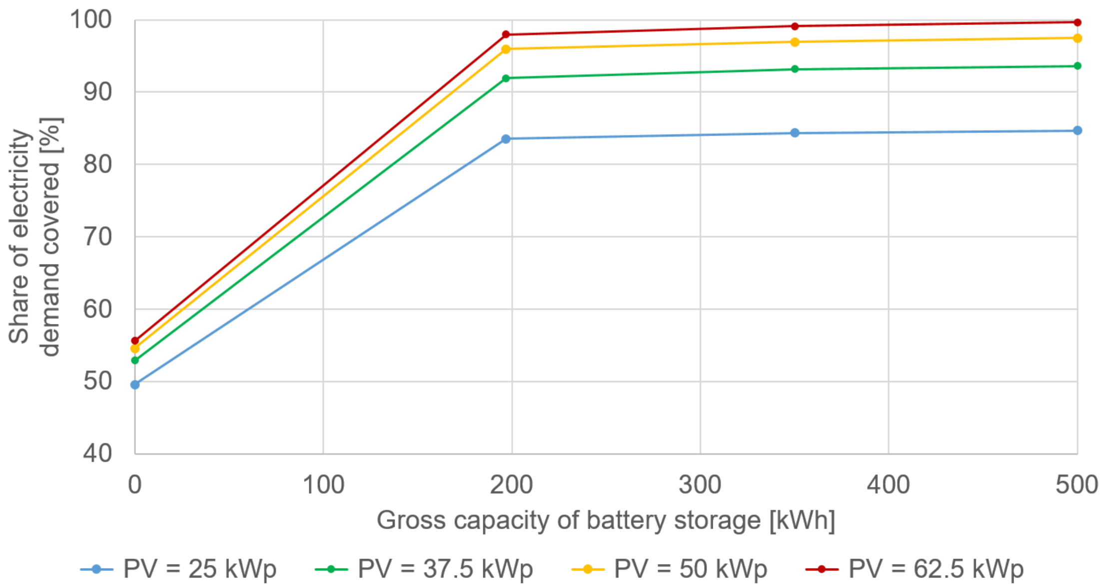

Figure 20: Share of electricity demand covered by the PV + Battery system for Ispaster 2.0.

Due to this, a rather high battery gross capacity of about 9,080 kWh is required to reduce the electricity purchase from the DSO down to 0 and so to achieve electric self-sufficiency for the PV + Battery system. For a PV peak power of 62.5 kW_p (= 250 PV panels), the battery gross capacity required to achieve self-sufficiency accounts for about 650 kWh, see Figure 21.

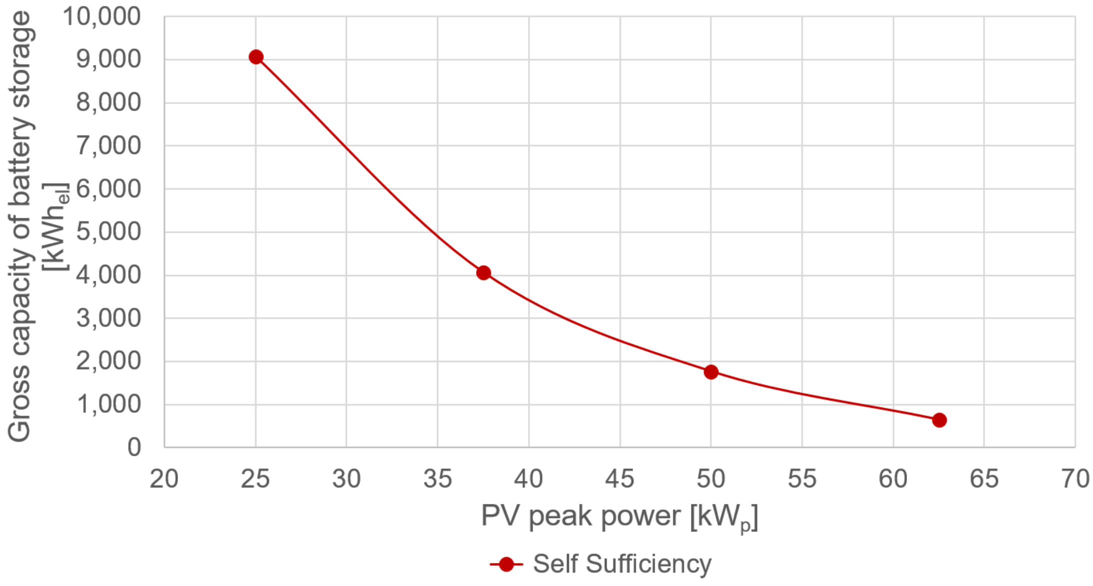

Figure 21: Required gross capacity of the battery storage depending on the installed PV peak power for the Ispaster Island case (self-sufficiency on the electricity side).

The thermal side, as was mentioned above, is completely independent of the electric side for the reference energy system. The annual gross heat demand of the DH network of about 108.4 MWh is covered by two sources: solar thermal collectors and a biomass (wood chips) boiler. For the currently installed collector gross area of 59 m², about one fourth of the DH heat demand is covered by solar heat as can be seen from Figure 22. If the installed collector gross area is doubled, about half of the heat demand is covered by solar thermal and by biomass, respectively. In case of a collector gross area of 177 m² (three times the currently installed area), solar thermal heat accounts for about 60 % of the annually required heat supply for the DH network.

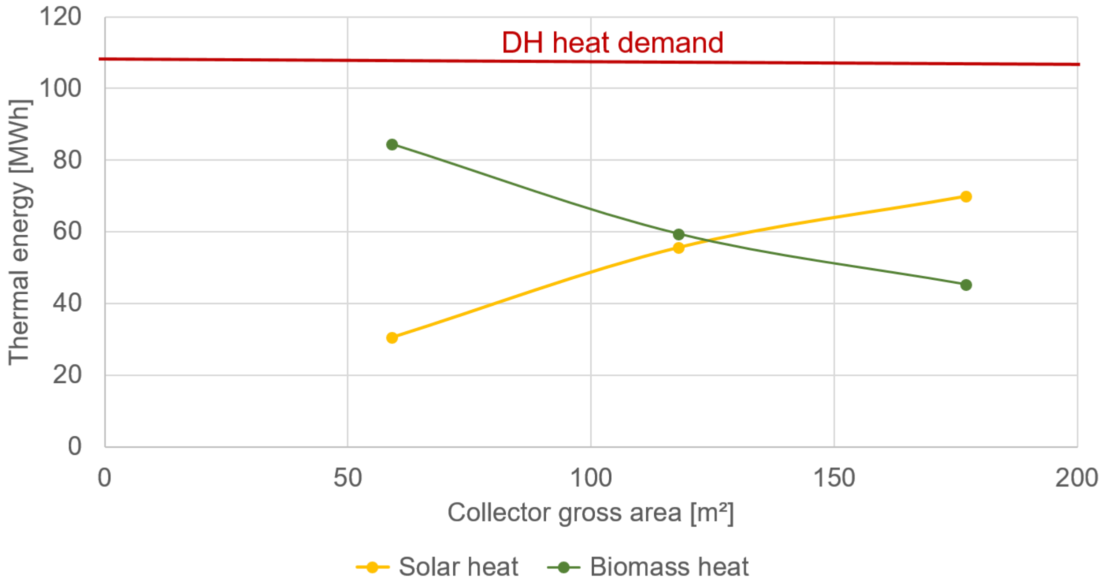

Figure 22: Dependence of solar and biomass heat on the solar thermal collector gross area for the reference energy system in the case of Ispaster 2.0.

5.2.2. Results for the CHEST system for Ispaster 2.0

The main question in the analysis of the CHEST system in Ispaster case study is if it is reasonable from an energetic, environmental and economic point of view to replace the currently installed lead-acid batteries by a CHEST system – or how such a CHEST system must be dimensioned and operated so that it is the favorable choice in comparison to the battery storage, respectively. So, the first run of simulations for the CHEST system was done for the current electric boundary conditions, i.e. for a PV peak power of 25 kW_p and a storage gross capacity of 197 kWh_{el}. As this storage capacity of the battery is purely electric, but in the CHEST system, energy is stored thermally, this electric storage capacity was converted to equivalent thermal storage capacity with the help of the following equation:

$$Equivalent\ thermal\ storage\ capacity = \frac{Electric\ storage\ capacity\ of\ the\ battery * Battery\ efficiency * Battery\ utilization\ factor}{Predicted\ ORC\ efficiency}$$

$$Equivalent\ thermal\ storage\ capacity = \frac{197 kWh_{el} * 70\% * 60\%}{11\%} \approx \boldsymbol{752\ kWh_{th}}$$

The partitioning of this storage capacity for the two storage parts of the HTTES was chosen to be about 420 kWh for the LHS and 332 kWh for the SHS, because this is about the ratio of latent to sensible heat in discharging operation for the combination of R1233zd(E) as refrigerant, KNO_3-$NaNO_3$-$NaNO_2$ as PCM and 70 °C as refrigerant-side ORC condensing temperature.

The run of simulations was done for a varying ORC nominal electric power of 0.5…4.5 kW_{el} and a fixed ratio of HP and ORC nominal powers of 4, i.e. the HP nominal electric power varied in the range 2…18 kW_{el}. All simulations were done for a solar thermal collector gross area of 118 m^2. Recharge of the SHS was only done if there is neither HP nor ORC operation and if the fluid level (= state of charge) of the HTWT lies below 35 %. This value of 35 % was found to be a good compromise to start the recharge neither too early (resulting in higher required amount of heat for the recharge) nor too late (resulting in too many hours of completely discharged SHS and therefore a blocking of the ORC operation).

Figure 23 shows the electricity consumption of the HP and the electricity generation of the ORC depending on the nominal electric power of the HP. As can be seen from that figure, the increase of HP electricity consumption and ORC electricity generation with increasing HP sizes is sharp for low HP sizes but begins to flatten at an HP nominal electric power of about 10 kW.

The P2P ratio is almost independent of the HP size and accounts for about 65 - 69 %. The same is noticed for the ORC efficiency (about 10.6 %) and the COP of the HP (ca. 5.8 - 6.2). These quite constant performance parameters are due to the constant evaporation and condensation temperature levels in the HP and ORC cycles. Again, it can be seen here that the P2P ratio is slightly higher than the product of COP * ORC-efficiency because of the recharge heat which leads to a slight increase of the electricity output of the CHEST system.

Figure 24 shows the decrease of the remaining grid electricity, which has to be purchased from the DSO depending on the size of the HP. For a CHEST system with a nominal electric power of the HP of 2 kW_{el}, the remaining grid electricity accounts for about 9.62 MWh/a, while it is only 3.94 MWh/a for a CHEST system with a nominal electric power of the HP of 18 kW_{el}. The battery storage with a gross capacity of 197 kWh_{el} results in an even lower value of only 3.83 MWh/a. Just for comparison: with no electric storage installed, the remaining grid electricity to be purchased from the DSO would account for 11.84 MWh/a.

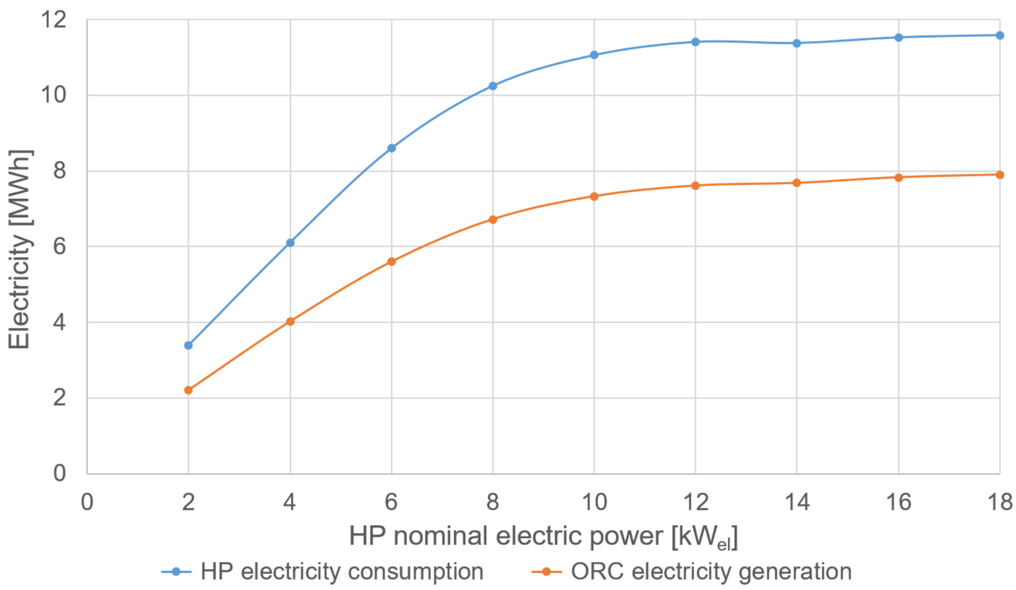

Figure 23: Dependence of HP electricity consumption and ORC electricity generation on the nominal electric power of the HP for a CHEST system with a HTTES capacity of 752 kWh_{th}.

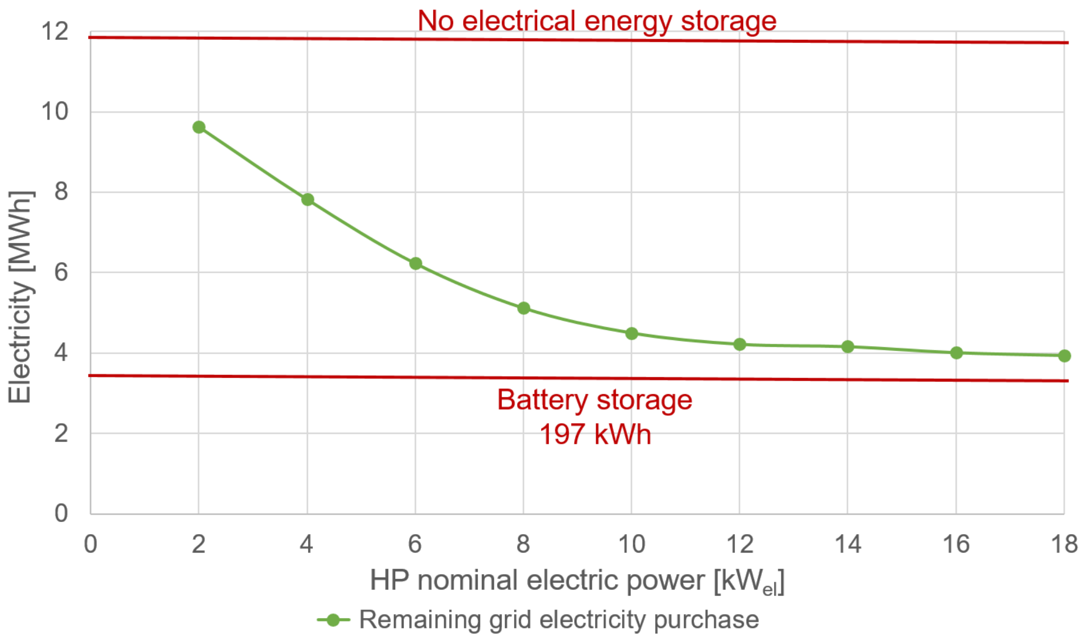

Figure 24: Dependence of remaining grid electricity purchase from the DSO on the nominal electric power of the HP for a CHEST system with a HTTES capacity of 752 kWh$_{th}$, compared to an equivalent battery storage and the situation without any electrical energy storage.

The conclusion based on these figures from the electric side is that the HP and ORC size and perhaps also the HTTES size needs to be slightly higher to result in a similar reduction of the purchased grid electricity from the DSO like the battery storage. More discussion on that is given below with Figure 27.

On the thermal side, as observed several times before, the operation of the CHEST system leads to an increased heat demand and thus to an increased demand of biomass compared to the situation without electrical energy storage or with battery storage as is shown in Figure 25. As was mentioned above, the battery storage does not influence the thermal side and therefore, the biomass demand is the same as for a situation without any electrical energy storage. The annual biomass demand in this reference energy system accounts for about 62.6 MWh. As can be seen from Figure 25, the biomass demand is always higher for the CHEST system and it increases with increasing size of the HP, at least for HP nominal powers of > 6 kW$_{el}$.

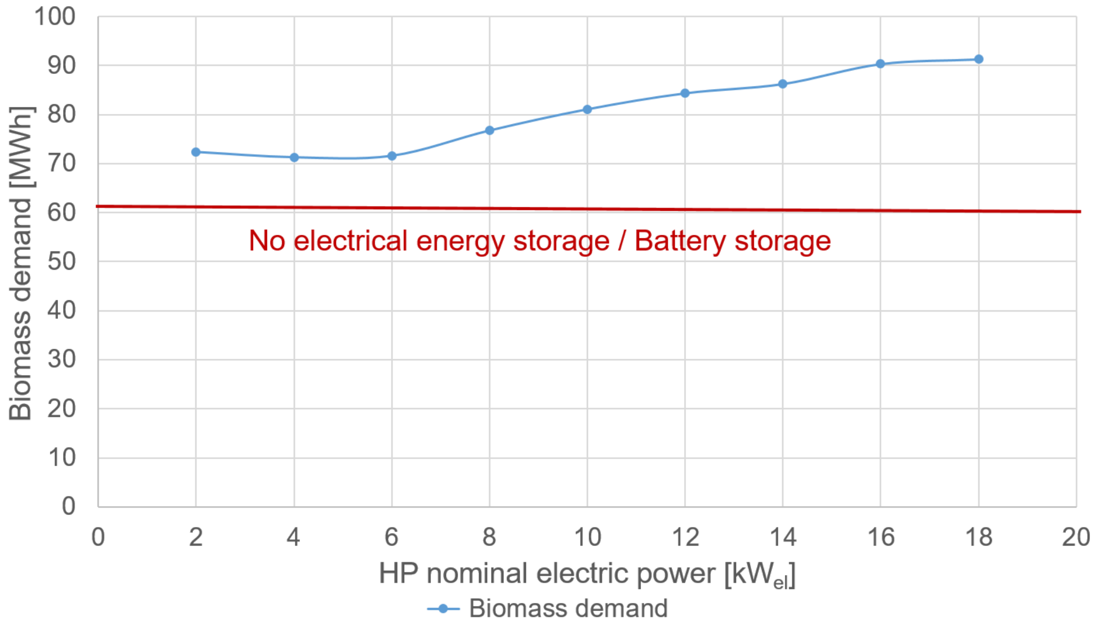

Figure 25: Dependence of the biomass demand on the nominal electric power of the HP for a CHEST system with a HTTES capacity of 752 kWh$_{th}$, compared to the battery storage and the situation without any electrical energy storage.

There are several reasons for the increased biomass demand of the CHEST system here:

First of all, the solar thermal yield is a bit lower, about 7 MWh/a lower, due to the higher temperatures needed at the HP evaporator compared to the DH forward temperature. This reduction of the solar thermal yield is quite independent of the HP size; the collector gross area is a more important influence factor and this was the same (118 m²) for both the CHEST system and the battery storage simulations.

Secondly, there is an additional biomass demand for the compensation of the SHS thermal losses (about 0.6 MWh/a) and thirdly, also for the SHS recharge (about 1.0 - 2.2 MWh/a). These two parts are also relatively independent of the HP size because they mainly depend on the SHS size and this was the same for all simulations.

The 3 effects summed up, results in an increase of the biomass demand of the CHEST system compared to the battery storage of roughly 10 MWh/a. This is visible in Figure 25 for HP nominal electric powers of 2 - 6 kW$_{el}$. For HP sizes > 6 kW$_{el}$, the difference of the biomass demand between CHEST system and battery storage increases further and the reason for this can be recognized by the two curves shown in Figure 26.

The yellow curve shows the total heat that is available at the ORC condenser, while the green curve stands for a part of this heat, which is transferred to the DH network, i.e. which is really used for heating purposes later. As can be seen from Figure 26, basically all the heat that is available at the ORC condenser is transferred to the DH network for HP nominal electric power of up to 6 kW$_{el}$. For higher HP sizes, the usable condenser heat in principle remains constant while the total available ORC condenser heat increases. This is due to the fact that there are times, especially in summer, when the available ORC condenser heat exceeds the heat demand of the DH network. This means, that the ORC condenser heat is only partly transferred to the DH network and partly, it must be transferred to the ambient and therefore, it is lost. As there is a certain heat input into the CHEST system at the HP evaporator, this lost thermal energy finally results in an increased biomass demand, which increases with increasing HP size.

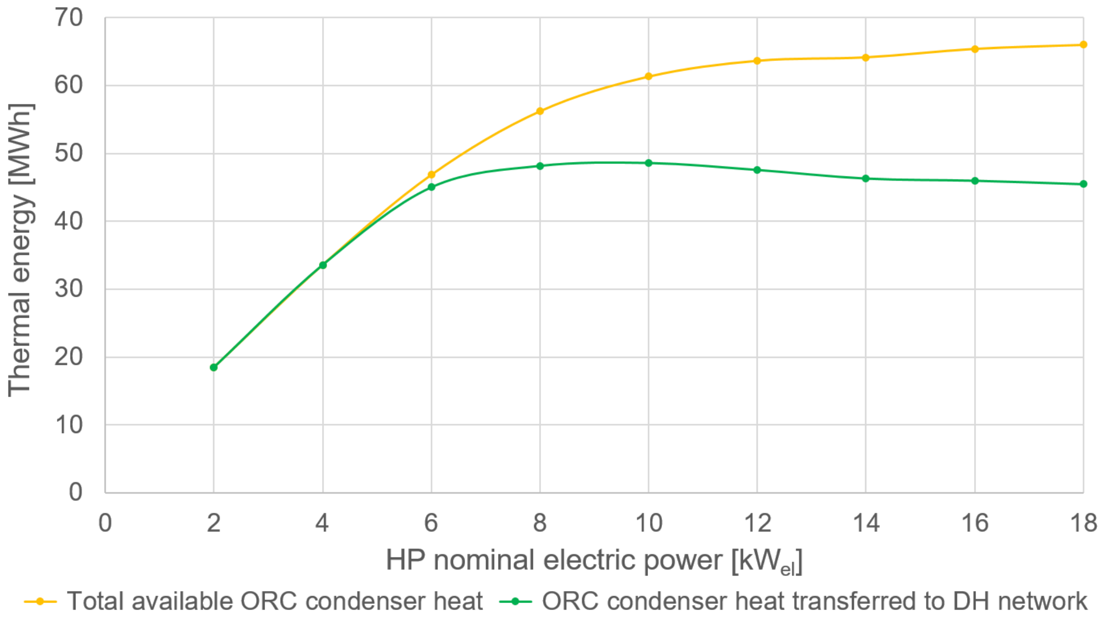

Figure 26: Dependence of the total available heat at the ORC condenser and the ORC condenser heat that was transferred to the DH network, on the nominal electric power of the HP for a CHEST system with a HTTES capacity of 752 kWh$_{th}$.

The conclusion from the figures above clearly is that the CHEST system is disadvantageous on the head side compared to the battery storage, because the CHEST system is a net heat consumer, whereas the battery system does not affect the heat demand at all.

In a second run of simulations, the installed PV peak power as well as the HTTES size were varied in order to analyze how this improves the reduction of the grid electricity purchase from the DSO. The main result of these simulations, carried out for two different HP and ORC sizes, is shown in Figure 27.

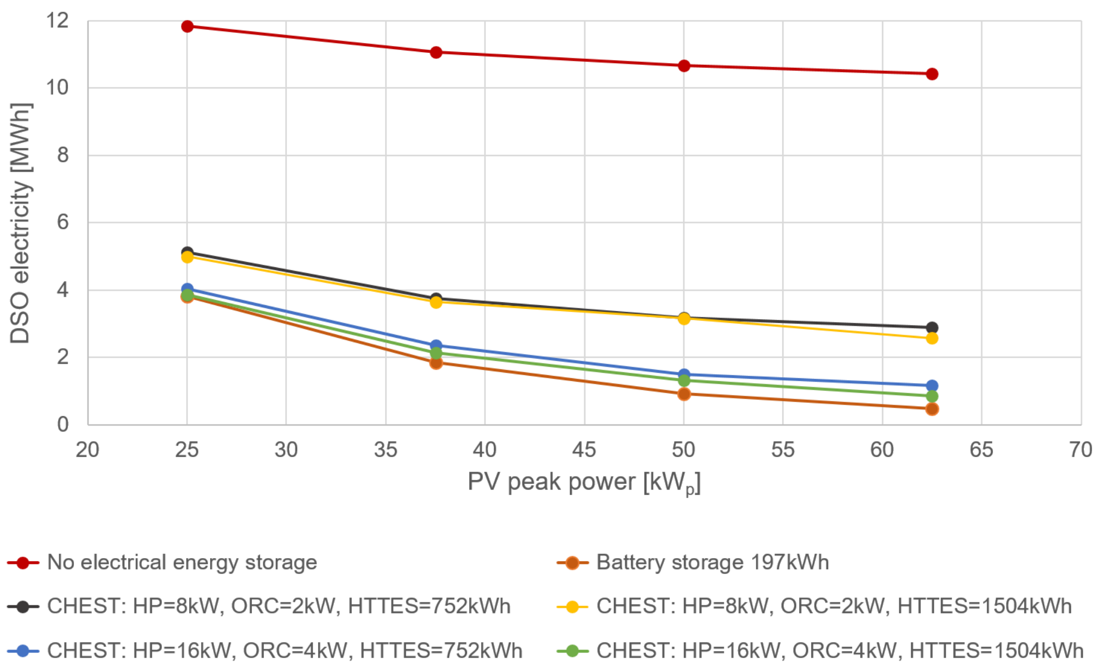

Figure 27: Dependence of remaining grid electricity purchase from the DSO on installed PV peak power and the HTTES storage capacity, compared to the battery storage and the situation without any electrical energy storage.

Figure 27 shows that doubling the storage capacity of the HTTES has almost no effect on the grid electricity to be purchased from the DSO. Rather, it is more decisive to increase the HP and ORC nominal power to reduce the electricity purchase. The battery storage is still the best option here despite the increase of the HTTES size for the CHEST system. This is partly due to the bit higher P2P ratio (70 % for the battery storage compared to about 65 - 69 % for the CHEST system), but mainly, this is due to the higher charging and discharging power of the battery of 20 kW_{el}.

Concerning the installed PV peak power, it must be said that for the Ispaster 2.0 case, the increase of the installed PV peak power only slightly reduces the electricity purchase from the DSO by few MWh per year. On the other hand, the PV curtailment is increased far more, from less than 10 MWh/a for an installed PV peak power of 25 kW_p up to almost 60 MWh/a for an installed PV peak power of 62.5 kW_p. This is due to the fact that the currently installed PV peak power of 25 kW_p is already quite sufficient to cover a high share of the electricity demand of Ispaster as was shown in Figure 20. So, the conclusion is that for Ispaster 2.0 case, the increase of the installed PV peak power is only slightly beneficial. In contrast to that, as will be shown in the next chapter, an increase of the installed PV peak power is more advantageous in the Ispaster Island case, because it reduces the required storage capacities for achieving electrical self-sufficiency considerably.

5.2.3. Results for the CHEST system for Ispaster Island

As was mentioned in Chapter 4.4, the refrigerant used for Ispaster Island simulations was R601 due to its higher P2P ratio compared to R1233zd(E). This reduces the required LHS capacity, which is the main factor of the investment costs of the CHEST system. The PCM used was the same as for Ispaster 2.0, i.e. KNO_3-$NaNO_3$-$NaNO_2$ with a melting temperature of 142 °C. The temperature levels for the HP evaporator and the ORC condenser (refrigerant-side) were 82 °C and 46 °C, respectively.

In contrast to Ispaster 2.0 simulations, a fixed partitioning of the HTTES into the two storage parts LHS and SHS was not applied here. The procedure was rather to get the lowest possible size for both parts to still achieve electrical self-sufficiency. The required size of the HTTES, i.e. of the LHS and the SHS, depends on the installed PV peak power and the HP nominal power. As for the battery storage, the installed PV peak power was varied in the range 25…62.5 kW_p (which is equal to a number of PV panels of 100…250). Regarding the HP nominal electric power, different relative HP/ORC sizes were chosen (see below). The ORC size (nominal electric power) was the same for all simulations. It accounted for 4.413 kW_{el}, according to the following equation:

$$Required\ ORC\ nominal\ electric\ power = \frac{Maximum\ electricity\ deficit}{Ratio\ between\ net\ and\ gross\ ORC\ electricity\ generation}$$

$$Required\ ORC\ nominal\ electric\ power = \frac{4.21 kW_{el}}{0.954} \approx \boldsymbol{4.413\ kW_{el}}$$

As was shown in Chapter 3.2.3, the maximum electric power demand accounts for about 5.5 kW, but this occurs at times when there is also PV electricity generation. So, the actual maximum electricity deficit that occurs during a year is smaller here, just 4.21 kW. The ORC must be able to generate this electric power, but as the net electricity generation of the ORC is a bit lower than its gross generation (its nominal power), the ratio between net and gross generation needs to be considered. For the given fluid and temperature levels in the ORC cycle, this ratio accounts for about 0.954.

For PV peak powers of 32.5, 50 and 62.5 kW_p, four different relative HP/ORC sizes were used for the simulations: 4.0, 3.0., 2.0 and 1.217, the latter one being the “optimum sizing ratio” used in the refrigerant and PCM analysis in Task 4.4. A ratio of 1.0 was by the way not used, because it turned out not to be possible to achieve self-sufficiency with such a small HP size. For a PV peak power of 25 kW_p, it was not even possible to achieve this for the ratio of 1.217, irrespective of the HTTES size; that is why the respective data point is missing in Figure 28 below. So, the HP nominal powers used for the aforementioned PV peak powers were: 17.652, 13.239, 8.826 and 5.371 kW.

All simulations were done for a solar thermal collector gross area of 118 m². Recharge of the SHS was only done if there is no HP operation at that point of time, i.e. recharge was also allowed to happen in parallel to the ORC operation. As was mentioned in Chapter 4.2, this was necessary, because otherwise, recharge would very rarely happen here. If the recharge is only allowed when there is neither HP nor ORC operation, then it only happens if this HP or ORC operation is limited by a completely charged or completely discharged LHS/SHS storage, respectively, because there is always an electric surplus or deficit and thus a demand for either driving the HP or the ORC. But for achieving electrical self-sufficiency, the LHS and the SHS storage are not allowed to get completely discharged, because otherwise, there would be no thermal energy to drive the ORC and thus, grid electricity would have to be purchased to compensate for the electricity deficit. So, recharge could only happen at a point of time when the LHS or SHS were completely charged (or if there is a heat availability limit for the HP evaporator). In principle, there are enough hours where this is given, however, only in summer, because in summer, there is a lot of excess PV electricity generation and thus HP operation, which charges both the LHS and the SHS. So, SHS recharge is not required in summer, but above all in winter, when the SHS gets more and more discharged due to the need for ORC operation since the PV generation is now lower than the electricity demand.

So, in order to allow for recharge also in winter and thus to be able to keep the SHS size small, recharge was also allowed to happen in parallel to the ORC operation. Beside the limit of the recharge concerning HP/ORC operation, the second condition for the initiation of the recharge was that the fluid level (= state of charge) of the HTWT lies below 30 %. The bit lower value of 30 % compared to 35 % used in Ispaster 2.0 case (see Chapter 5.2.2). was found to give better results in the Ispaster Island case.

Figure 28 shows, which HTTES capacities are required to achieve electrical self-sufficiency, dependent on the PV peak power and the relative HP/ORC size. It can be seen from this figure that the required HTTES capacity, which is a main factor of the investment costs of the CHEST system, decreases with increasing HP/ORC relative size. However, a HP/ORC relative size of 3.0 is actually enough, because a further increase of the relative HP/ORC size has only negligible effects.

Furthermore, the currently installed PV peak power of 25 kW_p leads to quite high required HTTES capacities and therefore, the PV peak power should be increased to 50 kW_p. A further increase to 62.5 kW_p has only small effects on the required HTTES capacity.

For comparison, the required gross capacity of the battery storage (cf. Figure 21) is also plotted in Figure 28, but note that this is an electrical storage capacity (MWh_{el}), whereas the HTTES storage capacity is thermal (MWh_{th}).

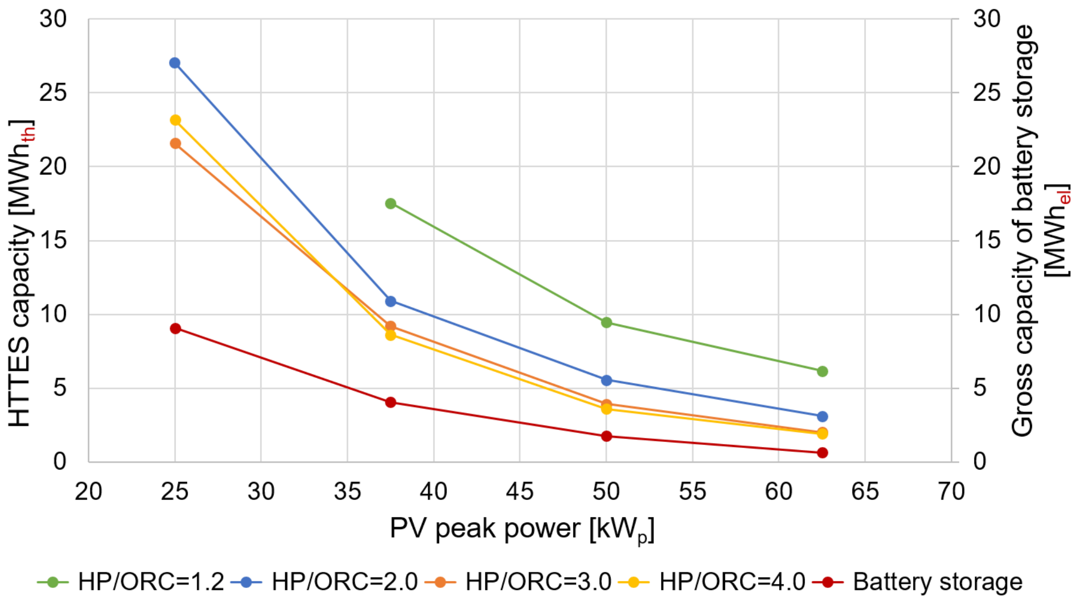

Figure 28: Dependence of the required HTTES capacity on the installed PV peak power and the HP/ORC relative size to achieve electrical self-sufficiency.

The COP of the heat pump accounts for about 6.2 - 6.4 and the ORC efficiency accounts for about 14.1 %. Both the COP and the ORC efficiency are almost independent of the CHEST size, because, as mentioned above for the Ispaster 2.0 simulations, the decisive temperature levels do not change and this is the main factor for the HP and ORC efficiency. The P2P ratio is quite high here, about 95 - 101 %. If you just multiply COP and ORC efficiency, this number seems a bit too high, but the reason for this comes from the heat side. Namely, there is the additional heat input of the SHS recharge, which is partly also taken for converting stored heat back into electricity.

Taking a look at the thermal behavior of the CHEST system again shows that the CHEST system is a net heat consumer. The heat input into the CHEST system accounts for about 68 - 85 MWh/a, whereas the **useful** heat output of the system accounts for just 54 - 61 MWh/a. Figure 29 highlights the origin of this gap. The curves shown in this figure were generated from the average values of the simulation results for the different HP/ORC relative sizes.

First of all, there is a certain amount of heat required for the compensation of the thermal losses of the SHS (blue line). It can be recognized that these thermal losses decrease with increasing PV peak power. This is given by the fact that the required HTTES capacity (and as a part of it also the SHS storage) decreases with increasing PV peak power as was shown in Figure 28.

The thermal losses of the LHS are not compensated by an external heat source. That is why the heat required for this is not visible in Figure 29. However, the thermal losses of the LHS also affect the thermal balance of the CHEST system, because the compensation of the LHS thermal losses eventually requires an increase of the HP operation and this needs heat at the HP evaporator.

As was mentioned in Chapter 5.2.2, there is a certain amount of ORC condensation heat that cannot be transferred to the DH network, because especially in summer, there is more ORC condensation heat than there is heat demand of the DH network. As you can see from Figure 29, this unused ORC condensation heat (green line) is almost independent of the PV peak power.

It is also almost independent of the HP size (not shown here), because the ORC size is the decisive parameter for the amount of heat available at the ORC condenser and the ORC size was always the same (nominal electric power of 4.413 kW_{el}).

A further effect on the thermal balance of the CHEST system is given by the heat that is required for the recharge of the SHS (orange line). This heat accounts for about 9 - 14 MWh/a, with no clear dependence on PV peak power and on HP size.

The red line in Figure 29 shows the sum of the three effects indicated by the blue, the orange and the green line. A clear decrease of the total additional heat required with increasing PV peak power (and thus with decreasing CHEST storage size) can be recognized. This is in line with the previous findings, namely, that the CHEST system is a net heat consumer and this net heat consumption will be more pronounced the bigger the CHEST system is.

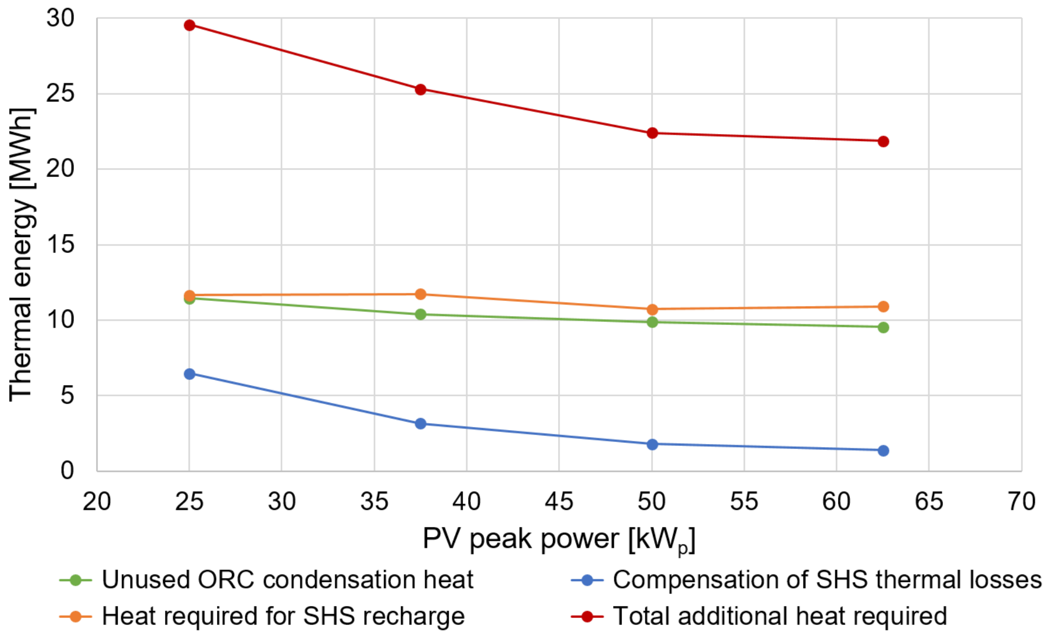

Figure 29: Contributors to the additional heat requirement for the CHEST system, depending on the installed PV peak power.

The consequence of this additional heat required for the CHEST system is a higher biomass demand compared to the battery storage. As was mentioned several times before, battery storage does not affect the thermal side and therefore, the biomass demand is always the same (62.6 MWh/a), irrespective of the battery capacity.

Figure 30 shows this comparison as regards to the annual biomass demand between the CHEST system and the battery storage. For the CHEST system, the blue curve was generated from average values for the different HP/ORC relative sizes.

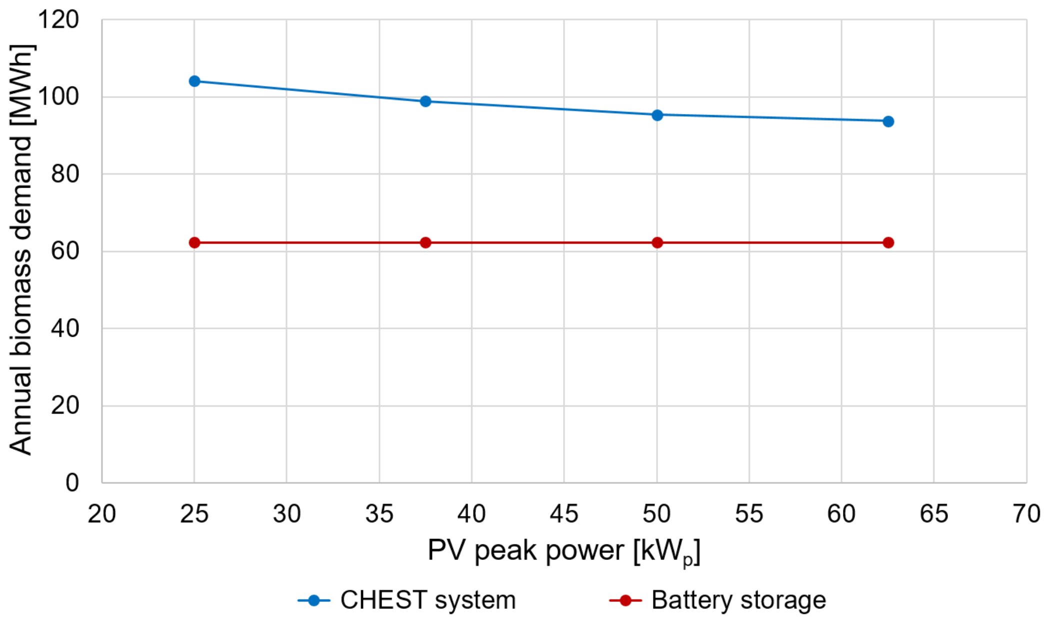

Figure 30: Dependence of the annual biomass demand on the installed PV peak power to achieve electrical self-sufficiency.

If you compare Figure 29 and Figure 30, you can see, that the additional biomass demand (Figure 30) is higher than the total additional heat (Figure 29) required. On the one hand, this is due to the conversion factor between heat and biomass, i.e. the efficiency of the biomass boiler, which is 95 % here. On the other hand, the CHEST system also leads to lower solar yields and thus to a higher biomass demand due to the fact that in the simulations, one collective thermal storage for covering DH heat demand and HP evaporator heat demand was modelled and the relatively high HP evaporator temperature (refrigerant-side) of 82 °C compared to only 60 °C forward temperature required for the DH network reduces the useful solar yield into the storage.

A more detailed modelling of the thermal circuit of the Ispaster case study with single storages for the solar collectors, the biomass boiler, the DH system and the HP evaporator would probably improve this solar yield. Nevertheless, it gets very clear from the results shown above that there is an increase of biomass demand for the CHEST system compared to the battery storage.

6. Techno-economic assessment

Several KPIs, particularly of the first and second group (technical and operational KPIs) were already shown in Chapter 5 of this deliverable in the simulation results. Chapter 6 will therefore deal with the KPIs of the other three groups (energetic, environmental and economic KPIs).

As was already said in the introduction, the environmental KPIs and some of the energetic KPIs (energetic payback time) will be treated more in detail in the upcoming Task 4.6, because at the moment, no sound correlations for the primary energy demand and for the CO_2 emissions for the production, installation and removal of a CHEST system are available. Preliminary values that were used for this analysis are yet presented in Chapter 6.

6.1. Overview on boundary conditions used for the analysis

6.1.1. Energetic and environmental assessment

For the assessment of the CHEST system from energetic and environmental point of view, the following factors have to be defined:

- **PEF** (Primary energy factor) and **CEF** (CO_2 emission factor) of the respective energy source/carrier:
  - Aalborg case study: grid electricity, excess heat, natural gas
  - Ispaster case study: grid electricity, photovoltaics (PV), solar thermal, wood chips
- **CED** (Cumulative energy demand) and **GWF** (Global warming factor) for the production, (installation) and removal of the respective energy system:
  - CHEST system consisting of an HP, an ORC and the HTTES (LHS + SHS)
  - lead-acid batteries (Ispaster case study only)

As was stated in Chapter 2.4.3, the primary energy factors consider the **non-renewable share** of primary energy. And as was mentioned in Chapter 2.5.1, the CED values consider a period of 100 years for the global warming potential (GWP_{100}) of the respective source of emission. Table 3 shows the PEF and CEF values that were used in the analysis for the respective energy carrier in each case study.

For Aalborg case study, PEF and CEF values provided by PlanEnergi for the Danish electricity mix and for the several heat generators in Aalborg (for details see also Deliverable 4.3) were used. Electricity in Denmark is characterized by a high share of renewables of 71 %, which mostly comes from wind and biomass and to a smaller extent from PV and biogas. Around 20 % of the Danish electricity is generated by coal-fired power plants, another 6 % comes from natural gas and the remaining 3 % from oil and other combustible sources. This gives a relatively low non-renewable PEF value of 0.389 and a CEF value of 0.157 t/MWh. In contrast to that, the PEF and CEF values of the Aalborg excess heat are considerably higher since a high share of the heat comes from coal-fired CHP plants.

The Spanish electricity mix is characterized by a much lower share of renewables of < 40 % and significant shares of fossil fuels (coal, natural gas, oil and others) of 40 % and nuclear power of around 20 %. This gives a much higher non-renewable PEF value and also a higher CEF value compared to Denmark. The PEF and CEF values for the renewable sources PV, solar thermal and biomass (wood chips) are naturally very low.

Table 3: Primary energy factors (PEF) and CO_2 emission factors (CEF) used for the analysis.

Energy carrier	$PEF_{non-renewable}$ [-]	CEF [t/MWh]	Reference/remark
Aalborg case study			
Grid electricity	0.389	0.157	[PlanE 2020]
Excess heat	0.603	0.238	[PlanE 2020]
Natural gas	1.100	0.185	[PlanE 2020]
Ispaster case study			
Grid electricity (Spain)	2.007	0.214	PEF from [RITE 2016], CEF from [TEC 2020]
PV (polycrystalline)	0	0.040	PEF per definition, CEF from [IWU 2020]
Solar thermal (vacuum tube collectors)	0	0.034	PEF per definition, CEF from [IWU 2020]
Wood chips	0.0085	0.018	[RITE 2016]

As was stated above, it is at the moment very difficult to estimate the cumulative energy demand and the carbon emissions for the production, installation and removal of a CHEST system. Due to very little data, it was decided only to consider the production phase, but no installation and removal phase. Available data from earlier projects and the literature were related to the characteristic size parameter of the respective component. Table 4 lists the values that were used for the analysis:

Table 4: Cumulative energy demand (CED) and Global warming factors (GWF) used for the analysis.

Component	CED_P	GWF_P	Reference/remark
CHEST system			
Heat pump	0.035 MWh/kW_{el}	24.11 kg/kW_{el}	[TEC 2020]
ORC engine	0.311 MWh/kW_{el}	82.26 kg/kW_{el}	[TEC 2020]
LHS	0.00863 MWh/kg + 0.005 MWh/m^3	2.85 kg/kg + 1.29 kg/m^3	[ECO 2014] [TEC 2020]
SHS	0.005 MWh/m^3	1.29 kg/m^3	[TEC 2020]
Electrical energy storage			
Lead-acid batteries	0.034 MWh/kWh_{el}	9.52 kg/kWh_{el}	[Valv 2009]

As will become more obvious later with the presentation of the results, the PCM is the major factor for the cumulative energy demand and the CO_2 emission of the production of a CHEST system. In the literature, quite different values are reported for several PCMs, for example by Johannson and Norrman [Joh 2019], Lamnatou et al. [Lam 2018], Carbonaro et al. [Carb 2015], Noel et al. [Noel 2015] and Miro et al. [Miro 2015]. The PCMs discussed in these sources do not really match the PCMs used in T4.3, i.e. $LiNO_3$-$NaNO_3$-KCl (45-50-5 wt.-%) for Aalborg case study and KNO_3-$NaNO_3$-$NaNO_2$ (53-6-41 wt.-%) for Ispaster case study. Therefore, data from the ecoinvent 3.1 database [ECO 2014] were used, which contains datasets for the single salts that the two PCMs are composed of, except for $LiNO_3$. As the lithium salt is not listed in the ecoinvent database, only the PCM of the Ispaster case study could be calculated, based on the respective weight percentages of the single salts given above. The CED and GWF values for this PCM were then also used for the Aalborg case study.

Since the mass-based values of the ecoinvent database only apply to the production of the PCM itself, but not to the whole LHS, the volume-based values of the SHS are added in order to also consider the storage tank and not just the storage medium.

6.1.2. Economic assessment

The economic assessment was based on the calculation of the economic KPIs presented in Chapter 2.6, where applicable. The calculation period for the economic assessment was defined to be 30 years, which is the expected lifetime for the CHEST system; for more details, see Chapter 6.1.3. The following general boundary conditions apply to the dynamic economic calculations:

- interest rate (nominal): 5.0 %
- inflation: 1.5 %
- interest rate (real): 3.5 %
- average increase in energy prices (real): 3.0 %

In Aalborg case study, a CHEST system is installed to make profit from the participation in both the spot and regulation electricity market. The electricity price profiles of these two markets used for the economic calculations were shown in Chapter 3.1.3. The heat required to operate the HP of the CHEST system was not considered as a fuel cost because it is free excess/waste heat. The heat delivered by the ORC of the CHEST system is not classified as useful heat due to its low temperature level. Therefore, there are no revenues from the sale of heat and thus, electricity is the only form of energy to consider in the economic calculations.

In the Ispaster case study, the storage costs for the two storage solutions CHEST system vs. lead-acid batteries were compared with each other and for Ispaster 2.0 also with the case without EES. For Ispaster Island it does not make sense to consider the case without EES, because then an island system would not be possible.

In addition, PV revenues were not considered, i.e., it is assumed that PV generation is curtailed, since the injection of PV electricity into an electrical energy storage system does not provide an economic advantage compared to a situation without EES. Considering PV yields would worsen the economic evaluation of both the CHEST system and the battery storage system compared to the situation without electrical storage, since the available PV surplus and thus the electricity export is higher in the situation without electrical energy storage. And in the case of Ispaster Island, no grid connection is considered anymore anyway; thus, PV power injection is not physically possible in this case. In addition, no cost reduction for terminating the DSO contract was considered in the Ispaster Island case. Fuel costs arise from the purchase of biomass (wood chips) at a price of €25.6/MWh, as indicated in Section 3.2.3.

The direct CO2 emission costs were not considered.

In terms of lifetimes and investment costs, the following values apply, most of them have already been reported in D6.2:

Table 5: Lifetimes and specific investment costs used for the economic analysis.

Component	Lifetime [a]	Specific investment costs
CHEST system		
Heat pump	30*	500,000 €/MW_{th}
ORC engine	30	800,000 €/MW_{el}
LHS	30	90,000 €/MWh_{th}
SHS	30	830 €/m^3
Electrical energy storage		
Lead-acid batteries	15/(10)	180 €/kWh_{el}

*Need for major replacements after 20 years, estimated half of the specific investment costs

In some scenarios, as will be shown later with the results, future reduced costs of the CHEST components apply. For this, we assumed that the HP and the ORC are no longer two separate components, but a single one. Therefore, the average of the two component´s costs was taken in this case, and no replacement costs after 20 years arise then. Furthermore, it was also analyzed how a shorter lifetime of the batteries of only 10 instead of 15 years affects the Ispaster business case. A more detailed discussion on the assumed lifetimes is given in Chapter 6.1.3.

Table 6 lists the assumed specific operation and maintenance costs (O&M costs) for the CHEST system and for the battery storage. The values were directly taken from D6.2.

The O&M costs for the batteries are expressed in € per kW charging/discharging power and year. In Ispaster case study, the charging and discharging power of the batteries is 20 kW; so, the O&M costs account for 178 € per year. For the CHEST system, the O&M costs are expressed in € per MWh of electricity that were consumed by the HP or generated by the ORC, respectively. O&M costs, as the name infers, include all costs (e.g. personnel costs) required for the operation and maintenance of the system. Fuel costs, i.e. electricity and heat required for charging, are not included in the O&M costs, but accounted for separately.

Table 6: Specific O&M costs used for the economic analysis.

Component	Specific investment costs
CHEST system	
Heat pump	10 €/MWh_{el}
ORC engine	15 €/MWh_{el}
HTTES (LHS + SHS)	0
Electrical energy storage	
Lead-acid batteries	8.9 €/(kW*a)

6.1.3. Assumed lifetimes

The assumption of the lifetime of a storage system or its components can have a major influence on the outcome of the economic assessment, but also on the environmental assessment. As several experts in this field of research agree, a lifetime of 30 years is absolutely reasonable for types of thermomechanical storage in general and the CHEST system in particular. [Olym 2021]. However, it is also important to look at the single components of a storage system and identify critical parts that might have to be replaced earlier. Therefore, a more detailed discussion of the values presented above in Table 5 is given in the following to show that the lifetime assumptions are justified.

<u>HP and ORC</u>

The heat pump (HP) is probably the most critical component with regard to lifetime, with the compressor as the most vulnerable part, especially its impeller, bearings and shaft seal. For large-scale heat pumps with a thermal output of > 1 MW_{th}, David et al. reported that also other parts of the heat pump, such as engine, gears, coupling, tubes in heat exchangers and computer systems might require replacement after 20 - 30 years of operation. On the other hand, the authors also reported that the world´s largest seawater heat pumps with a thermal output of 250 MW_{th} operate for more than 30 years at average seawater temperatures as low as 3 °C [David 2017]. For large heat pumps applied in district heating systems, Wang assumed 25 years as lifetime for his cost calculations [Wang 2018].

Given the unusually high heat supply temperatures of the HTHP in a CHEST system of up to 150 °C and even beyond, the HTHP can be evaluated as the least mature component of the CHEST system. However, HTHPs, exist for several years, with maximum heat supply temperatures reaching about 165 °C at the moment [Arp 2018]. Furthermore, HP technology in the CHEST system can be quite similar to ORC and there is a clear tendency even to have the same equipment for compression and expansion. Both for HP and ORC technology, for the MW sizes considered in real CHEST systems, turbomachinery will be used which is mature technology with regular maintenance plans and without new developments. In ORC technology, heat source (turbine inlet) temperatures of more than 300 °C are standard technology and manufacturers have experience with a wide range of working fluids [Turbo 2021] [Quo 2013]. Since the beginning of the installation of commercial ORC plants in the 1970s, more than 700 projects have been realized in a wide range of power and belonging to four main applications (waste heat recovery, geothermal power generation, biomass combined heat and power, solar power plants) [Quo 2013] [Tar 2017]. Concerning the turbine as the central part of an ORC plant, Quoilin et al. reported a lifetime of 30 years in contrast to steam turbines having a lifetime of only 15 - 20 years. Since in ORC turbines, the working fluid usually remains superheated, there is no condensation, which reduces the risk of corrosion on the turbine blades like it happens in steam turbines [Quo 2013].

Taking into account all the above sources, it is reasonable to assume a 30-year lifetime for the ORC component, as it is a mature technology and experience is available from numerous projects in different applications and for a range of powers and temperatures. However, for the HP, the conclusion is that an overall lifetime of 30 years for the HP is possible, but the replacement of several parts of the HP will certainly be necessary after a lower period of time. Therefore, it was decided to include into the economic assessment replacement costs that account for half of the original specific investment costs of the HP and arise after 20 years of HP operation.

LHS and SHS

In general, rather high lifetimes of 30 years or more can be considered for large scale thermal energy storage considering state-of-the-art examples such as molten salt storage for CSP plants and seasonal (pit) thermal energy storage for district heating systems.

A lifetime of 30 years for a CSP plant including its molten salt storage is an assumption that has been often used in the literature, e.g. for LCA studies conducted by Adeoye et al. [Adeo 2014], Burkhardt et al. [Burk 2011] and Ko et al [Ko 2018]. Admittedly, there are also studies which assume shorter lifetimes for the CSP plant or its molten salt TES, e.g. from Lalau et al. [Lal 2016] assuming 25 years and from Oro et al [Oro 2012] and Piemonte et al. [Pie 2011] assuming only 20 years. For existing CSP plants like Andasol in Spain that started operation between 2008 and 2011, only the expected service life is known which is 40 years [Dint 2014].

Pit storages are large seasonal storages that are often (partly) buried and therefore designed for long time of operation. The most critical part of them is not the construction itself, but the polymer liner. From recent developments in that field (polypropylene instead of polyethylene liners), lifetimes of > 30 years can be expected [Held 2021].

For PCM-based thermal energy storage like the LHS of the CHEST system, there is very few experience in that large-scale application, but it is expected to be similar to molten salt storage, e.g. concerning wall construction and issues like corrosion, since the PCMs used are mixtures of similar salts. For SHS, a lifetime of 30 years can be seen as a justified assumption given the much lower technological complexity (merely pressurized water tanks) compared to the other main components of the CHEST system. Such pressurized water tanks are state-of-the-art technology for decades; an SHS manufactured today is expected to last at least 30 years.

All in all, it seems reasonable to assume a lifetime of 30 years for both the LHS and the SHS.

Lead-acid batteries

The lifetime of lead-acid batteries varies significantly depending on the application, discharge rate and number of deep discharge cycles [EPRI 2010]. Therefore, different assumptions concerning the lifetime of lead-acid batteries can be found in the literature. While for instance Schmidt et al. reported a shelf life of only 10 years used for their calculations of LCOS of different EES technologies [Schm 2019], Rastler assumed 15 - 20 years for “advanced lead-acid” batteries [EPRI 2010]. Dufo-López et al. analyzed more in detail the lifetime of lead-acid batteries applied in stand-alone PV systems and reported significant differences between the lifetimes that appear in the datasheets of the manufacturers (typically 10 - 20 years) and the real battery life (even as low as 6 years, but for a small household system analyzed) [Dufo 2014]. Olympios et al. reported the lifetime of any type of large-scale battery system to be in the range of 10 - 15 years [Olym 2021]. Given these analyzed sources for lead-acid batteries, it was decided to consider two cases concerning lifetime of the batteries in the Ispaster case study: 15 and 10 years.

6.2. Aalborg case study

6.2.1. Energetic assessment of the CHEST system

As mentioned beforehand, the CHEST system in the Aalborg case study operates exclusively based on the electricity prices of the Danish spot and tertiary regulation market. There is no information given about the hourly generation and consumption of electricity. The assumption here is that there is no grid limitation for the CHEST system to exchange electricity with the grid, as long as the electricity prices make it beneficial for the CHEST system to do so. The only limitation for the exchange of electricity with the grid originates from the CHEST system itself, i.e. due to a certain nominal electric power of the HP and the ORC and a charging and discharging limitation given by a completely charged or discharged LHS/SHS, respectively.

Due to this unlimited available power of the electricity grid on the demand side, it is not possible here to quantify the KPIs "**Reduction of peak deficit power**" because there is no maximum electricity deficit, neither in the case with nor in the case without CHEST system. Given the assumption mentioned in Chapter 2.4.1 that all the electricity taken up by the CHEST system is excess electricity from renewable sources, the KPI "**Curtailment reduction**" is directly given by the amount of electricity that was taken up by the heat pump. For the exemplary CHEST system with the flexible setting concerning the buy-limit shown in Table 2 in Chapter 5.1, this KPI accounts for **4,275 MWh per year**.

Again assuming that all the electricity the CHEST consumed was excess electricity from renewable sources (that otherwise would have been curtailed), the net electricity generation of the ORC can be seen as the **savings of electricity**, cf. Chapter 2.4.1. For the same exemplary CHEST system shown in Table 2 in Chapter 5.1, the ORC net electricity generation accounted for **5,780 MWh/a**.

Concerning heat, there is no saving of thermal energy by the CHEST system, but additional heat required. The heat balance of the CHEST system is highly negative here due to the following reasons:

- A high P2P ratio of > 100 % is beneficial for the electrical side, but it eventually means that part of the heat was transformed into electricity and thus, the heat output of the CHEST system must be less than the heat input into the CHEST system.
- The **useful** heat output is 0 here, because none of the available heat at the ORC condenser is transferred to the DH system. This is due to the fact that the refrigerant-side condensing temperature of the ORC (45 °C) is too low to be able to transfer heat to the DH system, which has a return temperature of 45 °C as well.
- The HTTES with its latent and sensible part has thermal losses, which need to be compensated.
- There is some extra heat required for the recharge of the SHS.

As the state of charge of the LHS and of the SHS is not the same at the beginning and at the end of the simulation, the change of energy content of the LHS and the SHS was included in the following calculation of the CHEST heat balance:

$$\begin{aligned}CHEST\ heat\ balance\\ &= Useful\ heat\ output\ of\ CHEST - Heat\ input\ of\ CHEST\\ &+ Change\ of\ energy\ content\ of\ HTTES\ considered\end{aligned}$$

The detailed results of this calculation are listed in Table 7.

Table 7: Heat balance for the exemplary CHEST system.

Heat input/output	Thermal energy [MWh_{th}/a]
Useful heat output of the CHEST system	**+0**
Heat transferred to DH system	+0
Heat input into the CHEST system	**-30,456**
Excess heat required for HP evaporator	-22,687
Excess heat required for compensation of SHS thermal losses	-113
Excess heat required for SHS recharge	-7,656
Auxiliary heat required for HP evaporator	-0
Auxiliary heat required for compensation of SHS thermal losses	-0
Auxiliary heat required for SHS recharge	-0
Change of energy content of HTTES	**+401**
Change of energy content of LHS	+254
Change of energy content of SHS	+147
CHEST heat balance	**-30,055**

Note: the thermal losses of the LHS account for about 27 MWh/a here. They are not given in the table above, because they are not directly compensated for by external heat like the SHS thermal losses. Instead, they are indirectly compensated for at every heat pump operation. So, the thermal losses of the LHS are eventually a part of the heat required for the HP evaporator.

The main reason for the highly negative CHEST heat balance clearly is the lack of heat transfer from the ORC condenser to the DH system, because actually, there are about 27,245 MWh of heat available at the ORC condenser. But as said above, the temperature level of this heat is too low to be usable for the DH system.

As regards to the quantification of the KPI "**Savings of thermal energy**", the question is in how far this excess heat required was truly "excess", i.e. not usable otherwise. If so, the savings of thermal energy of the CHEST system compared to a situation without CHEST system would basically be **0** (neglecting the change of energy content of the HTTES). If not, then there are some 30,000 MWh/a of "negative savings", i.e. additional heat required.

Looking at the profiles of excess heat and heat demand in Aalborg (see Figure 5 in Chapter 3.1.3), you can see that the DH heat demand is in most cases higher than the available excess heat. On a yearly basis, the heat demand is about twice the available excess heat. This means that most of the time when the CHEST system consumes excess heat, this amount is missing for the DH system.

For a detailed analysis of this, the DH heat demand, the excess heat available and the heat consumed by the CHEST system were plotted for every point of time. Whenever the DH heat demand is higher than the available excess heat, then the heat consumed by the CHEST is true additional demand. In case that the available excess heat is higher than the DH demand + the heat consumption of the CHEST, the heat required for the CHEST is true excess heat, because this heat would not have been used otherwise, anyway. And in case that the available excess heat is higher than the DH demand, but not higher than DH demand + CHEST heat consumption, then the heat required for CHEST is partly excess heat and partly means an additional heat demand.

For the exemplary CHEST system considered here, it turns out that from the 30,456 MWh/a as heat input into the CHEST system, only 4,040 MWh/a were true excess heat, that means, this heat would not have been usable otherwise, anyway. The remaining 26,416 MWh/a, however, could have been used for covering the DH demand and therefore, this must be seen as additional required heat. Taking into account the 401 MWh/a as a plus in the energy content of the HTTES, this in total gives “negative savings” of thermal energy of the CHEST system of 26,015 MWh/a.

Therefore, on a final energy basis, you can say that the exemplary CHEST system considered here leads to the saving of 5,780 MWh/a of electricity, but on the other hand causes an additional heat demand of 26,015 MWh/a.

Taking into account the primary energy factors (PEF) listed in Table 3, the CHEST system does not save primary energy, but does consume an additional amount of about 13,400 MWh/a in primary energy. This also means that an energetic payback time cannot be calculated here.

Assuming a situation with so much availability of excess heat that the heat consumption of the CHEST system is not done on the expense of available heat for the DH network (only true excess heat used for CHEST, see above), the savings of 5,780 MWh/a of electricity would be equal to **primary energy savings of 2,248 MWh/a**. In this case, the **energetic payback time** would be about **29 years** given the cumulative energy demand for the production of the CHEST system presented in Table 8.

Table 8: Calculation of the cumulative energy demand (CED) for the production of the CHEST system.

Component	Component size	CED_P (specific)	CED_P (total)
CHEST system			
Heat pump	5 MW_{el}	0.035 MWh/kW_{el}	175 MWh
ORC engine	5 MW_{el}	0.311 MWh/kW_{el}	1,555 MWh
LHS	7,373 t / 3,210 m³	0.00863 MWh/kg + 0.005 MWh/m³	63,645 MWh
SHS	2 x 5,058 m³	0.005 MWh/m³	51 MWh
Total			**65,426 MWh**

$$\tau_{payback,en,P} = \frac{CED_P}{S_{el+th,prim}} = \frac{65{,}426 MWh}{2{,}248 MWh/a} \approx \mathbf{29.1\ a}$$

6.2.2. Environmental assessment of the CHEST system

Following the assumption made above concerning the excess heat availability, the savings of 5,780 MWh/a of grid electricity would be equal to **savings of CO_2 emissions of about 907 t/a**. Considering the CO_2 emissions for the production of the CHEST system as given in Table 9 , this gives an **CO_2 payback time of about 24 years**.

Table 9: Calculation of the CO_2 emissions for the production of the CHEST system.

Component	Component size	GWF_P (specific)	GWF_P (total)
CHEST system			
Heat pump	5 MW_{el}	24.11 kg/kW_{el}	121 t
ORC engine	5 MW_{el}	82.26 kg/kW_{el}	411 t
LHS	7,373 t / 3,210 m³	2.85 kg/kg + 1.29 kg/m³	21,017 t
SHS	2 x 5,058 m³	1.29 kg/m³	13 t
Total			**21,562 t**

$$\tau_{payback,CO2,P} = \frac{GWF_P}{E_{CO2}} = \frac{21{,}562 t}{907 t/a} \approx \mathbf{23.8\ a}$$

6.2.3. Economic assessment of the CHEST system

Due to the very low operation hours of the CHEST system, which is a consequence of the unfavorable Danish electricity price profiles, the Danish tax scheme and the operation and maintenance costs, no profitable business case is possible under these boundary conditions as is shown in Table 10.

Table 10: Electric profit balance for exemplary CHEST system.

Costs (-) /revenues (+)	Value [€]
Electricity purchase	
Turnover for electricity purchase	+65,345
O&M costs for HP	-42,750
Tax/fee-addon for electricity purchase	-92,041
Electricity purchase balance	**-69,446**
Electricity sale	
Turnover for electricity sale	+237,211
Turnover for availability payment	+5,385
O&M costs for ORC	-86,700
Tax/fee-addon for electricity sale	-3,006
Electricity sale balance	**+152,890**
Electric profit balance	
Annual profit from electricity purchase and sale	**+83,444**
Investment costs	
Investment costs of the HP	15,700,000
Investment costs of the ORC	4,000,000
Investment costs of the LHS	49,000,000
Investment costs of the SHS	8,400,000
Total investment costs of the CHEST system	**77,100,000**

As can be seen from Table 10, there is even a certain revenue for the uptake of electricity by the CHEST system due to the purchase of electricity at negative electricity prices. However, including the taxes and fees to pay for the electricity purchase and the O&M costs for the operation of the HP, the uptake of electricity costs about 69,000 € per year.

At the electricity generation side, the taxes and fees are almost negligible, but there are considerable O&M costs for the operation of the ORC. The availability payments are also quite negligible.

Finally, this results in an annual profit of about 83,000 €, which is very low compared to the expected investment costs of the system. Although it is very clear from these numbers, that this is not a profitable business case, a dynamic economic calculation was carried out to determine the most important economic KPIs for this case study.

Table 11 lists the calculated KPIs where applicable/reasonable. As detailed already above, the initial investment costs account for about 77.1 million €. Furthermore, after 20 years, a major replacement of several parts of the HP becomes necessary, which costs another 5.1 million € (discounted value). The operational costs including O&M costs and taxes and fees account for about 224,500 €/a and 5.0 million as a cumulative, discounted sum over the whole lifetime of 30 years, respectively. On the other hand, there is a cumulative, discounted sum for the turnover of about 8.3 million €. This results in an NPV of -78.8 million € after the 30 years, which means a highly negative business case for this exemplary CHEST system.

Table 11: Relevant economic KPIs for the exemplary CHEST system in the Aalborg case study.

Economic KPI	Value
Investment costs (CAPEX)	
Initial investment costs	77,077,363 €
Investment for replacement of HP parts after 20 years (discounted)	5,117,500 €
Cumulative Investment costs after 30 years (discounted)	**82,194,863 €**
Operational costs (OPEX)	
Annual O&M costs (1st year)	129,450 €
Annual fuel costs for HP heat requirement (1st year)	0 €
Annual taxes and fees (1st year)	95,046 €
Cumulative operational costs after 30 years (discounted)	**4,973,808 €**
Turnover	
Annual turnover for electricity purchase (1st year)	65,345 €
Annual turnover for electricity sale (1st year)	237,212 €
Annual turnover for availability payments (1st year)	5,385 €
Cumulative turnover after 30 years (discounted)	**8,327,896 €**
Economic payback	
Net present value (NPV) after 30 years	**-78,840,775€**
Return on investment (ROI)	n.a.
Internal rate of return (IRR)	n.a.
Economic payback time	n.a.
Levelized costs	
Levelized costs of energy (LCOE)	**820 €/MWh**
Levelized costs of storage (LCOS)	**471 €/MWh**

Concerning levelized costs, the equations presented in Chapter 2.6.9 for LCOE and LCOS need to be adapted for this case study or several levelized costs could actually be determined here, respectively. The question is about what can be determined as the useful energy output in the denominator, since both consumption and supply of electricity contribute to the revenues of the storage system. It seems reasonable, from energy (system) point of view, to account only the electricity supply (net ORC electricity generation) for LCOE. However, for LCOS, it seems reasonable to account both electricity consumption and supply. For the numerator, it is reasonable to consider the total accounted sum of investment and operation costs, but no costs for charging, since charging rather generates revenues and these revenues are already accounted for by putting the consumed electricity into the denominator. As was stated in Chapter 2.6.9, the idea behind levelized costs is to determine a minimum price at which a unit of energy has to be sold to cover all costs, i.e. to reach break-even point.

As was presented in Chapter 6.2.1, the annual amount of electricity consumed by the HP and the annual amount of net electricity generated by the ORC account for 4,275 MWh and 5,780 MWh, respectively. This results in cumulative discounted sums of 78,626 MWh and 106,306 MWh, respectively.

$$LCOE = \frac{\sum_{t=1}^{n} \frac{I_t + O\&M_t}{(1+j)^t}}{\sum_{t=1}^{n} \frac{E_{Discharge,t}}{(1+j)^t}} = \frac{82{,}194{,}863€ + 4{,}973.808€}{106{,}306 MWh} \approx \mathbf{820\ €/MWh}$$

$$LCOS = \frac{\sum_{t=1}^{n} \frac{I_t + O\&M_t}{(1+j)^t}}{\sum_{t=1}^{n} \frac{E_{Charge,t} + E_{Discharge,t}}{(1+j)^t}} = \frac{82{,}194{,}863€ + 4{,}973.808€}{78{,}626 MWh + 106{,}306 MWh} \approx \mathbf{471\ €/MWh}$$

The interpretation of these levelized cost values is that for every MWh the ORC generates or for every MWh that either the HP consumes or the ORC generates, an electricity price (before taxes) of 820 € or 471 €, respectively, would have to be realized at the electricity market to operate cost-effective. This is far beyond the electricity prices currently present in the Danish electricity markets; cf. Chapter 3.1.3.

6.3. Ispaster case study (Ispaster 2.0)

6.3.1. Energetic assessment of the CHEST system

In Chapter 5.2.2, it was already shown which savings of electricity are achieved by the CHEST system in Ispaster 2.0 case dependent on the size of the HP and ORC compared to a situation without electrical energy storage (cf. Figure 24). It was also illustrated that battery storage with an equivalent electric storage capacity showed higher savings of electricity due to the relatively low P2P ratio of the CHEST system of about 65 - 68 % and due to the higher charging and discharging power of the battery storage. Furthermore, the CHEST system is a net heat consumer, i.e. additional heat is required for the operation of the CHEST system, which leads to an increased biomass demand. Concerning primary energy, there are savings of the CHEST system compared to a situation without any electrical energy storage, but the battery storage performs better as can be seen in Figure 31.

Compared to a situation without any electrical energy storage, a battery storage with a storage capacity of 197 kWh leads to annual savings of primary energy of about 16.1 MWh. The **primary energy savings of a CHEST** system with equivalent thermal storage capacity range from **4.4 MWh/a to 15.6 MWh/a**, depending on HP and ORC size. Although there is a higher biomass demand by the CHEST system, this hardly affects the primary energy savings, because the primary energy factor (PEF) of wood chips is very low, especially in comparison to the PEF for grid electricity (cf. Table 3).

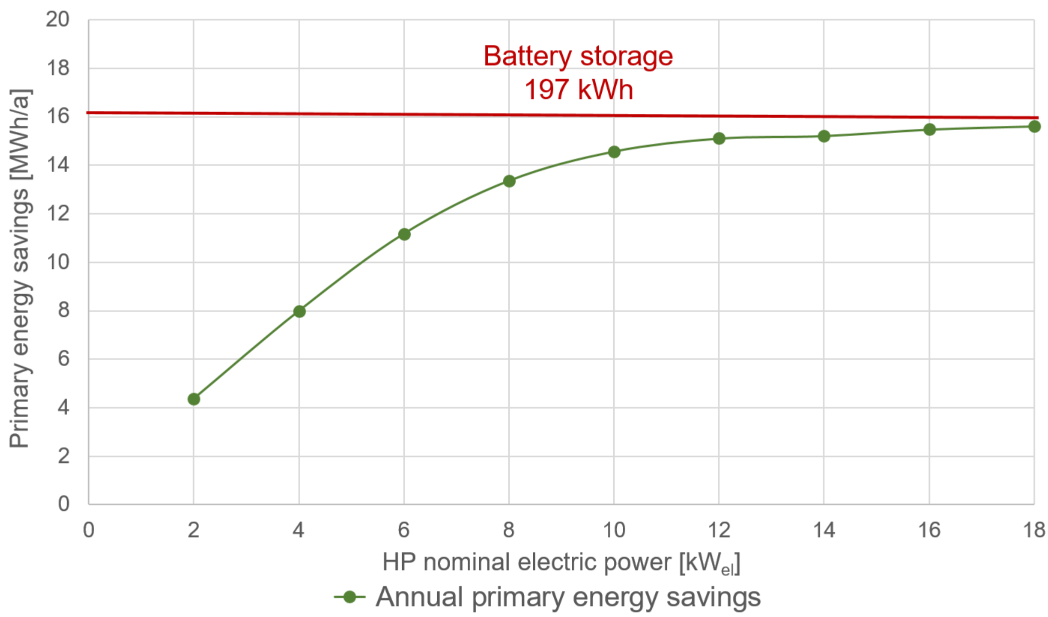

Figure 31: Dependence of the annual primary energy savings on the nominal electric power of the HP for a CHEST system with a HTTES capacity of 752 kWh_{th}, compared to an equivalent battery storage and the situation without any electrical energy storage.

Figure 32 shows the primary energy savings of the CHEST system and the battery storage cumulated for the whole lifetime of 30 years, compared to the situation without any electrical energy storage. For the battery storage with a capacity of 197 kWh, in total 482.3 MWh of primary energy are saved compared to the situation without EES. For the CHEST system, the cumulated primary energy savings account for between 131.2 MWh and 468.3 MWh dependent on the HP size.

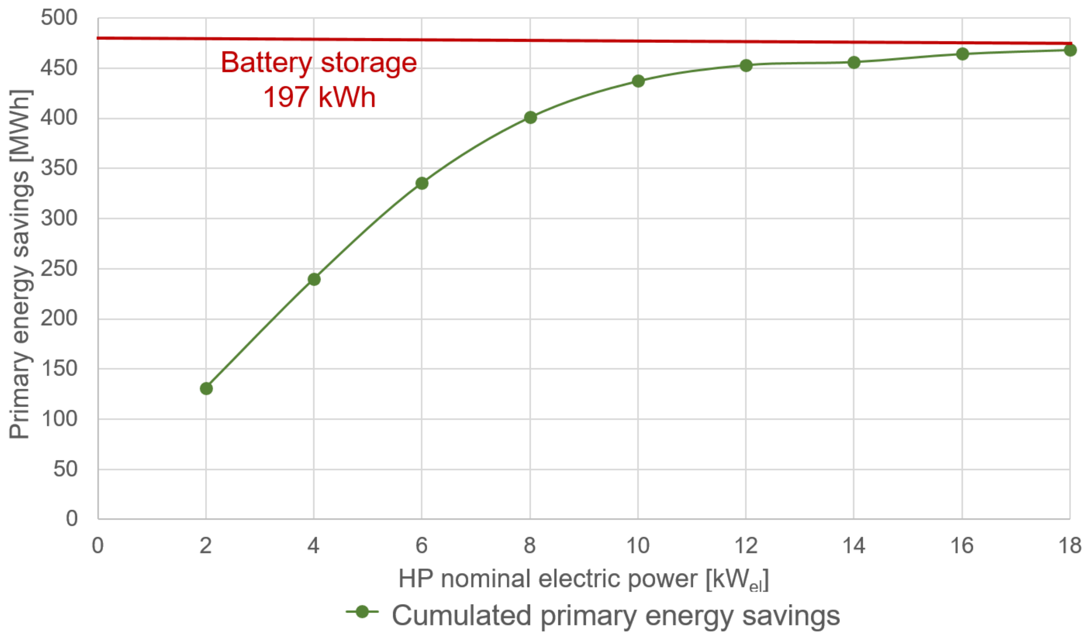

Figure 32: Dependence of the cumulated primary energy savings on the nominal electric power of the HP for a CHEST system with a HTTES capacity of 752 kWh$_{th}$, compared to an equivalent battery storage and the situation without any electrical energy storage.

In order to determine the energetic payback time, the primary energy demand was calculated for one exemplary CHEST system with HP and ORC nominal electrical powers of 8 kW and 2 kW, respectively, along with values for the battery storage, see Table 12.

Table 12 shows that the primary energy demand for the production of the CHEST system is about the factor 18 higher than the primary energy demand for the production of the battery storage. Furthermore, it can be recognized that the LHS accounts for more than 99 % of this primary energy demand due to the high PCM mass and its high specific CED value.

Table 12: Calculation of the cumulative energy demand (CED) for the production of the CHEST system and for the production of the battery storage.

Component	Component size	CED_P (specific)	CED_P (total)
CHEST system			
Heat pump	8 kW_{el}	0.035 MWh/kW_{el}	0.28 MWh
ORC engine	2 kW_{el}	0.311 MWh/kW_{el}	0.62 MWh
LHS	13,742 kg / 6.85 m^3	0.00863 MWh/kg + 0.005 MWh/m^3	118.63 MWh
SHS	2 x 2.57 m^3	0.005 MWh/m^3	0.03 MWh
Total			**119.56 MWh**
Battery storage			
Lead-acid batteries	197 kWh_{el}	0.034 MWh/kWh_{el}	**6.70 MWh**

Considering the abovementioned 16.1 MWh/a of annual primary energy savings for the battery storage and a primary energy demand for its production of 6.70 MWh, this gives an energetic payback time of 0.4 a. The CHEST system with the abovementioned size for HP of 8 kW_{el} and ORC of 2 kW_{el} as well as a HTTES storage capacity of 752 kWh_{th} saves 13.4 MWh/a in primary energy. Considering the cumulative energy demand of 119.6 MWh required for the production of the CHEST system, this gives an **energetic payback time of roughly 9 years**.

$$\tau_{payback,en,Battery} = \frac{CED_P}{S_{el+th,prim}} = \frac{6.70MWh}{16.08MWh/a} \approx \mathbf{0.4\ a}$$

$$\tau_{payback,en,CHEST} = \frac{CED_P}{S_{el+th,prim}} = \frac{119.56MWh}{13.37MWh/a} \approx \mathbf{8.9\ a}$$

Another KPI of interest in terms of energetic performance of the CHEST system and the battery storage is the **reduction of peak deficit power**. This is due to the fact that reducing the peak deficit power could reduce the contracted maximum connection power to the DSO and this in turn could reduce costs. However, it must be said that in this case, neither the CHEST system nor the battery storage reduce the peak deficit power, because the storage systems are still too small for that. The peak deficit power in any case accounted for 4.21 kW_{el}.

Concerning the **reduction of PV curtailment**, Figure 33 shows how many MWh of excess PV electricity are curtailed annually for the CHEST system, for the battery storage and for the situation without any electrical energy storage. The figure shows that depending on the HP and ORC size, the CHEST system reduces the PV curtailment by about **3.4 to 11.6 MWh**. The battery storage with a storage capacity of 197 kWh reduces the PV curtailment by about 11.4 MWh per year down to 10.2 MWh/a. Without any EES, there are 21.6 MWh/a of curtailed PV electricity generation.

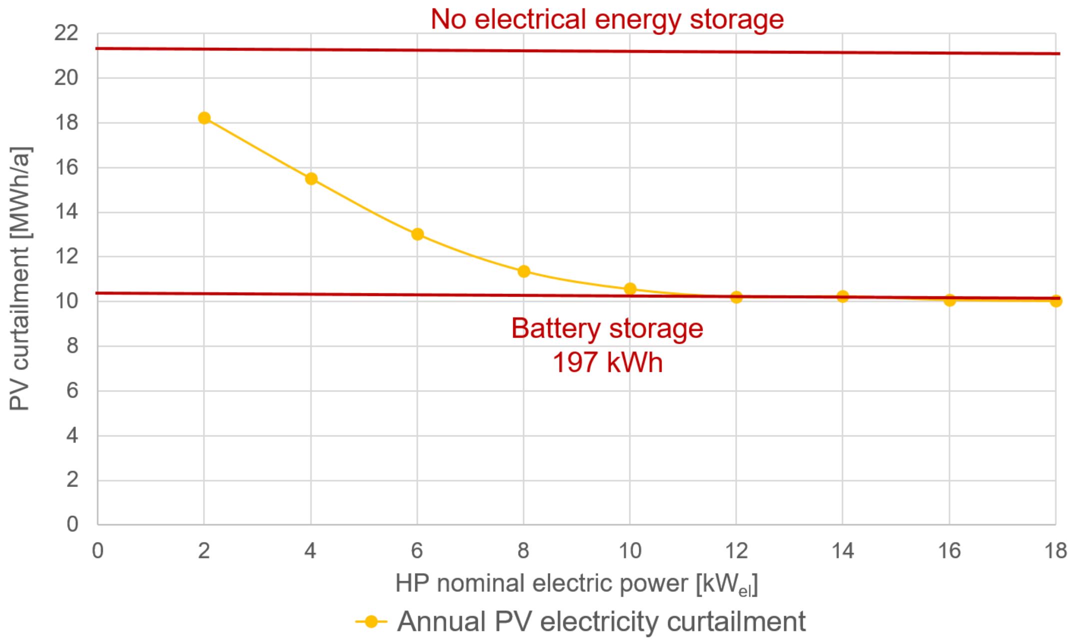

Figure 33: Dependence of the annual PV electricity curtailment on the nominal electric power of the HP for a CHEST system with a HTTES capacity of 752 kWh$_{th}$, compared to an equivalent battery storage and the situation without any electrical energy storage.

Figure 34 shows the PV electricity curtailment for the CHEST system and the battery storage cumulated for the whole lifetime of 30 years, compared to the situation without any electrical energy storage. Without EES, there is a total of 648.9 MWh of curtailed PV electricity. For the battery storage with a capacity of 197 kWh, the curtailed PV electricity accounts for 307.2 MWh and for the CHEST system, it accounts for between 301.2 MWh and 546.6 MWh dependent on the HP size.

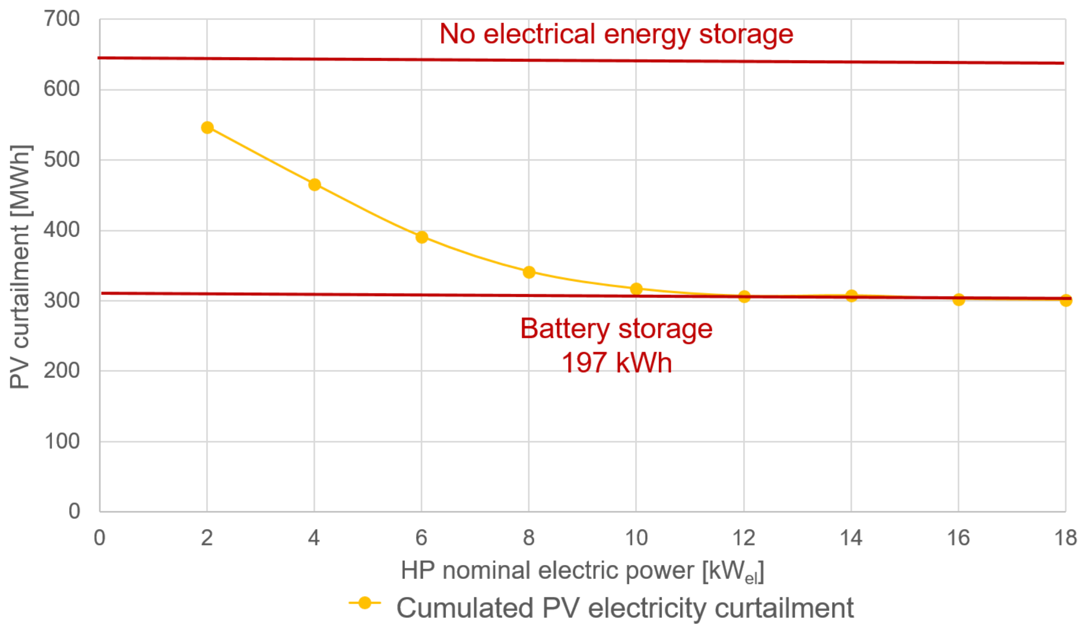

Figure 34: Dependence of the cumulated PV electricity curtailment on the nominal electric power of the HP for a CHEST system with a HTTES capacity of 752 kWh$_{th}$, compared to an equivalent battery storage and the situation without any electrical energy storage.

6.3.2. Environmental assessment of the CHEST system

Similar to the savings of primary energy, also the **savings of CO_2 emissions** can be calculated, with the help of the CEF values given in Table 3. Again, the increased biomass demand of the CHEST system has only a minor effect, because the CEF value for the wood chips is quite low. The savings of grid electricity are therefore much more important for the savings of CO_2 emissions. As can be seen from Figure 35, the battery storage saves about 1.71 t of CO_2 per year, while the CHEST system saves **between about 0.55 and 1.44 t of CO_2 per year**. The fact that the operation of the CHEST system reduces the solar thermal yield due to the high HP evaporation temperatures is actually beneficial for the environmental assessment of the CHEST system, because the CO_2 emissions per MWh of solar heat are higher than those per MWh of heat from wood chips, cf. Table 3.

Figure 36 shows the savings of CO_2 emissions of the CHEST system and the battery storage cumulated for the whole lifetime of 30 years, compared to the situation without any electrical energy storage. For the battery storage with a capacity of 197 kWh, in total 51.4 t of CO_2 emissions are saved compared to the situation without EES. For the CHEST system, the cumulated savings of CO_2 emissions account for between 16.6 t and 43.1 t dependent on the HP size.

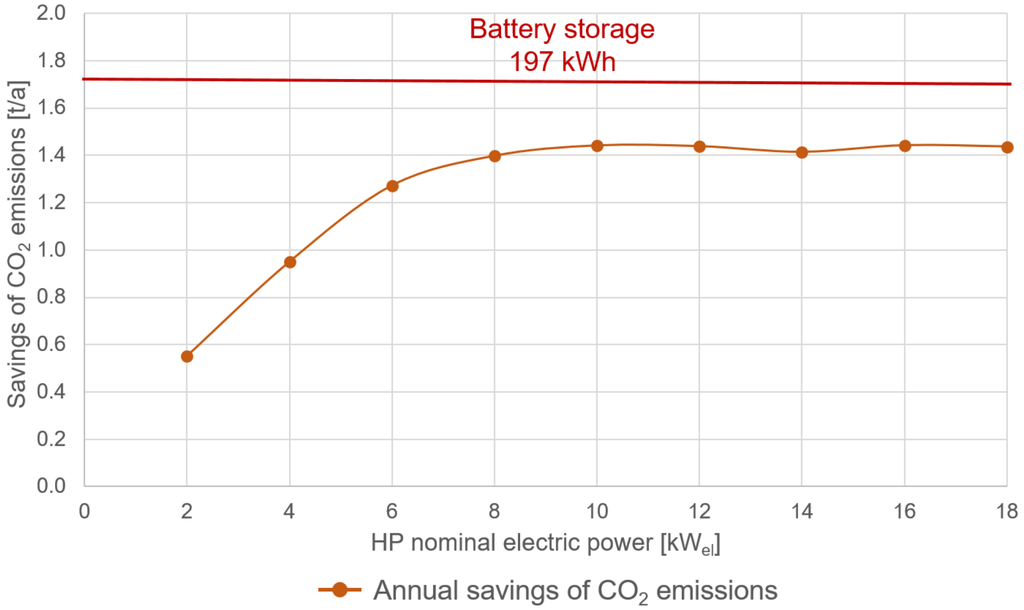

Figure 35: Dependence of the annual savings of CO_2 emissions on the nominal electric power of the HP for a CHEST system with a HTTES capacity of 752 kWh_{th}, compared to an equivalent battery storage and the situation without any electrical energy storage.

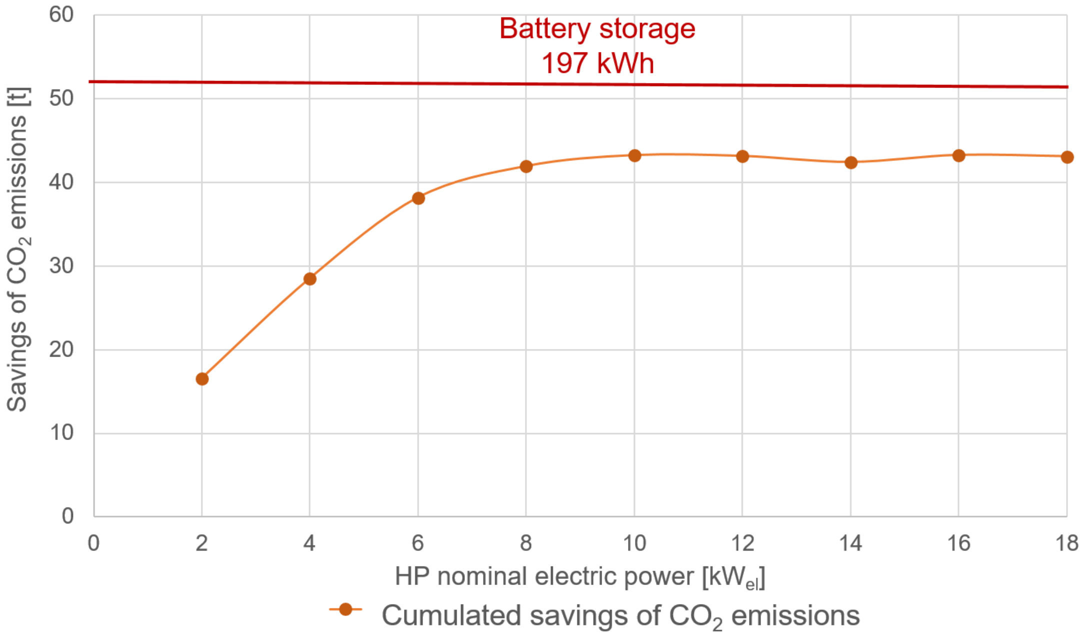

Figure 36: Dependence of the cumulated savings of CO_2 emissions on the nominal electric power of the HP for a CHEST system with a HTTES capacity of 752 kWh_{th}, compared to an equivalent battery storage and the situation without any electrical energy storage.

The calculation of the CO_2 payback time shows a similar picture like for the energetic payback time. As can be seen from Table 13, the production of the CHEST system leads to about 20 times higher CO_2 emissions compared to the battery storage.

Table 13: Calculation of the CO_2 emissions for the production of the CHEST system and for the production of the battery storage.

Component	Component size	GWF_P (specific)	GWF_P (total)
CHEST system			
Heat pump	8 kW_{el}	24.11 kg/kW_{el}	0.19 t
ORC engine	2 kW_{el}	82.26 kg/kW_{el}	0.16 t
LHS	13,742 kg / 6.85 m^3	2.85 kg/kg + 1.29 kg/m^3	39.17 t
SHS	2 x 2.57 m^3	1.29 kg/m^3	0.01 t
Total			**39.53 t**
Battery storage			
Lead-acid batteries	197 kWh_{el}	9.52 kg/kWh_{el}	**1.88 t**

As was presented above, the battery storage saves about 1.71 t of CO_2 per year. Given the CO_2 emissions of 1.88 t for the production of the battery storage, this results in a CO_2 payback time of about one year. The CHEST system saves 1.40 t of CO_2 per year. This gives a **CO_2 payback time of about 28 years**.

$$\tau_{payback,CO2,Battery} = \frac{GWF_P}{E_{CO2}} = \frac{1.88t}{1.71t/a} \approx \mathbf{1.1\ a}$$

$$\tau_{payback,CO2,CHEST} = \frac{GWF_P}{E_{CO2}} = \frac{39.53t}{1.40t/a} \approx \mathbf{28.2\ a}$$

6.3.3. Economic assessment of the CHEST system

A dynamic economic calculation was carried out with the boundary conditions presented in Chapter 6.1.2 for the CHEST system with an HP and ORC nominal electric power of 8 and 2 kW, respectively, and for the battery storage. Figure 37 shows the development of the total costs of both the CHEST system and the battery storage in comparison to the situation without any electrical storage over the lifetime of 30 years. Total costs comprise all costs (investment, O&M, electricity + biomass purchase) discounted to the respective year (=net present values). For the battery storage, as can be seen in the figure, two different lifetimes of 10 and 15 years were assumed. The currently expected costs of the CHEST system were calculated according to the component costs listed in Table 5. For the future expected costs, it is assumed that HP and ORC are one single component, cf. the explanations in Chapter 6.1.2.

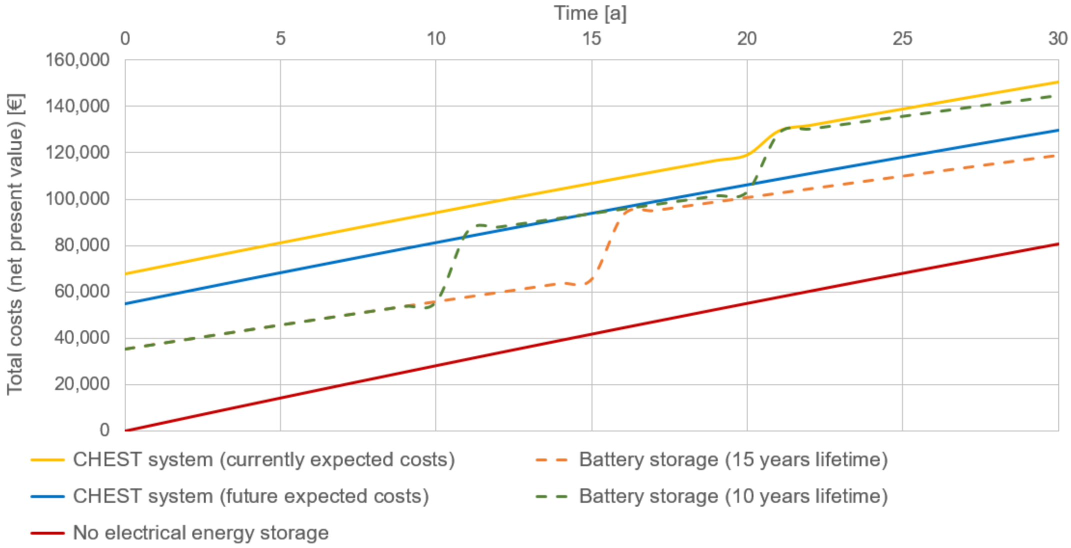

Figure 37: Development of the total costs (net present value) over the lifetime for the CHEST system and the battery storage.

At the beginning of the period, investment costs of about 67,600 € arise for the CHEST system (currently expected costs) and after 20 years of operation, another 7,800 € (discounted value) are necessary for the replacement of HP parts. The initial investment costs for the battery storage account for only 35,500 €. However, as can be recognized from Figure 37, a second investment for the battery storage has to be made after 15 years due to the shorter lifetime of the battery. Despite this second investment, the battery storage is the economically favorable option here compared to the CHEST system. Assuming the HP and the ORC to be a single component in the future reduces the initial investment costs from 67,600 € down to 54,800 € and there is no replacement of HP parts after 20 years. Compared to a battery storage with a lifetime of 15 years, the battery storage is still the economically favorable option. However, as can be recognized in the figure, the lifetime of the battery storage is a key parameter for the outcome of the comparison between the two technologies. Assuming a lifetime of only 10 years, the CHEST system could be the better option assuming future cost reduction for CHEST.

Finally, none of the two systems achieve an economic payback over the lifetime, since installing no electrical energy storage clearly causes least total costs over the 30 years. This means that from economic point of view, the best option is to install no electrical energy storage at all. This is due to the relatively low annual savings of some hundred € per year that arise from the savings of electricity purchase from the DSO when using EES. This is too low compared to the massive investment costs of EES to achieve economic payback.

Table 14 lists the main economic KPIs for the four different EES solutions/variants. It shows that not installing EES is by far the best solution with total cumulative costs of some 81,000 € over the 30 years. From the four EES solutions, lead-acid batteries with a lifetime of 15 years cause least cumulative costs of about 119,000 €.

Table 14: Relevant economic KPIs for the exemplary CHEST system in Ispaster 2.0 case study.

Economic KPI	CHEST (now)	CHEST (future)	Battery (15 a)	Battery (10 a)	No EES
Investment costs (CAPEX)					
Initial investment costs	67,626 €	54,846 €	35,460 €	35,460 €	0 €
Replacement investments costs (discounted)	7,835 €	0 €	25,567 €	51,378 €	0 €
Cumulative Investment costs after 30 years (discounted)	**75,461 €**	**54,846 €**	**61,027 €**	**86,838 €**	**0 €**
Operational costs (OPEX)					
Annual O&M costs (1st year)	215 €	215 €	178 €	178 €	0 €
Annual costs for electricity purchase (1st year)	633 €	633 €	473 €	473 €	1,461€
Annual costs for biomass purchase (1st year)	1,965 €	1,965 €	1,521 €	1,521 €	1,521 €
Cumulative operational costs after 30 years (discounted)	**75,036 €**	**75,036 €**	**57,863 €**	**57,863 €**	**80,650 €**
Economic payback					
Total costs (discounted) after 30 years	**150,497 €**	**129,882 €**	**118,890 €**	**144,701 €**	**80,650 €**
Return on investment (ROI)	n.a.	n.a.	n.a.	n.a.	n.a.
Internal rate of return (IRR)	n.a.	n.a.	n.a.	n.a.	n.a.
Economic payback time	n.a.	n.a.	n.a.	n.a.	n.a.
Levelized costs					
Levelized costs of storage (LCOS)	**746 €/MWh**	**579 €/MWh**	**441 €/MWh**	**616 €/MWh**	n.a.

As can be seen from the table, also levelized costs of storage (LCOS) were calculated for the four EES solutions. LCOS were defined the following way for Ispaster case study:

$$LCOS = \frac{\sum_{t=1}^{n} \frac{I_t + O\&M_t + C_{Charge,t}}{(1+j)^t}}{\sum_{t=1}^{n} \frac{E_{Discharge,t}}{(1+j)^t}} = \frac{\sum_{t=1}^{n} \frac{I_t + O\&M_t + C_{Biomass,add,t}}{(1+j)^t}}{\sum_{t=1}^{n} \frac{Elec_{Discharge,t}}{(1+j)^t}}$$

The output of EES in Ispaster is clearly the discharged electricity, since the electricity consumption has no economic value, it comes (for free) from the PV system. Heat output is not present with the batteries, and with CHEST, there is no revenue for it. The costs for charging are defined here by the additional biomass costs compared to the situation without EES, since these are charging costs related to the storage. For the batteries, it is 0, since the batteries do not change the heat balance and thus, they do not cause a higher biomass demand. However, the CHEST system has a higher heat demand than heat output and therefore causes additional biomass demand. For the first year of operation, this is given by (1,965 - 1,521) € = 444 €. The cumulative discounted sum of these additional biomass costs is about 12,015 €. This results in the following LCOS equations:

$$LCOS_{CHEST,now} = \frac{\sum_{t=1}^{n} \frac{I_t + O\&M_t + C_{Biomass,add,t}}{(1+j)^t}}{\sum_{t=1}^{n} \frac{Elec_{Discharge,t}}{(1+j)^t}} = \frac{75{,}461€ + 4{,}759€ + 12{,}015€}{123.6MWh} \approx \mathbf{746\ €/MWh}$$

$$LCOS_{CHEST,future} = \frac{\sum_{t=1}^{n} \frac{I_t + O\&M_t + C_{Biomass,add,t}}{(1+j)^t}}{\sum_{t=1}^{n} \frac{Elec_{Discharge,t}}{(1+j)^t}} = \frac{54{,}846€ + 4{,}759€ + 12{,}015€}{123.6MWh} \approx \mathbf{579\ €/MWh}$$

$$LCOS_{Battery,15a} = \frac{\sum_{t=1}^{n} \frac{I_t + O\&M_t + C_{Biomass,add,t}}{(1+j)^t}}{\sum_{t=1}^{n} \frac{Elec_{Discharge,t}}{(1+j)^t}} = \frac{61{,}027€ + 3{,}944€ + 0€}{147.3MWh} \approx \mathbf{441\ €/MWh}$$

$$LCOS_{Battery,10a} = \frac{\sum_{t=1}^{n} \frac{I_t + O\&M_t + C_{Biomass,add,t}}{(1+j)^t}}{\sum_{t=1}^{n} \frac{Elec_{Discharge,t}}{(1+j)^t}} = \frac{86{,}838€ + 3{,}944€ + 0€}{147.3MWh} \approx \mathbf{616\ €/MWh}$$

For the case “No EES”, there is no LCOS definition, since no storage is installed. In principle, also levelized costs of **energy** (LCOE) could be calculated for the whole Ispaster energy system, but was not conducted here due to the following reasons. First of all, also the investment costs for PV, solar thermal collectors and the biomass boiler would have to be taken into account to get actual energy system costs. Second, actually, heat and electricity would have to be separated; otherwise an LCOE value for minimum price per unit energy has little meaning. For the battery, this can easily be done, since PV + battery are responsible for electricity supply and solar thermal collectors + biomass boilers are responsible for heat supply. For CHEST, one could apply a similar approach like above, i.e. only the additional biomass costs are included in the levelized costs of **electricity** (LCOE) definition. However, levelized costs of **heat** (LCOH) would then be the same for all variants and LCOE (electricity) would show similar differences like for LCOS, since just the investment costs for PV, solar thermal and biomass boiler are included and they are the same for all variants.

Furthermore, it should be noted that LCOS values calculated for Ispaster case study are not really comparable to the LCOS values calculated for Aalborg case study. In Aalborg, although showing a highly negative heat balance, no additional fuel costs are included for the CHEST system since heat for the HP evaporator is assumed to come exclusively from free waste/excess heat. Moreover, in Aalborg case study, also the HP electricity consumption was included in LCOS definition since it generates revenues through payments from the electricity market. That´s why it was stated in Chapter 2.6.9 that a comparison of LCOS should only be made application-specific.

6.4. Ispaster case study (Ispaster Island)

6.4.1. Energetic assessment of the CHEST system

Depending on the installed number of PV panels, the CHEST system as well as the battery storage save between 10.4 and 11.8 MWh of electricity, which otherwise would have to be purchased from the DSO grid. As was already mentioned, the CHEST system leads to an increase of the heat demand and therefore of the biomass demand, whereas the battery storage does not affect the heat side.

Concerning the **annual savings of primary energy**, Figure 38 shows that both the CHEST system and the battery storage account for very similar values in the range **20.7 - 23.8 MWh/a**. This is logical, because the savings of electricity are the same, as the storage system is dimensioned so that no electricity has to be purchased from the DSO grid anymore. The CHEST system shows slightly lower annual savings of primary energy due to the increased biomass demand. However, as mentioned above, this is negligible for primary energy assessment due to the low primary energy factor (PEF) of wood chips.

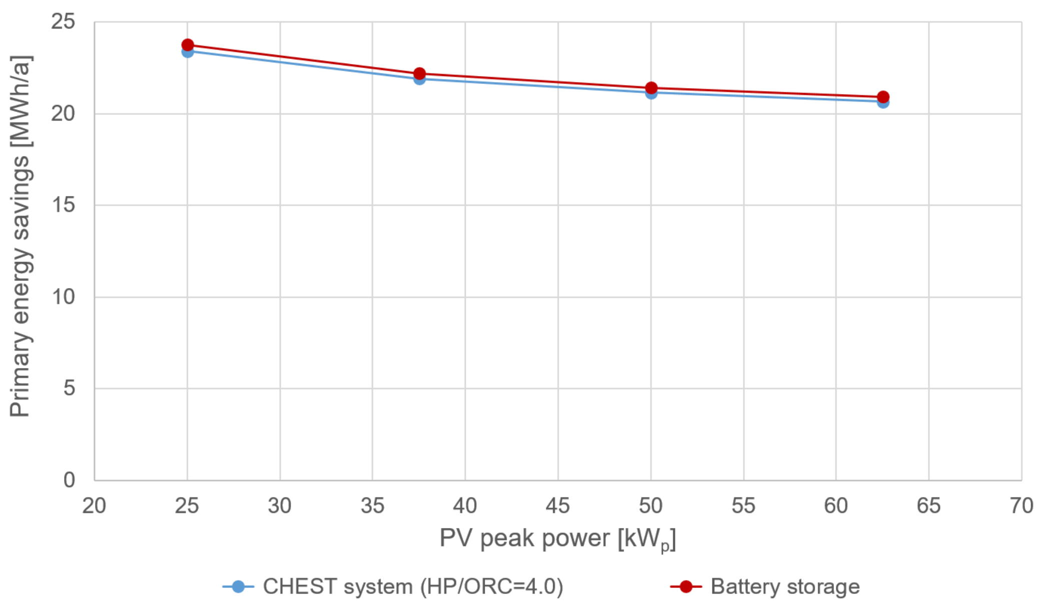

Figure 38: Dependence of the annual primary energy savings for both the CHEST system and the battery storage on the installed PV peak power.

Figure 39 shows the primary energy savings of the CHEST system and the battery storage cumulated for the whole lifetime of 30 years, compared to the situation without any electrical energy storage. For the battery storage, in total between 627.4 MWh and 712.9 MWh of primary energy are saved compared to the situation without EES, dependent on the installed PV peak power. For the CHEST system, the cumulated primary energy savings account for between 619.7 MWh and 702.3 MWh.

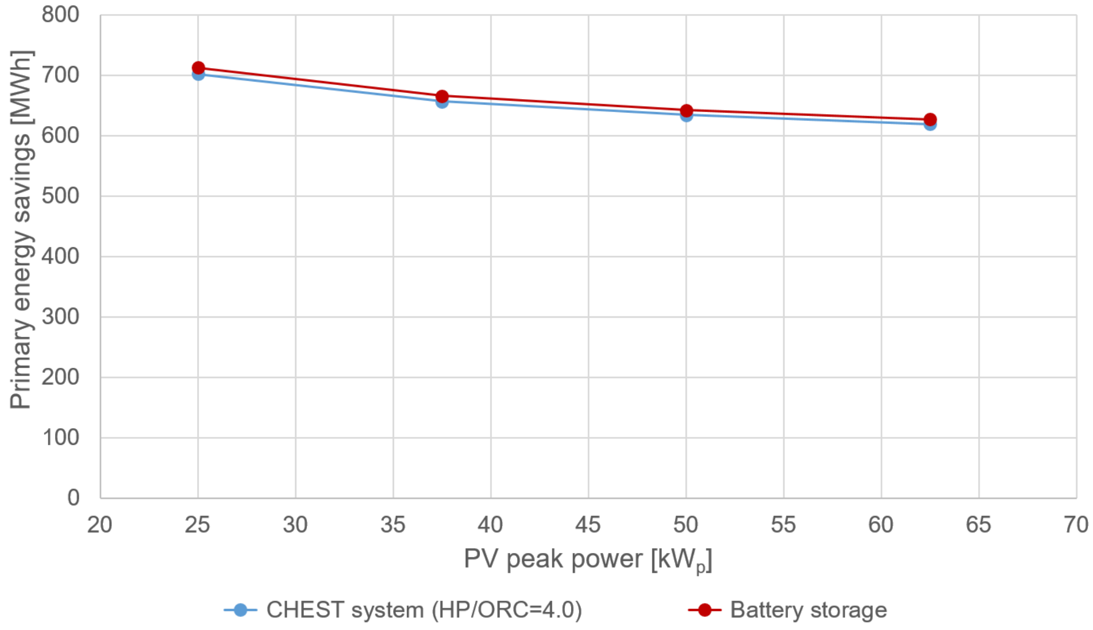

Figure 39: Dependence of the cumulated primary energy savings for both the CHEST system and the battery storage on the installed PV peak power.

For the example of an installed PV peak power of 50 kW_p, Table 15 shows the cumulative energy demand required for the production of the CHEST system and the battery storage.

Table 15: Calculation of the cumulative energy demand (CED) for the production of the CHEST system and for the production of the battery storage.

Component	Component size	CED_P (specific)	CED_P (total)
CHEST system			
Heat pump	17.652 kW_{el}	0.035 MWh/kW_{el}	0.62 MWh
ORC engine	4.413 kW_{el}	0.311 MWh/kW_{el}	1.37 MWh
LHS	77,372 kg / 38.57 m^3	0.00863 MWh/kg + 0.005 MWh/m^3	667.91 MWh
SHS	2 x 9.69 m^3	0.005 MWh/m^3	0.10 MWh
Total			**670.00 MWh**
Battery storage			
Lead-acid batteries	1,770 kWh_{el}	0.034 MWh/kWh_{el}	**60.18 MWh**

Like already mentioned for the Ispaster 2.0 case, the cumulative energy demand for the production of the CHEST system is considerably higher than for the battery storage, which affects the energetic payback time. For an installed PV peak power of 50 kW_p, the energetic payback time of the battery storage accounts for about 3 years. In contrast to this, the CHEST system does not show energetic payback within the lifetime of the system since the calculated **energetic payback time** accounts for about **32 years** in this case.

$$\tau_{payback,en,Battery} = \frac{CED_P}{S_{el+th,prim}} = \frac{60.18MWh}{21.41MWh/a} \approx \mathbf{2.8\ a}$$

$$\tau_{payback,en,CHEST} = \frac{CED_P}{S_{el+th,prim}} = \frac{670.00MWh}{21.15MWh/a} \approx \mathbf{31.7\ a}$$

It should be added that the energetic payback time in Ispaster Island case depends strongly on the installed PV peak power since, as shown in Figure 28, the required storage size becomes significantly reduced with increasing PV peak power. For an installed PV peak power of 25 kW_p, the battery storage has an energetic payback time of about 13 years while it accounts for only about one year in case of an installed PV peak power of 62.5 kW_p. For the CHEST system, there is an energetic payback given within its lifetime only for an installed PV peak power of 62.5 kW_p. In this case, the energetic payback time accounts for about 12.6 years. Note: the cumulative energy demand of the PV panels is not taken into account here since only the storage system is considered.

The **peak deficit power** was reduced for all systems **from 4.21 kW_{el} down to zero**. This is due to the fact that in an island energy system, the PV + storage system must be dimensioned in a way that there is no electricity purchase from the DSO anymore. The **PV curtailment** is a bit smaller for the battery storage, but the decisive factor for the PV curtailment clearly is the installed PV peak power.

6.4.2. Environmental assessment of the CHEST system

Similar to the savings of primary energy, there are only small differences between the two technologies in terms of **savings of CO_2 emissions** as is shown in Figure 40. Dependent on the installed PV peak power, the CHEST system saves between **2.07 t and 2.21 t of CO_2**, while the battery saves between 2.23 t and 2.54 t of CO_2. This is due to the fact that the saving of grid electricity is the dominating factor and this was the same for both technologies at a certain installed PV peak power.

Figure 41 shows the savings of CO_2 emissions of the CHEST system and the battery storage cumulated for the whole lifetime of 30 years, compared to the situation without any electrical energy storage. For the battery storage, in total between 67.0 t and 76.1 t of CO_2 emissions are saved compared to the situation without EES. For the CHEST system, the cumulated savings of CO_2 emissions account for between 62.2 t and 66.3 t dependent on the installed PV peak power.

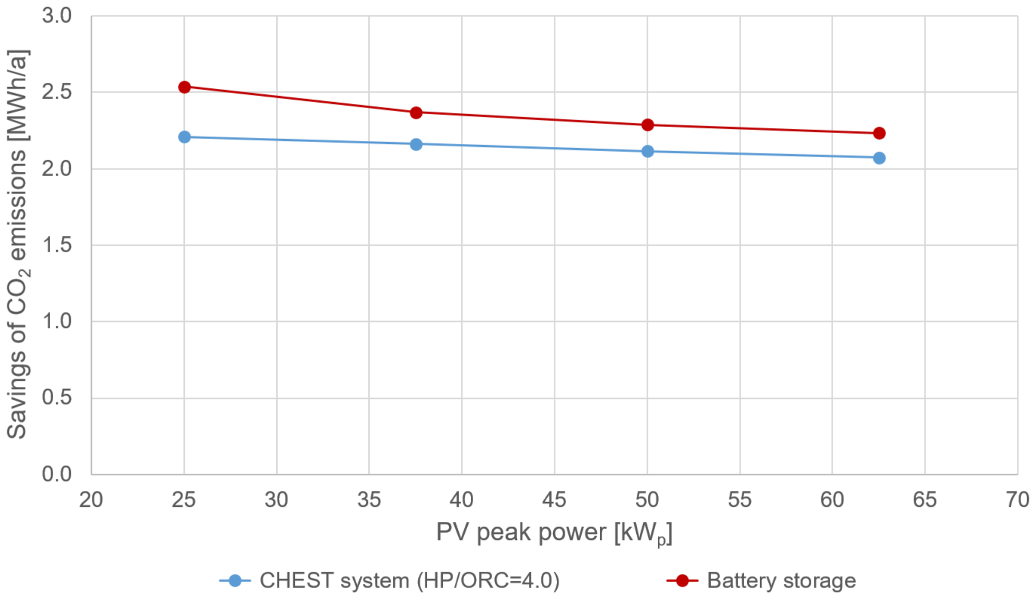

Figure 40: Dependence of the annual savings of CO_2 emissions for both the CHEST system and the battery storage on the installed PV peak power.

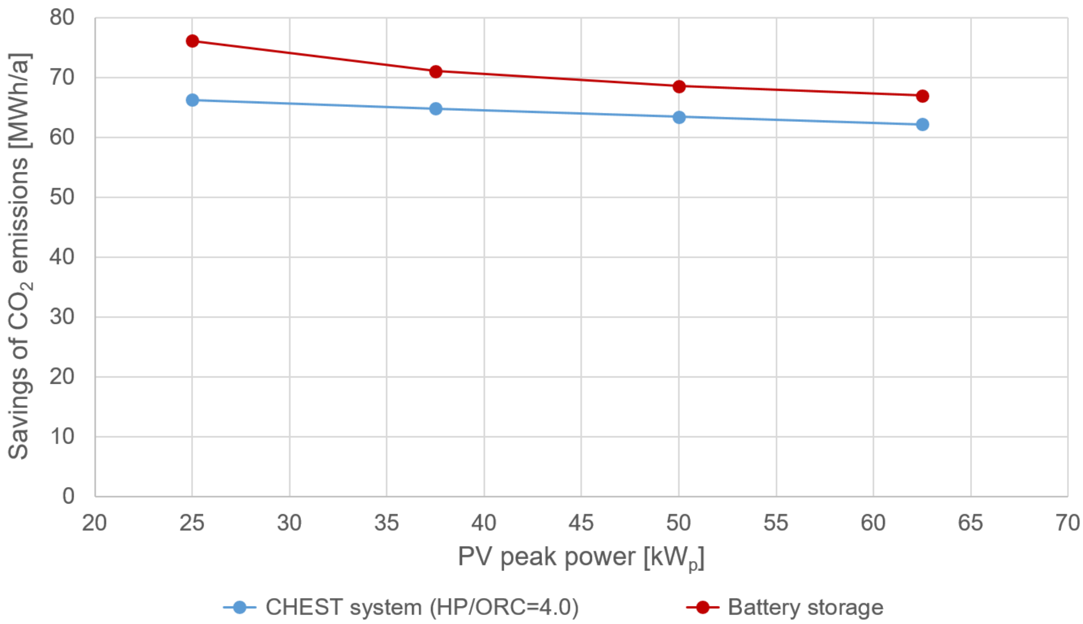

Figure 41: Dependence of the cumulated savings of CO_2 emissions for both the CHEST system and the battery storage on the installed PV peak power.

Table 16 shows the CO_2 emissions for the production of the CHEST system and the battery storage, respectively. As was already shown above, the CHEST system causes considerably higher CO_2 emission at its production due to the PCM. This does not lead to a **CO_2 payback time** for the CHEST system, whereas the battery storage saves as much CO_2 as has been emitted during its production after about 7.4 years.

Table 16: Calculation of the CO_2 emissions for the production of the CHEST system and for the production of the battery storage.

Component	Component size	GWF_P (specific)	GWF_P (total)
CHEST system			
Heat pump	17.652 kW_{el}	24.11 kg/kW_{el}	0.43 t
ORC engine	4.413 kW_{el}	82.26 kg/kW_{el}	0.36 t
LHS	77,372 kg / 38.57 m^3	2.85 kg/kg + 1.29 kg/m^3	220.56 t
SHS	2 x 9.69 m^3	1.29 kg/m^3	0.03 t
Total			**221.38 t**
Battery storage			
Lead-acid batteries	1,770 kWh_{el}	9.52 kg/kWh_{el}	**16.85 t**

$$\tau_{payback,CO2,Battery} = \frac{GWF_P}{E_{CO2}} = \frac{16.85t}{2.29t/a} \approx \mathbf{7.4\ a}$$

$$\tau_{payback,CO2,CHEST} = \frac{GWF_P}{E_{CO2}} = \frac{221.38t}{2.12t/a} \approx \mathbf{104.4\ a}$$

Like for the energetic payback time, also the results for the CO_2 payback time are strongly dependent on the installed PV peak power in Ispaster Island case study. For an installed PV peak power of 25 kW_p, the battery storage has a CO_2 payback time of about 34 years while it accounts for about 2.8 years in case of an installed PV peak power of 62.5 kW_p. The CHEST system in Ispaster Island case does not achieve CO_2 payback, irrespective of the installed PV peak power.

6.4.3. Economic assessment of the CHEST system

Before presenting the outcome of the dynamic economic calculation, a brief look is taken at the annual costs and the investment costs of both the CHEST system (with its currently expected costs) and the battery storage. Figure 42 shows the annual costs dependent on the installed PV peak power for the CHEST system and the battery storage. As there is no electricity purchase from the DSO grid in Ispaster Island case, only biomass has to be purchased. The annual biomass costs in case of the CHEST system are higher, which is due to the increased biomass demand, cf. Figure 30. The annual O&M costs were calculated according to the values listed in Table 6. They are slightly higher for the CHEST system. As a conclusion, the annual costs of the CHEST system are definitely higher compared to the battery storage.

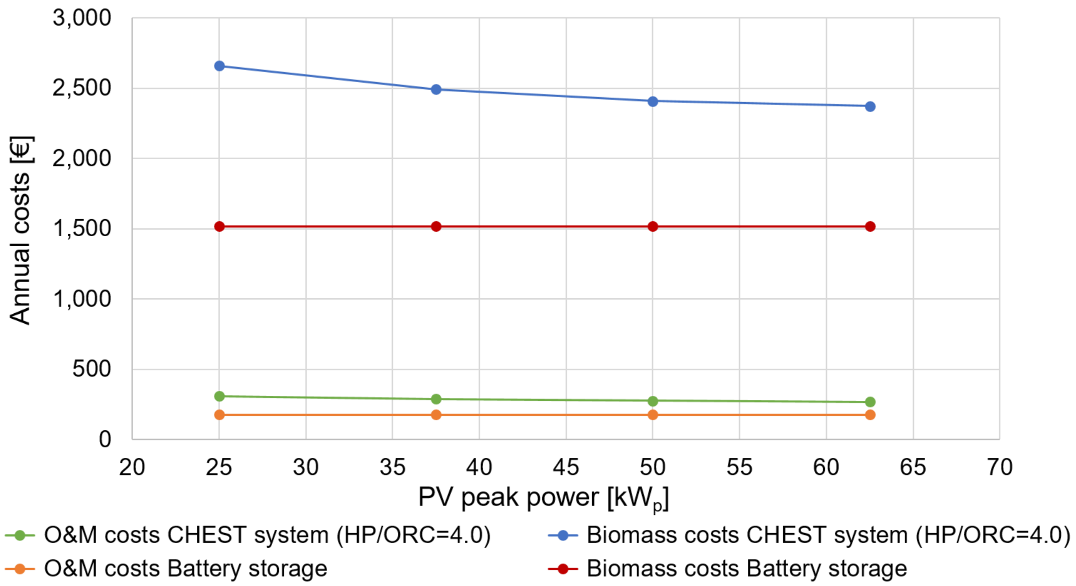

Figure 42: Dependence of annual costs for both the CHEST system and the battery storage on the installed PV peak power.

Figure 43 shows the (initial) investment costs dependent on the installed PV peak power for both the CHEST system and the battery storage. As it was shown in Chapter 5.2.3, an increase of the installed PV peak power means a decrease of the required storage capacity: both for CHEST and the battery (cf. Figure 28). As a first conclusion of Figure 43, it can be said that for this island energy system, the investment costs of the CHEST system and of the battery storage are quite in the same order of magnitude. For small system sizes (= for high installed PV peak powers), the battery storage shows slightly lower investment costs, but the larger the storage system, the more advantageous becomes the CHEST system compared to the battery storage. Furthermore, as was already mentioned, the battery storage has a lower expected lifetime, which makes the CHEST system even more advantageous here.

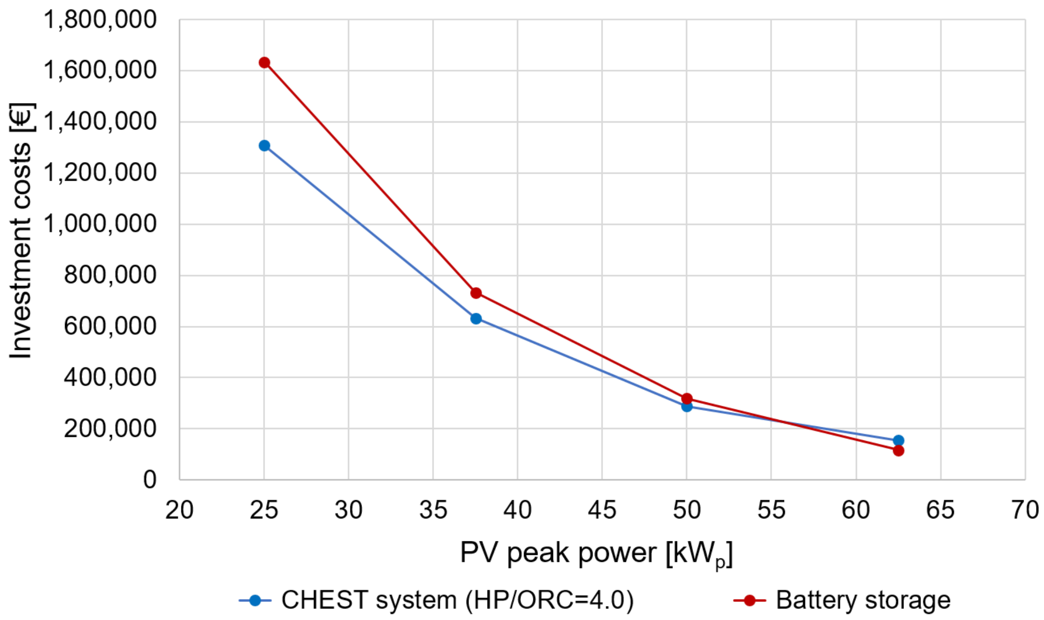

Figure 43: Dependence of investment costs for both the CHEST system and the battery storage on the installed PV peak power.

A dynamic economic calculation was carried out with the boundary conditions presented in Chapter 6.1.2 for the CHEST system and for the battery storage for the two different installed PV peak powers of 25 kW_p (100 panels) and 62.5 kW_p (250 panels).

Figure 44 shows for the case 25 kW_p installed PV peak power the development of the total costs of both the CHEST system and the battery storage over the lifetime of 30 years. Total costs comprise all costs (investment, O&M, electricity + biomass purchase) discounted to the respective year (=net present values). For the battery storage, as can be seen in the figure, two different lifetimes of 10 and 15 years were assumed. The currently expected costs of the CHEST system were calculated according to the component costs listed in Table 5. For the future expected costs, it is assumed that HP and ORC are one single component, cf. the explanations in Chapter 6.1.2.

For the lower installed PV peak power of only 25 kW_p, as said above, the storage system sizes are higher and so are the investment costs (cf. Figure 43). For the installed PV peak power of 25 kW_p, the initial investment costs of the CHEST system account for about 1.31 million € according to the currently expected costs. Assuming a single component for both HP and ORC reduces the investment costs only marginally down to 1.28 million €. This is because the PCM is the dominating factor of the CHEST´s investment costs in such an island energy system.

As can be seen from Figure 44, the battery storage is clearly disadvantageous from economic point of view compared to the CHEST system, irrespective of the assumed lifetime for the batteries. The cheapest solution again would be to install no EES at all (total costs after 30 years: 80,650 €), because the annual savings are very low in relation to the investment costs However, then, such an island energy system cannot be realized. Thus, if the decision is to be completely independent of the DSO, a CHEST system should be selected as electrical energy storage solution rather than the batteries for this case of an installed PV peak power of 25 kW_p.

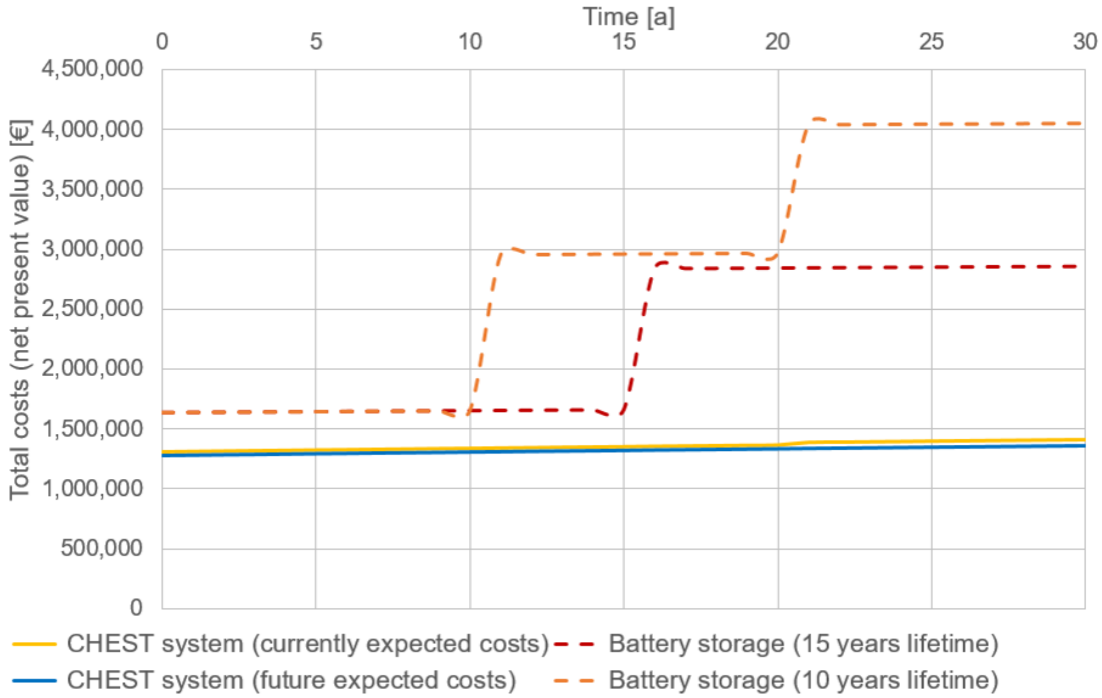

Figure 44: Development of the total costs (net present value) over the lifetime for the CHEST system and the battery storage for an installed PV peak power of 25 kW_p.

Table 17 shows the main economic KPIs for the four different EES solutions/variants. The values for "No EES" are shown in the table for informative purpose, but as said above, it is not a fair comparison to the storage solution since no island energy is possible then. LCOS definition was the same as presented in Chapter 6.3.3 for Ispaster 2.0 case, namely:

$$LCOS = \frac{\sum_{t=1}^{n} \frac{I_t + O\&M_t + C_{Charge,t}}{(1+j)^t}}{\sum_{t=1}^{n} \frac{E_{Discharge,t}}{(1+j)^t}} = \frac{\sum_{t=1}^{n} \frac{I_t + O\&M_t + C_{Biomass,add,t}}{(1+j)^t}}{\sum_{t=1}^{n} \frac{Elec_{Discharge,t}}{(1+j)^t}}$$

The levelized costs between Ispaster 2.0 and Ispaster Island are directly comparable, since the application, the LCOS definition and also the boundary conditions are the same. As can be seen from the comparison with Chapter 6.3.3, the levelized costs of storage are significantly higher for Ispaster Island case. This is comprehensible, because achieving complete independence from the grid requires huge storage capacities in comparison to the other components.

Table 17: Relevant economic KPIs for the exemplary CHEST system in Ispaster Island case study for the case of an installed PV peak power of 25 kWp.

Economic KPI	CHEST (now)	CHEST (future)	Battery (15 a)	Battery (10 a)	No EES
Investment costs (CAPEX)					
Initial investment costs	1,308,751 €	1,278,654 €	1,634,400 €	1,634,400 €	0 €
Replacement investments costs (discounted)	18,529 €	0 €	1,178,429 €	2,368,084 €	0 €
Cumulative Investment costs after 30 years (discounted)	**1,327,279 €**	**1,278,654 €**	**2,812,829 €**	**4,002,484 €**	**0 €**
Operational costs (OPEX)					
Annual O&M costs (1st year)	309 €	309 €	178 €	178 €	0 €
Annual costs for electricity purchase (1st year)	0 €	0 €	0 €	0 €	1,461 €
Annual costs for biomass purchase (1st year)	2,659 €	2,659 €	1,521 €	1,521 €	1,521 €
Cumulative operational costs after 30 years (discounted)	**78,762 €**	**78,762 €**	**44,943 €**	**44,943 €**	**80,650 €**
Economic payback					
Total costs (discounted) after 30 years	**1,406,041 €**	**1,357,416 €**	**2,857,772 €**	**4,047,427 €**	**80,650 €**
Return on investment (ROI)	n.a.	n.a.	n.a.	n.a.	n.a.
Internal rate of return (IRR)	n.a.	n.a.	n.a.	n.a.	n.a.
Economic payback time	n.a.	n.a.	n.a.	n.a.	n.a.
Levelized costs					
Levelized costs of storage (LCOS)	**6,226 €/MWh**	**6,004 €/MWh**	**12,848 €/MWh**	**18,275 €/MWh**	n.a.

$$LCOS_{CHEST,now} = \frac{\sum_{t=1}^{n} \frac{I_t + O\&M_t + C_{Biomass,add,t}}{(1+j)^t}}{\sum_{t=1}^{n} \frac{Elec_{Discharge,t}}{(1+j)^t}} = \frac{1{,}327{,}279€ + 6{,}847€ + 30{,}778€}{219.2MWh} \approx \mathbf{6,226\ €/MWh}$$

$$LCOS_{CHEST,future} = \frac{\sum_{t=1}^{n} \frac{I_t + O\&M_t + C_{Biomass,add,t}}{(1+j)^t}}{\sum_{t=1}^{n} \frac{Elec_{Discharge,t}}{(1+j)^t}} = \frac{1{,}278{,}654€ + 6{,}847€ + 30{,}778€}{219.2MWh} \approx \mathbf{6,004\ €/MWh}$$

$$LCOS_{Battery,15a} = \frac{\sum_{t=1}^{n} \frac{I_t + O\&M_t + C_{Biomass,add,t}}{(1+j)^t}}{\sum_{t=1}^{n} \frac{Elec_{Discharge,t}}{(1+j)^t}} = \frac{2{,}812{,}829€ + 3{,}944€ + 0€}{219.2MWh} \approx \mathbf{12,848\ €/MWh}$$

$$LCOS_{Battery,10a} = \frac{\sum_{t=1}^{n} \frac{I_t + O\&M_t + C_{Biomass,add,t}}{(1+j)^t}}{\sum_{t=1}^{n} \frac{Elec_{Discharge,t}}{(1+j)^t}} = \frac{4{,}002{,}484€ + 3{,}944€ + 0€}{219.2MWh} \approx \mathbf{18,275\ €/MWh}$$

Figure 45 shows for the case 62.5 kW_p installed PV peak power the development of the total costs of both the CHEST system and the battery storage over the lifetime of 30 years. For this higher installed PV peak power of 62.5 kW_p, as illustrated in Figure 43, the storage system sizes are smaller and so are the investment costs. The initial investment costs of the CHEST system account for about 155,000 € according to the currently expected costs. Assuming a single component for both HP and ORC reduces the investment costs down to 125,000 €.

As can be seen from Figure 45, the battery storage is still disadvantageous from economic point of view compared to the CHEST system. However, the differences between CHEST and the battery are small compared to the example shown above for an installed PV peak power of 25 kW_p. This is because of the lower differences in investment costs for this installed PV peak power. The cheapest solution again would be to install no EES at all (total costs after 30 years: 75,911 €). However, as already stated above, an island energy system would not be possible in this case.

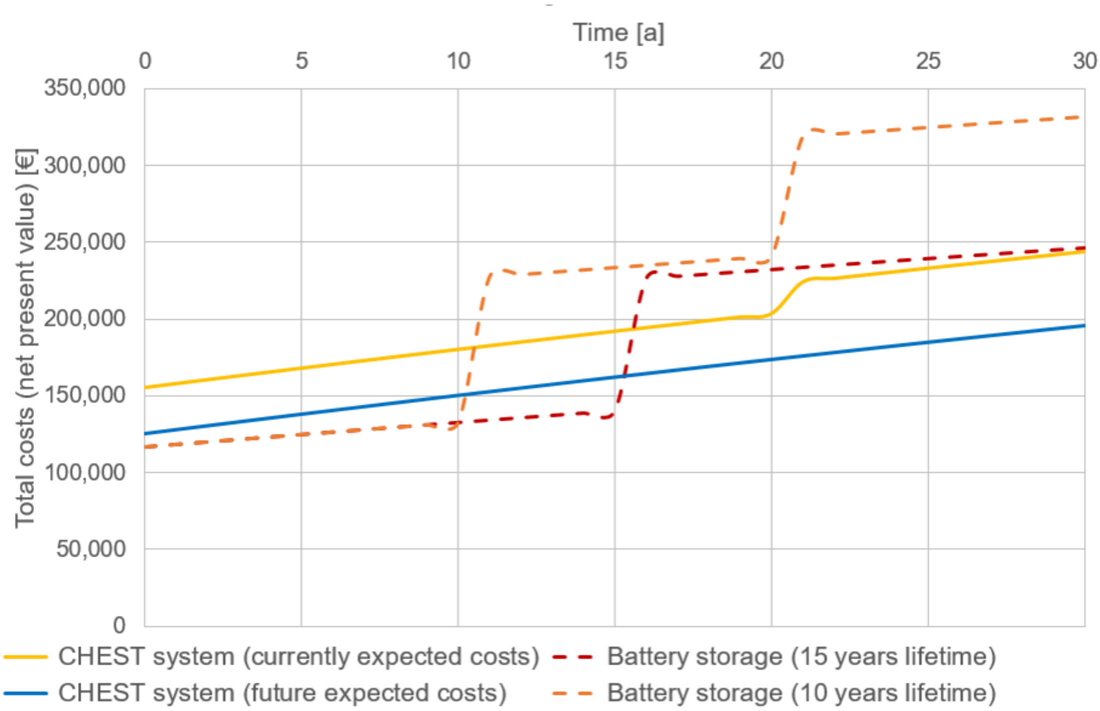

Figure 45: Development of the total costs (net present value) over the lifetime for the CHEST system and the battery storage for an installed PV peak power of 62.5 kW$_p$.

Table 18 shows the main economic KPIs for the four different EES solutions/variants.

Table 18: Relevant economic KPIs for the exemplary CHEST system in Ispaster Island case study for the case of an installed PV peak power of 62.5 kW_p.

Economic KPI	CHEST (now)	CHEST (future)	Battery (15 a)	Battery (10 a)	No EES
Investment costs (CAPEX)					
Initial investment costs	155,247 €	125,327 €	117,000 €	117,000 €	0 €
Replacement investments costs (discounted)	18,413 €	0 €	84,359 €	169,521 €	0 €
Cumulative Investment costs after 30 years (discounted)	**173,661 €**	**125,327 €**	**201,359 €**	**286,521 €**	**0 €**
Operational costs (OPEX)					
Annual O&M costs (1st year)	268 €	268 €	178 €	178 €	0 €
Annual costs for electricity purchase (1st year)	0 €	0 €	0 €	0 €	1,286 €
Annual costs for biomass purchase (1st year)	2,372 €	2,372 €	1,521 €	1,521 €	1,521 €
Cumulative operational costs after 30 years (discounted)	**70,094 €**	**70,094 €**	**44,943 €**	**44,943 €**	**75,911 €**
Economic payback					
Total costs (discounted) after 30 years	**243,754 €**	**195,421 €**	**246,302 €**	**331,464 €**	**75,911 €**
Return on investment (ROI)	n.a.	n.a.	n.a.	n.a.	n.a.
Internal rate of return (IRR)	n.a.	n.a.	n.a.	n.a.	n.a.
Economic payback time	n.a.	n.a.	n.a.	n.a.	n.a.
Levelized costs					
Levelized costs of storage (LCOS)	**1,050 €/MWh**	**800 €/MWh**	**1,064 €/MWh**	**1,506 €/MWh**	n.a.

$$LCOS_{CHEST,now} = \frac{\sum_{t=1}^{n} \frac{I_t + O\&M_t + C_{Biomass,add,t}}{(1+j)^t}}{\sum_{t=1}^{n} \frac{Elec_{Discharge,t}}{(1+j)^t}} = \frac{173{,}661€ + 5{,}934€ + 23{,}022€}{192.9MWh} \approx \mathbf{1,050\ €/MWh}$$

$$LCOS_{CHEST,future} = \frac{\sum_{t=1}^{n} \frac{I_t + O\&M_t + C_{Biomass,add,t}}{(1+j)^t}}{\sum_{t=1}^{n} \frac{Elec_{Discharge,t}}{(1+j)^t}} = \frac{125{,}327€ + 5{,}934€ + 23{,}022€}{192.9MWh} \approx \mathbf{800\ €/MWh}$$

$$LCOS_{Battery,15a} = \frac{\sum_{t=1}^{n} \frac{I_t + O\&M_t + C_{Biomass,add,t}}{(1+j)^t}}{\sum_{t=1}^{n} \frac{Elec_{Discharge,t}}{(1+j)^t}} = \frac{201{,}359€ + 3{,}944€ + 0€}{192.9MWh} \approx \mathbf{1,064\ €/MWh}$$

$$LCOS_{Battery,10a} = \frac{\sum_{t=1}^{n} \frac{I_t + O\&M_t + C_{Biomass,add,t}}{(1+j)^t}}{\sum_{t=1}^{n} \frac{Elec_{Discharge,t}}{(1+j)^t}} = \frac{286{,}521€ + 3{,}944€ + 0€}{192.9MWh} \approx \mathbf{1,506\ €/MWh}$$

As a conclusion of the two cases with 25 kW_p and 62.5 kW_p installed PV peak power, it can be stated that regardless of the installed PV peak power, the CHEST system is the economically more favorable storage solution compared to the batteries for the Ispaster Island case.

7. Conclusions

A first major outcome of this Task 4.3 was the definition of a number of key performance indicators (KPIs) that were grouped into five categories. These KPIs describe and assess the performance of the CHEST system and its components from a technical, operational, energetic, environmental and economic point of view. Based on these KPIs, an evaluation and decision can be made in how far a CHEST system is a reasonable energy storage solution for a certain use case. The KPIs defined in Task 4.3 will also be used in the CHEST public tool of Task 6.5 to supply information on the expected performance of a CHEST system to the user of this web tool who wants to analyze the feasibility of the CHEST system under the boundary conditions of an energy system defined by the user.

Furthermore, the work in this Task 4.3 dealt with the dynamic simulation and subsequent techno-economic assessment of two very different use cases of a CHEST system:

- on the one hand, a CHEST system that uses the fluctuating electricity prices in order to make a profit with the purchase and sale of electricity from and to the national electricity grid (Aalborg case study),
- on the other hand, a CHEST system, which is used together with photovoltaic panels (PV) to reduce the dependence on the local DSO to a large extent (Ispaster 2.0) or even completely (Ispaster Island).

Also in terms of the availability of heat, the two case studies are different. While in Aalborg case study, there is plenty of excess heat available at quite a high temperature level, the heat in Ispaster case study comes from solar thermal collectors and a wood chips boiler.

The simulation results and the techno-economic assessment of the CHEST system in the **Aalborg** case study show that with the current Danish electricity prices and tax schemes in place, no profitable operation of the CHEST system is possible for the business case considered here. The unfavorable electricity prices also affect the energetic and environmental performance of the CHEST system, because the annual primary energy savings and the annual savings of CO_2 emissions are low due to the low operation time of the CHEST system. An energetic and CO_2 payback is achieved within the lifetime of the CHEST system, however, it takes very long (> 20 years) and it is only given under the assumption that heat consumption of the CHEST system is completely covered by true excess heat, which would not have been usable otherwise.

However, these not very positive outcomes of the Aalborg case study do not mean that this envisaged business case and the role that the CHEST system can play in such a case for the stability of the electricity grid, do not work. First of all, the electricity prices and tax schemes in other European countries might give very different results here. Secondly, there will be an increased demand of electrical energy storage (EES) in the coming years due to the increase of renewable electricity sources, which will certainly change the electricity prices and tax schemes for EES. At the moment, no electrical energy storage at all is economically the best option, but this is not an option for the close future. Therefore, the regulation situation for electrical energy storage and the electricity prices will have to change.

Furthermore, as is pointed out in Deliverable 4.4, changes of the HP and ORC process and optimization of the control strategies of the CHEST system pose a huge potential for increased operation times and performance of the CHEST system. This can increase the electrical and thermal efficiency and/or reduce the required CHEST system size, which then reduces the investment costs of the system.

For the **Ispaster** case study, it was shown that the CHEST system is already today the economically favorable storage solution compared to lead-acid batteries. It was also illustrated that indeed, it is always cheaper to have no electrical energy storage at all, because the annual savings of electricity are quite low compared to the investment costs of electrical energy storage. However, if independence from the DSO is to be achieved, EES is required and then, CHEST is the more beneficial option from an economic point of view compared to the battery and this benefit gets even more pronounced the bigger the storage size gets.

Due to the high cumulative energy demand and CO_2 emissions originating from the production of the CHEST system, the battery storage is the favorable option from an energetic and environmental point of view. For relatively small storage system sizes like in Ispaster 2.0, the CHEST system still achieves energetic and CO_2 payback within its lifetime, although it is very long. For achieving electrical self-sufficiency in Ispaster Island case, the CHEST system needs to be increased mainly by its HTTES size and as the PCM is by far the domination factor regarding cumulative energy demand and CO_2 emissions, there is no energetic and CO_2 payback within the lifetime of the CHEST system for Ispaster Island case.

In general, from an energetic point of view, it became very clear that the CHEST system is a net heat consumer, i.e. its operation leads to additional heat demand (i.e. an increase of the heat demand compared to the original heat demand of the DH network). This means that the benefit on the electricity side is achieved at the expense of the thermal output. Whether this affects the assessment of the CHEST from primary energy and CO_2 emission point of view, strongly depends on where the heat for the CHEST system is taken from. If it is excess heat that could not be used otherwise or if it is heat that almost exclusively comes from renewables, which is indeed the concept behind CHEST, then the energetic and the environmental assessment is affected only slightly. If there is not enough excess heat for the CHEST system or if it has to be generated by fossil fuels, this will worsen the energetic and the environmental assessment of the CHEST system significantly compared to other EES solutions like batteries, which do not affect the thermal production and demand side.

The assessment of the CHEST system regarding the energetic and environmental payback time was generally bad here, which is due to a very high cumulative energy demand and very high CO_2 emissions for the production of the PCM. However, the characterization of the PCM storage was very preliminary here and will further be analyzed in the upcoming Task 4.6.

References

[Adeo 2014]. Adeoye, J. T.; Amha, Y. M.; Poghosyan, V. H.; Torchyan, K.; Arafat, H. A.: Comparative LCA of two thermal energy storage systems for Shams1 concentrated solar power plant: molten salt vs. concrete. Journal of Clean Energy Technologies 2 (2014), pp. 274-281, https://doi.org/10.7763/JOCET.2014.V2.139.

[Arp 2018]. Arpagaus, C.; Bless, F.; Uhlmann, M.; Schiffmann, J.; Bertsch, S.: High Temperature Heat Pumps: Market Overview, State of the Art, Research Status, Refrigerants, and Application Potentials. In: 17th International Refrigeration and Air Conditioning Conference, Purdue, 2018.

[Burk 2011]. Burkhardt, J. J.; Heath, G. A.; Turchi, C. S.: Life cycle assessment of a parabolic trough concentrating solar power plant and the impacts of key design alternatives. Environmental Science and Technology 45 (2011), pp. 2457-2464, https://doi.org/10.1021/es1033266.

[Carb 2015]. Carbonaro, C.; Cascone, Y.; Fantucci, S.; Serra, V.; Perino, M.; Dutto, M.: Energy assessment of a PCM-embedded plaster: embodied energy versus operational energy. Energy Procedia 78 (2015), pp. 3210-3215, https://doi.org/10.1016/j.egypro.2015.11.782.

[David 2017]. David, A.; Mathiesen, B. V.; Averfalk, H.; Werner, S.; Lund, H.: Heat Roadmap Europe: large-scale electric heat pumps in district heating systems. Energies 10 (2017), 578, https://doi.org/10.3390/en10040578.

[Dint 2014]. Dinter, F.; Gonzalez, D. M.: Operability, reliability and economic benefits of CSP with thermal energy storage: first year of operation of Andasol 3. Energy Procedia 49 (2014), pp. 2472-2481, https://doi.org/10.1016/j.egypro.2015.11.782.

[Dufo 2014]. Dufo-López, R.; Lujano-Rojas, J. M.; Bernal-Agustín, J. L.: Comparison of different lead-acid battery lifetime prediction models for use in simulation of stand-alone photovoltaic systems. Applied Energy 115 (2014), pp. 242-253, https://doi.org/10.1016/j.apenergy.2013.11.021.

[ECO 2014]. ecoinvent: Ecoinvent database 3.1, https://www.ecoinvent.org/database/older-versions/ecoinvent-31/ecoinvent-31.html

[EPRI 2010]. Rastler, D.: Electricity energy storage technology options. A white paper primer on applications, costs and benefits. EPRI (Electric Power Research Institute) report No. 1020676, 2010, http://large.stanford.edu/courses/2012/ph240/doshay1/docs/EPRI.pdf

[Held 2021]. Van Helden, W.; Reisenbichler, M.; Leusbrock, I.; Muser, C.; Wallner, G.; Ochs, F.; Moser, M.; Kremnitzer, P.; Maier, G.: Giga-scale thermal energy storage for renewable districts; First giga_TES results. Online conference Solarthermie und innovative Wärmesysteme, 27th-30th April 2021.

[IWU 2020]. Institut Wohnen und Umwelt. Kumulierter Energieaufwand und CO_2-Emissionsfaktoren verschiedener Energieträger und -versorgungen. Retrieved 02/10/2020 from https://www.iwu.de/fileadmin/tools/kea/kea.pdf.

[Joh 2019]. Johansson, E.; Norrman, F.: Life cycle analysis on phase change materials for thermal energy storage. Bachelor thesis KTH School of Industrial Engineering and Management Stockholm (2019), https://www.diva-portal.org/smash/get/diva2:1373953/FULLTEXT01.pdf.

[Ko 2018]. Ko, N.; Lorenz, M.; Horn, R.; Krieg, H.; Baumann, M.: Sustainability assessment of concentrating solar power (CSP) tower plants: Integrating LCA, LCC and LCWE in one framework. Procedia CIRP 69 (2018), pp. 395-400, https://doi.org/10.1016/j.procir.2017.11.049.

[Lal 2016]. Lalau, Y.; Py, X.; Meffre, A.; Olives, R.: Comparative LCA between current and alternative waste-based TES for CSP. Waste and Biomass Valorization 7 (2016), pp. 1509-1519, https://doi.org/10.1007/s12649-016-9549-6.

[Lam 2018]. Lamnatou, C.; Motte, F.; Notton, G.; Chemisana, D.; Cristofari, C.: Cumulative energy demand and global warming potential of a building-integrated solar thermal system with/without phase change material. Journal of Environmental Management 212 (2018), pp. 301-310, https://doi.org/10.1016/j.jenvman.2018.01.027.

[Miro 2015]. Miro, L.; Oro, E.; Boer, D.; Cabeza, L. F.: Embodied energy in thermal energy storage (TES) systems for high temperature applications. Applied energy 137 (2015), pp. 793-795, https://doi.org/10.1016/j.apenergy.2014.06.062.

[Noel 2015]. Noel, J. A.; Allred, P. M.; White, M. A.: Life cycle assessment of two biologically produced phase change materials and their related products. International Journal of Life Cycle Assessment 20 (2015), pp. 367-376, https://doi.org/10.1007/s11367-014-0831-1.

[Olym 2021]. Olympios, A. V.; McTigue, J. D.; Farres-Antunez, P.; Tafone, A.; Romagnoli, A.; Li, Y.; Ding, Y.; Steinmann, W.-D.; Wang, L.; Chen, H.; Markides, C. N.: Progress and prospects of thermo-mechanical storage – a critical review. Progress in Energy 3 (2021), 022001, https://doi.org/10.1088/2516-1083/abdbba.

[Oro 2012]. Oro, E.; Gil, A.; de Gracia, A.; Boer, D.; Cabeza, L. F.: Comparative life cycle assessment of thermal energy storage systems for solar power plants. Renewable Energy 44 (2012), pp. 166-173, https://doi.org/10.1016/j.renene.2012.01.008.

[Pie 2011]. Piemonte, V.; De Falco, M.; Tarquini, P.; Giaconia A.: Life cycle assessment of a high temperature molten salt concentrated solar power plant. Solar Energy 85 (2011), pp. 1101-1108, https://doi.org/10.1016/j.solener.2011.03.002.

[PlanE 2020]. PlanEnergi: Data provided by PlanEnergi for Danish electricity mix and Aalborg heat generation based on own calculations and several sources, e.g. (in Danish) Retrieved 26/10/2020 from https://ens.dk/sites/ens.dk/files/Energibesparelser/energifaktorer_ved_energiberegning.pdf.

[Quo 2013]. Quoilin, S.; Van den Broek, M.; Declaye, S.; Dewallef, P.; Lemort, V.: Techno-economic survey of Organic Rankine Cycle (ORC) systems. Renewable and Sustainable Energy Reviews 22 (2013), pp. 168-186, https://doi.org/10.1016/j.rser.2013.01.028.

[RITE 2016]. Reglamento de Instalaciones Térmicas en los Edificios (RITE): FACTORES DE EMISIÓN DE CO2 y COEFICIENTES DE PASO A ENERGÍA PRIMARIA DE DIFERENTES FUENTES DE ENERGÍA FINAL CONSUMIDAS EN EL SECTOR DE EDIFICIOS EN ESPAÑA. Retrieved 02/10/2020 from https://energia.gob.es/desarrollo/EficienciaEnergetica/RITE/Reconocidos/Reconocidos/Otros%20documentos/Factores_emision_CO2.pdf.

[Schm 2019]. Schmidt, O.; Melchior, S.; Hawkes, A.; Staffell, I.: Projecting the future levelized cost of electricity storage technologies. Joule 3 (2019), pp. 81-100, https://doi.org/10.1016/j.joule.2018.12.008..

[Tar 20017]. Tartière, T.; Astolfi, M.: A world overview of the Organic Rankine Cycle market. Energy Procedia 129 (2017), pp. 2-9, https://doi.org/10.1016/j.egypro.2017.09.159.

[TEC 2020]. Tecnalia: Energy and environmental data based on earlier research project results. 2020

[Turbo 2021]. Turboden S.p.A.: Website of Italian ORC manufacturer Turboden. Retrieved 01/09/2021 from https://www.turboden.com/products/2463/orc-system

[Valv 2009]. Garcia-Valverde, R.; Miguel, C.; Martinez-Bejar, R.; Urbina, A.: Life cycle assessment of a 4.2 kW_p stand-alone photovoltaic system. Solar Energy 83 (2009), pp. 1434-1445, https://doi.org/10.1016/j.solener.2009.03.012.

[Wang 2018]. Wang, Z.: Heat pumps with district heating for the UK´s domestic heating: individual versus district level. Energy Procedia 149 (2018), pp. 354-362, https://doi.org/10.1016/j.egypro.2018.08.199.